

OFFICE OF ADVANCED RESEARCH AND TECHNOLOGY  
SPACE VEHICLES DIVISION

PROCEEDINGS OF CONFERENCE ON  
**THERMAL JOINT CONDUCTANCE**



GPO PRICE \$ \_\_\_\_\_

CFSTI PRICE(S) \$ \_\_\_\_\_

Hard copy (HC) 4.00

Microfiche (MF) 1.00

ff 653 July 85

FEBRUARY 19, 1964  
NASA HEADQUARTERS  
WASHINGTON, D. C.

FACILITY FORM 602	<b>N66 37806</b>	<b>N66 37810</b>
	(ACCESSION NUMBER)	(THRU)
	<u>134</u>	<u>1</u>
	(PAGES)	(CODE)
	<u>TMX-56300</u>	<u>33</u>
	(NASA CR OR TMX OR AD NUMBER)	(CATEGORY)

FOR NASA INTERNAL USE ONLY


## Table of Contents

List of Attendees	2
Conference Agenda	3
Conference Notes, Conrad P. Mook	6
"Results of Contract NAS 8-5207 'Thermal Contact Conductance in a Vacuum' and Related Parameter Study" Harry L. Atkins, Marshall Space Flight Center	7 ✓
"Measurements of Thermal Contact Conductance in a Vacuum" Walter E. Kaspereck and Richard M. Daily, Marshall Space Flight Center	61 ✓
"Thermal Joint Conductance" J. M. F. Vickers, Jet Propulsion Laboratory	97 ✓
"Thermal Conductance of Molybdenum and Stainless Steel Interfaces in a Vacuum Environment" R. D. Sommers and W. D. Coles, Lewis Research Center	119 ✓

NASA Headquarters Conference on Thermal Joint Conductance  
February 19, 1965

List of Attendees

Aaron Fisher	GSFC
John F. Rogers	GSFC
Joe Boyle	GSFC
Robert Kidwell	GSFC
J. Michael Vickers	JPL
John W. Lucas	JPL
Ralph D. Sommers	Lewis
Herman Mark	Lewis
John P. Mugler, Jr.	Langley
Robert G. Thomson	Langley
Doyle P. Swofford	Langley
Lenwood Clark	Langley
Charles Smith	MSFC
W. S. Jensen	MSFC (R-P&VE-PTP)
Richard Dailey	MSFC
Walter E. Kaspereck	MSFC
Robert F. Elkin	MSFC
Billy P. Jones	MSFC (RP)
Harry L. Atkins	MSFC (Research Projects)
Robert G. Brown	MSC
Conrad P. Mook	HDQS.



Space Vehicle Division  
Office of Advanced Research and Technology  
NASA Headquarters  
Washington, D.C.

Thermal Joint Conductance Research Review and Planning Conference  
February 19, 1964

AGENDA

- 9:00 - 9:15 a.m. Welcome and Introduction
- 9:15 - 9:30 a.m. Brief Summary of Status of Government, University and Industry Research on Thermal Conductivity across Unbonded Joints in the High Vacuum Environment of Space - Conrad P. Mook - OART
- 9:30 - 10:00 a.m. Contract Efforts on Thermal Interface Conductance - Harry L. Atkins - MSFC

ABSTRACT

The past year's efforts under NASA Contract NAS8-5207 (General Electric Company, Mr. Erwin Fried) will be discussed. Slides will be used to show the equipment, test samples, and data plotted on graphs. This contract will be briefly compared with other work in the area of thermal interface conductance.

Next year's efforts under this contract will be discussed.

- 10:00 - 10:30 a.m. Model Studies in Conjunction with the Behavior of Thermal Interface Conductance - Harry L. Atkins - MSFC

ABSTRACT

Three models will be discussed in which their deformations as a function of loading is shown to be similar to the change of thermal interface conductance vs. loading. Slides will be used to show the deformed models and graphs of existing interface data. Some conclusions as to the nature of thermal interface conductance will be drawn from these deformed models.

One of the most complete bibliographies will be given in which some previously unknown Russian references will be presented.

- 10:30 - 10:45 a.m. BREAK



ABSTRACT

The apparatus used in obtaining experimental results of thermal contact conductance for metallic joints ranging in surface finish from 5 to more than 200 micro-inch CLA (Center Line<sub>2</sub> Average) with contact pressures ranging from 3 to 70 kg/cm<sup>2</sup> (40 to 1000 psi) is described.

Experimental results for the following materials are presented: 6061 T6 Aluminum, Casting Alloys Magnesium AZ91C, Almag 35 and Aluminum 356. Combinations of these materials expected in the Saturn program were tested. The addition of an interstitial material, i.e., high vacuum silicone grease was evaluated and the results are presented.

Detailed descriptions of the provisions made for the avoidance of radiation heat losses and the attempts made to improve measurement accuracies are given.

- 11:15 - 12:30 p.m.      Discussion of Research in Thermal Contact Resistance  
at Lewis and Goddard  
Ralph Sommers - Lewis Research Center  
Aaron Fisher - Goddard Space Flight Center
- 12:30 - 1:30 p.m.      LUNCH
- 1:30 - 2:30 p.m.      Thermal Joint Conductance - Dr. J. M. F. Vickers - JPL

ABSTRACT

The work of Drs. A. M. Clausing and B. T. Chao of the University of Illinois under a NASA Research Grant, for which Jet Propulsion Laboratory was the technical monitor, will be described.

Many limitations are noted when an attempt is made to apply the available information on joint conductance to practical bolted or riveted joints.

A correlation of information from the literature on joint conductance has been prepared.

The problem of applying the uniform pressure information to an actual bolted joint by 1) carrying out a stress analysis of simplified models of bolted joints, and 2) determining the constriction effect of a region with variable joint conductance is being attacked.

Apparatus is presently under construction with which data can be generated to be compared with the results from the above analyses. Experimental investigation of certain other effects in joint conductance which have been largely neglected in the past will also be carried out.

2:30 - 4:30 p.m.

**Round Table Discussion on Future Research**

1. Theoretical Analyses of Laboratory Results
2. The Transient Pressure Problem
  - a. The Ascent Environment
  - b. Potential Usefulness as Thermal Switching Device
3. The need for Flight Experiments
4. The need for measurement standards.

4:30 p.m.

**Adjourn**

**BOTH MEETINGS WILL BE HELD AT 600 INDEPENDENCE AVENUE, S.W., FEDERAL OFFICE BUILDING 10B, ROOM 6032.**

## CONFERENCE NOTES

During the first half of 1964, a series of conferences was held at NASA Headquarters in Washington, dealing with research leading to advancements of the state-of-the-art in the thermal design of space vehicles. Of major importance in this program is research aimed at reducing uncertainties in the heat transfer which can be assumed to take place across unbonded joints in the vacuum environment of outer space.

This volume consists of four of the reports presented in the conference on Thermal Joint Conductance which was held in NASA Headquarters in Washington, D. C., on February 19, 1964, as a part of the series.

Some delay was encountered in publishing this volume due to efforts to overcome the need for more reproducible copy. This difficulty has not been alleviated and passage of time necessitates publication "as-is" with apologies to recipients who, it is hoped, will find the papers presented herein to be a useful summary.

The round-table discussion was held, as outlined in the agenda, with positive agreement reached as to the importance of continued research in this area, emphasizing further the need for transient data and flight experiments.

C. P. Mook  
NASA Headquarters  
Washington, D. C.

**N66 37807**

**RESULTS OF CONTRACT NAS 8-5207  
"THERMAL CONTACT CONDUCTANCE IN A  
VACUUM" AND RELATED PARAMETER STUDY**

by

**Harry L. Atkins  
Space Thermodynamics Branch  
Research Projects Laboratory  
Marshall Space Flight Center**

## INTRODUCTION

This paper shows the results of an in-house and contractual effort to better define the parameters associated with thermal contact conductance. Data for contact conductance vs. applied pressure, and the corresponding graphs are shown for samples of 304 Stainless Steel, AZ31 Magnesium, 6061-T6 Aluminum and Copper.

For a more thorough discussion of the contractual work, the reader is referred to the final report of this contract (NAS8-5207). A paper covering the results of this contract will also be presented at the AIAA 1st Annual Meeting and Technical Display June 29-July 1964, at the Sheraton Park Hotel, Washington, D.C.

In addition to the contractual interface data, an attempt is made to define the observed change of slope of 6061-T6 and 2024-T4 Aluminum when the data are plotted on log-log graph paper. It is shown that by deforming cones, hemispheres, and ellipses, a similar change of slope occurs. It is concluded that these models might possibly represent "scale-up" replicas of the macroscopic points of contact of two mating aluminum surfaces.

A reference list is included which is a revision and extension of the bibliography the author handed out at the February meeting. It contains many previously unknown Russian references.

## EXPERIMENTAL PROGRAM

A study of the problems in the early stages of the thermal contact conductance work, has indicated a need for experiments designed to (1) aid in the understanding of the heat transfer mechanism, (2) provide data to verify existing analyses, (3) provide data to aid in the development of new analytical methods.

Subsequently, a thermal contact conductance apparatus suitable for use in vacuum was developed which would permit accurate measurement of thermal conductance as a function of contact pressure. As opposed to the flat plate apparatus used in the investigations reported by Fried, the principal investigator of this study, this apparatus utilized cylindrical columns to minimize flatness deviations under load.

### Thermal Test Apparatus

A schematic of the test apparatus is shown in Fig. 1. Figure 2 shows the heat flow section of the apparatus, with a specimen in place, without the radiation shield.

The samples consisted of two metallic cylinders having a diameter of 5.08 cm (2 in.), and a length of 7.62 cm (3 in.) each. Each sample was instrumented with four copper constantan thermocouples to determine the axial temperature gradient due to the uniform heat flux passing between the electric heater and the liquid-cooled sink.

Contact pressure could be varied by means of a stainless steel bellows, pressurized in accordance with the desired load. The load was measured using a strain gage load washer on the heat sink side (Fig. 1).

The entire assembly was installed in a bell jar vacuum system with a right angle cold trap, utilizing a 4-inch oil diffusion pump preceded by a roughing pump to achieve a vacuum of  $10^{-4}$  mm Hg ( $1.33 \times 10^{-3}$  newton/m<sup>2</sup>) or better.

The heat source utilized in this test was a 100-watt electric resistance element embedded in the main heater assembly which is guarded by a ring heater and a rear guard heater, as shown in Fig. 1. This system is arranged such that there exists no temperature difference between the main heater and the guards. Each is separately controlled, so that all thermal energy from the main heater has only one direction to go -- into the test sample. In order to monitor this system, thermocouples were fastened to the several surfaces seeing each other.

Minimum cross-sectional area supports, made of tubes (Fig. 1), were used between the rear guard and the main heater, in order to minimize heat leak errors, even though the facing surfaces were kept at the same temperature. The desired range of temperature differences between potential heat lead points were kept at  $\Delta T$ 's of 1°C or less in order not to exceed 1/2 of 1% heat flow errors. Initially, these temperature differences were controlled by use of a deviation amplifier, but experience indicated that manual control, with proper judgment, resulted in less time delay between steady-state points.

The allowable temperature differences were dictated by the amount of heat passing through the test sample, since high heat fluxes through the sample permitted higher heat losses from the heater while permitting the percentage losses to remain the same.

The heat flux was determined by measuring the regulated d-c power input (i. e. , voltage and current), using precision instruments. In addition to this, the hot heater resistance was obtained by momentarily turning off the power. In order to eliminate leadline losses in the calculation, the ratio of heater winding resistance to total system resistance was measured and a correction applied to all readings. An ESI bridge having an accuracy of  $\pm 0.05\%$  was used.

A check was performed on the adequacy of the heat flow measurement by determining the thermal conductivity of a piece of ARMCO iron. The measured value came within 2% of the nominal value which, considering all possible variables, is quite good. If we were to perform only thermal conductivity measurements, this accuracy could probably be improved. However, for conductance measurements, with their many sources of error, the cost of improving this system is not quite worth the effort at present.

#### Temperature Measurement

Considerable attention was paid to accurate temperature measurement techniques in order to minimize possible measurement errors, since the quality of the temperature measurement directly affected the quality of the interface thermal contact conductance obtained. Thermocouple junctions were made of 40-gauge copper-constantan precision grade thermocouple wire. This grade of wire has a nominal tolerance of  $\pm 0.3^{\circ}\text{C}$  over the range of interest, but has been found by experience to be considerably better. Junctions were made by mercury pool arc welding techniques.



The thermocouples were installed in the test samples in 2.54-cm deep holes, to place the junction at the cylinder axis. The junction was embedded with Eccobond 56C, an epoxy base cement having a thermal conductivity equal to that of stainless steel. In order to assure that the thermocouple bead actually contacted the sample at the cylinder centerline, a 0.33-cm diameter hole was drilled at the desired axial thermocouple location and a tube of the same material as the sample was inserted with the thermocouple installed. This method had the advantage that there was less likelihood of drill runout when the hole was drilled. It also permitted more positive installation and location of the thermocouple junction. The only exception to the matching of material was that an aluminum tube was used with the magnesium sample. This was not expected to result in an error because: (1) the thermocouple junction was in contact with the sample magnesium, and (2) the thermal effect of different material was not adverse because of the higher thermal conductivity of the aluminum. This would not result in a delay to reach thermal equilibrium.

The choice of 40-gauge thermocouple wire was dictated by the desire to minimize conduction losses. Experience with several hundred thermocouples from such wire (purchased from Thermo-Electric Co.) with no adverse emf characteristics led to the selection of this diameter. The question as to the proper response of the thermocouples when embedded in the samples in a vacuum was circumvented by use of the Eccobond 56C, a fairly free-flowing epoxy cement inserted and packed around the thermocouple bead and wire. Thus, the bead was hermetically isolated from the surrounding atmosphere.

To assure proper response of these thermocouples, they were placed in a constant temperature oven after being installed in the sample and the consistency of the temperature readings was checked. Out of over 60 thermocouples tested, only 4 were found to require corrections in the computation of conductances for the range of temperatures of interest (25-50°C). Particular attention was paid to the precision with which the axial distances between thermocouples were controlled, since the axial distance vs. temperature plots were used to project the temperature gradients to the interface and thus obtain the interface temperature difference.

The constriction resistance effects at and near the interface require that thermocouples be located in the undisturbed region in order to correctly project the temperature gradient. Since only the sample half interfaces are of interest, the heat source and heat sink interfaces with the samples had high vacuum silicone grease applied as a heat transfer promoting device. Thus, no significant constriction effects resulted at these interfaces.

The temperature difference,  $\Delta T$ , is based on the temperature obtained experimentally, which are then extrapolated to the interface. The accuracy with which this  $\Delta T$  can be obtained is a function of the accuracy with which the temperature gradient in the sample can be obtained. For high values of contact conductances the  $\Delta T$  usually was quite low. Conversely, for low values of conductance the  $\Delta T$  was high. Since a high  $\Delta T$  resulted in a higher percent accuracy, the relative percent accuracy of contact conductance obtained was constant. A representative temperature gradient curve is shown in

Fig. 3. Of the thermocouples used in the samples, each had its own cold junction. Their emf was read on a Leeds and Northrop K-3 potentiometer, with individual couples switched by means of a transfer switch. Figure 4 shows the vacuum system, thermocouple recorder, power supply, and instrument panel.

### Surface Finish Measurements

One significant area of interest, which strongly affects the thermal contact resistance is the surface finish of the interface. Surface finish, by definition, can include surface roughness as well as waviness, which is described by Clausing and "microscopic and macroscopic effects," and by Fenech as "primary and secondary waviness."

In addition to the small asperities which constitute the roughness, a machine's surface can have larger peaks and valleys which constitute the waviness. The direction parallel to the ridges and valleys of the waviness is called the lay direction.

A Taylor-Hobson "Talysurf" stylus type profilometer was used to obtain single-line profiles of the various surface finishes prepared to this program. Due to difficulties of operating an in-house "Talysurf" instrument, all but one pair of samples (Nos. 15 and 16) were inspected after thermal contact conductance tests were completed. Thus, any deformation of asperities, which may have taken place during tests would, therefore, be observable. However, it is not very likely that any such effects could be observed, because the "Talysurf" trace is merely the record of a stylus motion following the contours of the surface in a straight line.

Any asperity, deformed or otherwise, on either side of this straight line would, therefore, not be recorded. Although there is no certainty that a trace parallel to or in continuation to an existing trace will resemble the existing trace, there will be a similarity of characteristics, provided the character of the surface is taken into consideration. For example, in the case of machined surfaces, traces should be taken in the direction of tool motion as well as in the perpendicular direction. Particular attention should be paid to lathe-turned finishes at the profile through the center of the surface, because of the non-flatness of the surface at that point. Figure 5 shows typical "Talysurf" traces through the center of a machined surface for a copper sample.

The traces as shown, do not represent a true pictorial representation of the surface, because of the scale differences. These asperities appear to be much more severe than they are in reality. Nevertheless, the traces do provide a significant amount of useful information and provide an excellent means for comparison of surface finishes.

As a result of the length of the stylus travel (1.27-cm max.) which is adjustable, and the use of the optical flat attachment, flatness deviations can also be observed. This is due to the fact that the stylus motion, relative to an optical flat, is recorded.

An additional feature of the "Talysurf" profilometer is its ability to provide a centerline average (CLA) roughness reading, by means of an electronic integrator circuit, for any surface of certain minimum length. Centerline average (CLA) is also known as arithmetic

average (AA) and runs somewhat lower than the corresponding root-mean-square (RMS) reading. The latter gives more weight to the larger deviations from the centerline.

Flatness measurements were made using a surface plate and a dial indicator reading 2.5 micrometers, (0.001 inches) which permitted estimation of half divisions (1.3 micrometers). The dial indicator point was set at the sample center and the dial was set at zero. With the dial indicator fixed, the sample was moved so that the point traveled to the interface edge, reading the vertical deviation at the center, one-fourth diameter and at the edge.

This was done at mutually perpendicular diameters. A secondary check was made initially by holding the sample fixed and moving the dial indicator support stand. No significant differences were observed between the two methods. Plus readings indicated high spots, whereas minus readings indicated low spots. Results are shown in Table I in which the maximum values are presented. It should be noted that these values are the maximum from a fictitious plane, i. e., the datum plane as described in the next major section, "Deformation Experiments." Thus, there may occur some matching of interfaces having deviations, which could result in a test assembly of better mating than would be expected on the basis of individual reading. For example, samples 3 and 4 could have a cumulative flatness deviation of only  $+1.2 \times 10^{-6}$  meters if they fitted into each other.

## Thermal Test Results

The material and the important surface properties of the test samples are shown in Table I. These include roughness, Rockwell hardness, flatness deviation and type of surface preparation. Actual data for these surfaces are shown in Table II.

### Stainless Steel 304

Figure 6 shows the results of the stainless steel interface tests. Of interest is the large difference in conductance at the maximum contact pressure. The flatness deviation of the 0.30 micrometer (RMS) roughness samples was 1.3 micrometer, whereas the 1.2 micrometer (RMS) roughness sample had a flatness deviation of approximately 1.5 micrometer, at best, and 3.8, at worst, depending on surface matching.

Of interest is the curvature of the fine finish contact conductance curve whose behavior was confirmed by the descending load curve. Hysteresis could be observed for this specimen for the loading-unloading cycle.

In contrast, the coarse finish sample curve shows no hysteresis and is almost linear.

It is of particular interest to note and compare these two curves in Fig. 6 with the corresponding results of Clausing. The resemblance of the Clausing results with Stainless Steel 303, for approximately the same degree of flatness deviation, to our results is remarkable. The importance of the approximate similarity of flatness deviation, as opposed to a marked difference in roughness (Clausing, 3 micro-in for both versus our 12 and 50 micro-in) is demonstrated well in this experiment.

## Magnesium

Figure 7 shows the results for Magnesium AZ31B, a widely used magnesium alloy. These samples, which had lathe-turned interfaces exhibited a rather unusual reversal of expected performance. The coarse finished surfaces exhibited higher thermal contact conductances than did the fine finished interfaces. One possible explanation would be the greater effect of a surface film on a fine-finished surface versus that on a coarse-finished surface. Oxide films and tarnish were visible on both sets of samples, since two months had elapsed between machining and use. The reason for conjecture that a film will have a lesser effect on a coarse surface finish, is that the fewer sharper ridges of this finish will result in higher loads per unit area and cause the film to break. Another, and perhaps more plausible, reason is the relatively large flatness deviation for both sample pair, but that the sample assembly may have resulted in a greater mismatch for the poorer performance.

It is of interest to note that Clausing obtained higher conductances for similar material having lower values of flatness deviation and much lower surface roughness.

## Aluminum

The resultant conductance versus pressure curves are shown in Fig. 8. It is of interest to note that there was no significant difference in the values of contact conductance for the two surface finishes considered. The results for the finer (0.3-micrometer RMS) finish 6061-T6 Aluminum should have been higher than for the coarse (1.4-micrometer RMS) finish, since the former had lower values of flatness

deviation. At present, no explanation can be found for this behavior. The general shape of this curve conforms to that shown by Clausing for 2024 Aluminum, with the conductance somewhat lower at maximum pressure.

### Copper

A test for electrical grade copper (OFHC oxygen-free, high-conductivity copper) was performed, because the only available data (Jacobs and Starr) indicated linear variation of conductance with load at moderate loads, whereas, most other materials change in a non-linear manner in that pressure region. As can be seen in Fig. 9, the curve is not linear at low pressures, but does appear to be linear at higher contact pressures. It is also of interest to note that no hysteresis could be observed for this copper joint.

### General Remarks

The results for specific metal joints are discussed under their respective headings. This section discusses common-ground observations.

When conductance versus pressure is plotted on log-log paper, a curve (as shown in Figs. 11-13) results, which is somewhat different from earlier observed and expected results. Initially, a slope of one-half to two-thirds was expected for elastic behavior as discussed in another section of this paper. However, plots of data obtained in this study indicate a definite two-regime behavior with a pronounced point of change in slope. The exact reason for this change in slope has not yet been defined, except to show that it possibly represents the change



from purely elastic to elastic-plastic deformation behavior. This is discussed in the next section dealing with an experimental study of this phenomenon.

## DEFORMATION EXPERIMENTS

The three models (2024-T4 Aluminum) described in this paper are shown in Fig. 10. The cone and hemisphere models were 2.54 cm (1 in.) in diameter and 1.27 cm (0.5 in.) in height. The ellipse semi-major axis was 1.27 cm with its semi-minor axis being .950 cm (.375 in.).

The models in Fig. 10 (column 1) were placed between two flat plates of a steel press with a piece of pressure-sensitive paper placed on their tops and bottoms and a load  $P_i$  was applied. A typical piece of the pressure-sensitive paper appears below the models. The blackened area is the deformed area for that particular load. After each specified loading, another paper was placed on the model. Over the entire range of loading from 0-250,000 Newtons (0-60,000 pounds), the deformed area remained circular, as indicated by the blackened area on the paper, and the deformed model. The diameter of this blackened area was measured several times and an average taken, thus leading to the recorded deformed area data in Table III. The tests were performed at room temperature (293° K).

The height of the model was measured by a dial micrometer placed between the two steel plates. The models in columns 2, 3, 4, and 5 of Fig. 10 were subjected to specific loads, and the areas and heights were compared to those of the previously described models in

which the load was cycled. No appreciable difference was noticed and, thus, the cycling of loads had produced little work hardening of the models.

As soon as the data were plotted, it was observed that an interesting resemblance existed between the published thermal interface data and the deformation of the model. Of particular interest is that of the area/height deformation versus loading when compared to the thermal interface conductance as a function of its mechanical loading. Figure 11 shows data of the models compared on a log-log plot with that of Fried and of Clausing. In an attempt to bring the data into the same order of magnitude, the following expression was used:

$$\left[ K_m \right]_{P=P_i} = k \left[ \frac{A}{Y} \right]_{P=P_i} \quad (1)$$

where

$k$  = conductivity of the models

$A_{P_i}$  = deformed area of the model at load ( $P_i$ )

$Y_{P_i}$  = height of the model at load ( $P_i$ )

$\left[ K_m \right]_{P=P_i}$  = computed conductance of the models

to compute a representative thermal conductance. It must be strongly emphasized that the plotted data in Figs. 11-13 taken from the Fried and Clausing reports should not be used in computation. This data has been shifted in magnitude for better visual observation.

It is particularly interesting that both the interface data and the model data experience a change of slope at certain loading values.

The factor that appears to cause this change of slope in the model data is the dependence of the deformed area on the loading. This became evident when the area versus the loading was plotted. The contribution of the model height versus loading did not undergo this sudden change. This critical point of loading at which the slope changes shall, hereafter, be designated  $P_{cI}$  for the interface data and  $P_{cM}$  for the model data.

As can be seen from Fig. 11, the values of  $P_{cI}$  and  $P_{cM}$  do not coincide. This might be partly explained by a temperature dependence. In comparing  $P_{cM}$  with  $P_{cI}$  of Clausen, it is to be noted that the models were at  $293^{\circ}\text{K}$  ( $70^{\circ}\text{F}$ ) while Clausen reported mean interface temperatures of approximately  $386^{\circ}\text{K}$  ( $234^{\circ}\text{F}$ ) for eight interfaces. Figure 12 is a plot of the data reported in this paper for 6061 aluminum and the computed model data. This mean interface temperature ( $T_M$ ) was approximately  $301^{\circ}\text{K}$  ( $82^{\circ}\text{F}$ ), this value being the average of all the  $T_1$  and  $T_2$  values of interface. Since for this sample  $T_m$  was near that of the model temperature, it appears that the slope change at  $P_{cI}$  is nearer the value of that of the models  $P_{cM}$  than the corresponding Clausen data. However, this comparison is not totally valid since the metals are different. This leads to the question of whether  $P_{cI}$  is dependent on the mean interface temperature. If  $P_{cI}$  is attributed to the changes of the physical properties of the metal, it would appear reasonable that its value should be lower for higher mean interface temperatures. Thus, it would appear that

$$K_{cI} \propto f(P_{cI}) \propto f\left(\frac{1}{T_m}\right) \quad (2)$$

If all the load values of the deformation models are divided by the corresponding deformed area, pressure values are recorded which are consistently near the yield strength of the metal, as can be expected for permanent deformation.

It seems that there are other factors which influence  $P_{CI}$  for the Clausing data. If the eight data groups are plotted, then  $P_{CI}$  appears at different load values for each specimen. This is partly shown by two curves of Fig. 11.

When all the eight samples of 2024-T4 Aluminum values are averaged and plotted, Fig. 13 shows that the two-slope regime is again evident. As can be seen, this corresponds to the included data for the models.

In order to study the functional relationship of the curves a computer program for best fitting the data to an equation was formed. This equation corresponds to the form presented earlier and is  $h = A + B P^C$ . The data from Clausing, data reported in this paper, and the deformation model data show similar values of the exponent  $c$  both before and after the change of slope. The values of  $A/Y$ ,  $h$ ,  $A$ ,  $B$ , do not coincide because the data used for the best fit curve were of different units as reported in the respective reports. On Figs. 12 and 13, only the functional notation has been shown for comparison.

The best fit curves are:

1. Model data

$$\frac{A}{Y} = -32.90 + 0.57 P^{0.72}$$

from  $P = 0$  to 10,000 pounds.

$$\frac{A}{Y} = -37.47 + 3.03 \times 10^{-4} P^{1.54}$$

from  $P = 10,000$  to  $60,000$  pounds,

where

$A$  = deformed area in inches<sup>2</sup>

$Y$  = deformed height in inches

$P$  = load in pounds

## 2. 6061-T6 Aluminum (Fig. 12)

$$h = 9.73 \times 10^{+2} + 1.17 \times 10^{+3} P^{0.09}$$

from  $P = 10.2$  to  $419$  p. s. i.

$$h = 1.14 \times 10^{+2} + 7.00 \times 10^{-2} P^{1.61}$$

from  $P = 419$  to  $1,117.0$  p. s. i.

where  $h$  is given in BTU/hr ft<sup>2</sup> °F .

## 3. Average data of Clausing for eight samples of 2024-T4 Aluminum

$$h = 35.41 + 7.59 p^{0.91}$$

from  $P = 10.4$  to  $67.0$  p. s. i.

$$h = 168.1 + 2.14 p^{1.16}$$

from  $P = 67.0$  to  $986.0$  p. s. i.

where  $h$  is given in BTU/hr ft<sup>2</sup> °F.

## CONCLUSIONS

1. The importance of the flatness deviation effects on thermal joint conductance has been demonstrated.

2. The proposed models, based on the elastic deformation relations of Hertz appear to provide an approach to understanding the heat transfer mechanism. This is represented by the approaches of Clausing and this paper.
3. Better surface definition methods are required.
4. More experimental data of suitable accuracy is needed to arrive at  
(a) semi-relations and (b) statistical correlation.

Barzelay, M. E., Tong, K. N., and Holloway, G. F., "Thermal Conductance of Contacts in Aircraft Joints," NACA TN-3167, March 1954.

Barzelay, M. E., Tong, K. N., and Holloway, G. F., "Effect of Pressure on Thermal Conductance of Contact Joints," NACA TN-3295, May 1955.

Barzelay, M. E., and Holloway, G. F., "Effect of an Interface on Transient Temperature Distribution in Composite Aircraft Joints," NACA TN-3824, April 1957.

Barzelay, M. E., and Holloway, G. F., "Interface Conductances of Twenty-Seven Riveted Aircraft Joints," NACA TN-3991, July 1957.

Barzelay, M. E., "Range of Interface Thermal Conductance for Aircraft Joints," NACA TN D-426, May 1960.

Barzelay, M. E., and Schaefer, John W., "Temperature Profiles and Interface Thermal Conductance of Stainless Steel and Titanium Alloy Panels under Combined Loading and Heating." Syracuse University Report ME 406-577F.

Barzelay, M. E., and Holloway, G. F., "The Effect of an Interface on the Transient Temperature Distribution in Composite Aircraft Joints," Syracuse University Research Institute Report No. 1620.290-1, March 1955.

Berman, R., "Some Experiments on Thermal Contact at Low Temperatures," Journal of Applied Physics, Vol. 27, No. 4, pp. 318-323, Apr. 1956.

Bernard, J. J., "La Resistance Thermique Des Joints," Groupe Consultatif Pour La Recherche et la Realisation Aeronautiques, Rapport 212, October 1958. ASTIA File Copy AD221-409.

Bloom, Mitchell, F., "A Review of the Parameters Influencing Thermal Control Conductance Between Interfaces," Douglas Aircraft Report SM-42082, August 9, 1962.

Bloom, Mitchell F., "Preliminary Results From a New Thermal Control Conductance Apparatus," Douglas Aircraft Engineering Paper 1672, August 1963.

Boeschoten, F., "On the Possibility to Improve the Heat Transfer of Uranium and Aluminum Surfaces in Contact." In the Proceedings of the International Conference on the Peaceful Uses of Atomic Energy, Vol. 9, p. 208-209, Geneva, August 1955.

Boeschoten and Van der Held, E., "The Thermal Conductance of Contacts Between Aluminum and Other Metals," Physics, Vol. 23, pp. 37-44, 1957.

Bory, C. and Cordier, H., "Thermal Contact Resistances," From French Institute of Fuels and Energy, Transmission of Heat Seminar.

Bowden, F. P., and Tabor, D., "The Area of Contact Between Stationary and Between Moving Surfaces," Proc. Roy. Soc. Lond. A. 169 (1939).

Brooks, Jr., W. A., Griffith, George E., and Strass, H. Kurt, "Two Factors Influencing Temperature Distributions and Thermal Stresses In Structures," NACA Technical Note 4052.

Brown, M. H. S. (Translator), "Thermal Conductance of Steel Joints," (Conductance Thermique Des Liaisons Acier) Sud-Aviation Report C.R. 72.013-50, March 1960. Royal Aircraft Establishment, Farnborough, England, Library Translation No. 950. ASTIA File Copy, AD262-820, July 1961.

Browning, J. W., "A Transient Study of Thermal Contact Resistance," A study performed at Southern Methodist University, Dallas, Texas, 1962.

Brunot, A. W. and Buckland, F. F., "Thermal Contact Resistance of Laminated and Machined Joints," Trans. ASME, Vol. 71, pp. 253-257, 1949.

Brutto, E., Casagrande, I., and Perona, G., "Thermal Contact Resistance Between Cylindrical Metallic Surfaces," Energia Nucleare Vol. 6, p. 532-540, 1959.



Carroll, T. W., "Statistical Calculation of Geometric Parameters for Semi-Smooth Contiguous Surfaces," M.S. Thesis, M.I.T., Jan. 1962.

Cetinkale, T. N., "Thermal Conductance of Metal Surfaces in Contact," PH.D. Thesis, London University, London, England, 1951.

Cetinkale, T. N., and Fishenden, M., "Thermal Conductance of Metal Surfaces Contact," General Discussion on Heat Transfer, Conference of Institution of Mech. Eng. and ASME, Sept. 1951.

Clark, W. T., Powell, R. W., "Measurement of Thermal Conduction by the Thermal Comparator," Journal of Scientific Instruments (E. B.) Vol. 39, No. 11, pp. 545-551, Nov. 1962.

Clausing, A. M., and Chao, B. T., "Thermal Contact Resistance in a Vacuum Environment," University of Illinois Experimental Station Report, ME-TN-242-1, August 1963.

Cordier, H., and Maimi, R., "Experimental Study of the Influence of Pressures on Thermal Contact Resistance," SLA Translation 63-10777 Translated from Acad. Des. Sciences, Compts Rendus 250:2853-2855, April 25, 1960

Cordier, H., "Experimental Studies of the Influence of Pressure on Thermal Contact Resistance," ANNALES DE PHYSIQUE, No. 1-2 5-19 (1961) Translation RSIC-116, Redstone Arsenal, Alabama.

Coulbert, C. D., "Thermal Resistance of Aircraft Structure Joints," WADC Technical Note 53-50, June 1953.

Davis, W., "Thermal Transients In Graphite Copper Contacts," British Journal of Applied Physics, Vol. 10 #12, pp. 516-522, Dec. 1959.

Dyban, E. P., and Kondak, N. M., "Research on Heat Exchange in Course of Contact Between Parts," IZV. AN SSSR OTD. TEKHN. NAUK pp. 62-79, 1955 (9). Translation ASLIB-GB 158.

Dyson, J., and Hirst, W., "The True Contact Between Solids," Proceedings of the Physical Society, Section B, Vol. 67, pp. 309-312, 1954.

Fenech, H. and Rohsenow, W. M., "Thermal Conductance of Metallic Surfaces in Contact," U. S. AEC Report NYO-2136, May 1959.

Fenech, H., and Rohsenow, W. M., "Prediction of Thermal Conductance of Metallic Surfaces in Contact," Jour. Heat Transfer, V. 85, pp. 15-24, Feb. 1963.

Fenech, H., and Henry, J. J., "An Analysis of Thermal Contact Resistance," Transactions of the American Nuclear Society, Nov. 1962.

Fenech, H., "The Thermal Conductance of Metallic Surface in Contact," PH.D. Thesis, M.I.T., May 1959.

Fishenden, M., and Kepinsky, A., "Resistance to heat transfer in gap between two parallel surfaces in contact," Proceedings of the Seventh Congress on Applied Mechanics, Vol. 3, pp. 193-195, 1948.

Frank, I., "Transient Temperature Distribution in Aircraft Structures," J. Aero. Sci., Vol. 25, No. 4, p. 265-267, April 1958.

Fried, E., and Costello, F. A., "Interface Thermal Contact Resistance Problem in Space Vehicles," American Rocket Society Conference, Palm Springs, California, April 1961 (See also ARS Journal, Vol. 32, pp. 237-243, 1962).

Fried, E., "The Thermal Conductance of Space Vehicle Interfaces- Experimental Results," General Electric Report No. 61GL65, March 1961.

Fried, E., "Thermal Joint Conductance in a Vacuum," ASME Paper No. AHGT-18, Aviation and Space Hydraulic and Gas Turbine Conference, Los Angeles, California, March 1963.

Fried, E., "Study of Thermal Contact Conductance," Final Report NASA (M-RP-T) Contract NAS8-5207.

Gardner, K. A., and Carnavos, T. C., "Thermal Contact Resistance In Finned Tubing," ASME paper (preprint 59-A-135) presented annual meeting, Nov. - Dec. 1959.

Gatewood, B. E., "Effect of Thermal Resistance of Joints Upon Thermal Stresses," Air Force Institute of Technology report 56-6, May 1956, Defense Documentation Center Number AD106-014.

Gex, Robert C., "Thermal Resistance of Metal-To-Metal Contacts," An Annotated Bibliography Lockheed Special Bibliography Report SB-61-39, July 1961.

Graff, W. J., "Thermal Conductance Across Metal Joints," Machine Design, Vol. 32, pp. 166-172, 1960.

Griffith, George E., and Miltonberger, Georgene H., "Some Effects of Joint Conductivity on the Temperatures and Thermal Stresses in Aerodynamically Heated Skin Stiffener Combinations," NACA Technical Note 3699.

Held, Wolfgang, "Heat Transfer Between Worked Metal Surfaces," Allgemeine Warmetechnik, Vol. 8, No. 1, pp. 1-8 (1957) "Der Wärmeübergang Zwischen Bearbeiteten Oberflächen." Trans. RSIC-76.

Henry, J. J., and Fenech, H., "The Use of Analogue Computers for Determining Surface Parameters Required for Prediction of Thermal Contact Conductance," ASME paper 63-WA-104, 1963.

Henry, J. J., "The Thermal Resistance of Metals In Contact," M. S. Thesis, M. I. T., August 1961.

Henry, J. J., "Some Methods of Surface Analysis for the Prediction of Thermal Resistance of Metal Contacts," AEC Report NYO 9457, Nov. 1961.

Henry, J. J., "Thermal Conductance of Metallic Surfaces in Contact," AEC Report NYO-9459, Feb. 1963.

Hertz, Heinrich, "Study on the Contact of Elastic Solid Bodies," Journal Fur die Reine und Angewandte Mathematik, Vol 29, p. 156-171, 1882. SLA translations SLA-57-1164.

Holloway, G. F., "The Effect on an interface on the Transient Distribution in Composite Aircraft Joints," Syracuse University Thesis, 1954.

Holm, R., Electrical Contacts, Handbook, Springer Verlag, Berlin, 3rd Ed., 1958. Includes many references on electrical contact conductance and contact problem in general.

Horton, J. C., "Electrical Contacts in Vacuum," (A) Brushes, Status Report No. 2, Marshall Space Flight Center Report MTP-R&VE-M-63-17, December 28, 1962.

Iwaki, A., and Mori, M., "Distribution of Surface Roughness When Two Surfaces are Pressed Together," Journal of the Japanese Society of Mechanical Engineering, Vol. 1, pp. 229-337, 1958.

Jacobs, R. B., and Starr, C., "Thermal Conductance of Metallic Contacts," Rev. of Scientific Instruments, Vol. 10, pp. 140-141, 1939.

Jelinek, D., "Heat Transfer of Proposed Structural Joints in the Rocket Package for the F-86D Airplane," North American Aviation Lab Report No. NA-49-831, Sept. 30, 1949.

Kapinos, V. M., and Il'chenko, O. T., "Determining the Contact Thermal Resistance of Mixed Pairs," KHARKOV. POLITEKHNICHESKII INST. TRUDY. SERIYA METALLURGICHESKAIA, Vol. 5, p. 217-223, 1959.

Kapinos, V. M., and Il'chenko, O. T., "Thermal Resistance of a contact layer," KHARKOV. POLITEKHNICHESKII INST. TRUDY. SERIYA METALLURGICHESKAIA, Vol. 5, pp. 160-181, 1959.

Karush, W., "Temperature of Two Metals in Contact," Atomic Energy Commission Report AECD-2967, Dec. 22, 1944.

Kaszubineki, L. J., "Determination of the Number of Contacts Between Two Surfaces Pressed Together," M.S. Thesis, M.I.T., Aug. 1962.

Kondo, S., "Thermodynamical Fundamental Equation for a Spherical Interface," J. Chem. Phys., Vol. 25, p. 662-669, New York, Oct. 1956.

Kouwenhoven, W. B., Tampico, J., "Measurement of Contact Resistance," Paper Presented at Annual Meeting of American Welding Society, Cleveland, Ohio, October 21-25, 1940.

Kouwenhoven, W. B. and Potter, J. H., "Thermal Resistance of Metal Contacts," J. Am. Weld. Soc., Vol 27, Part 2, pp. 515-520, 1948.

Laming, L. C., "Thermal Conductance of Machined Metal Contacts," 1961 International Heat Transfer Conference, Part 1, No. 8, pp. 65-76, Boulder, Colorado, Sept. 1961.

Ling, F. F., "On Asperity Distribution of Metallic Surfaces," Journal of Applied Physics, Vol. 24, No. 8, Aug. 1958

Ling, F. F., and Lucek, R. C., "On Model Studies of Metallic Surface Asperities," Air Force Office of Special Research, Report AFOSR TN 58-1134, DDC Number AD208-083, Dec. 1958.

Ling, F. F., "A Quasi-Iterative Method of Computing Interface Temperature Distribution," Air Force Office of Scientific Research Report AFOSR TN 58-1004, Defense Documentation Center Number AD206-147, Oct. 1958.

Massachusetts Institute of Technology, Progress Report, "Description of Method for Determining Geometric Parameters of Surfaces in Contact," AEC Report NYO-9456, May 1961.

Massachusetts Institute of Technology, Progress Report, "Some Methods of Surface Analysis for the Prediction of Thermal Resistance of Metal Contacts," AEC Report NYO-9457, Nov. 1961.

Meissner, Hans, "Studies of Contacts with Barriers in Between," John Hopkins University Report, DDC Report AD 225-070, Sept. 1959.

Mikesell, R. P., and Scott, R. B., "Heat Conduction Through Insulating Supports in Very Low Temperature Equipment," Journal of Research of the National Bureau of Standards, Vol. 57, No. 6, pp. 371-378, Dec. 1956.

Miller, V. S., "Effective Method of Reducing Thermal Contact Resistance," INZHENERNO-FIZICHESKII ZHURNAL, Vol. 6, pp. 371-74, April 1963. Entire Journal Translated.

Miller, V. S., "Peculiarities of Control Heat Exchange Transfer in Fuel Elements of a Reactor," IZV. UYSSH. UCHEB. ZAV ENERGETIKA, pp. 67-70, No. 3, 1962. Translation available from OTS, AEC translation AEC-TR-5410. Also, NASA Translation, NASA TT F-8849.

Miller, V. S., "Problems Concerning Contact Heat Resistances of Heat Emitting Elements," ZBIR. PRATS INST. TEPL. AN URSR, Vol. 24, pp. 133-139, 1962.

Miller, V. S., "Results of Investigation of Conductive Heat Exchange Between Plane Metallic Surfaces," AKADEMIYA NAUK USSR, KIEV. INSTITUT TEPLOENERGETIKI ZBIRNY PRATS, Vol. 20, pp. 44-53, 1960.

Miller, V. S., "Determining Thermal Resistance of Conductive Heat Exchange Between Metal Ceramic Surfaces," AKADEMIYA NAUK USSR KIEV. INSTITUT TEPLOENERGETIKI. ZBIRNY PRATS, Vol. 20, pp. 54-59, 1960.

Mizushina, T., Iuchi, S., Sasano, T., and Tamurs, H., "Thermal Contact Resistance Between Mercury and a Metal Surface," Int. J. Heat Mass Transfer, Vol. 1, pp. 139-146, 1960

Moon, J. S., and Keeler, R. N., "A Theoretical Consideration of Asymmetric Heat Flow at the Interface of Two Dissimilar Metals," International Journ. of Heat and Mass Transfer, Vol. 5, pp. 967-971, October 1962.

Mori, M., and Iwaki, A., "Distribution of Surface Roughness When Two Surfaces are Pressed Together," Journal of JSME, Vol. 1, pp. 329-337, 1958.

Mueller-Hillebrand, D., "Surface Contacts Under High Load Forces," WISS. VEROEFF. SIEMENSWERKE, (Scientific Publications of Siemenswerke) Vol. 20, pp. 85-103, 1941.

Nishiwai, J., and Hagi, S., "Thermal Conduction in Technology," KIKAINO KENKYU (Research on Machinery), Vol. 2, No. 2, 1950-1953.

Petri, F. J., "An Experimental Investigation of Thermal Contact Resistance in a Vacuum," ASME Paper 63-WA-156.

Podstrieach, S., "Temperature Field in a System of Solids Coupled by Means of a Thin Intermediate Layer," INZHENERNO-FIZICHESKII ZHURNAL, Vol. 6, No. 10, pp. 129-136, Oct. 1963, Trans. RSIC-148.

Pohle, F., Lardner, T., French, F., "Temperature Distributions and Thermal Stresses in Structures with Contact Resistances," Polytechnic Institute of Brooklyn Report, PIBA1 557, Air Force Report AFDSR TN 60-504, DDC Report AD237-149.

Potter, J. H., "Thermal Resistance of Metallic Contacts," Dissertation, John Hopkins, University, 1948.

Powell, R. W., Tye, R. P., and Jolliffe, B. W., "Heat Transfer at the Interface of Dissimilar Materials: Evidence of Thermal Comparator Experiments," International Journal of Heat and Mass Transfer, Vol. 5, pp. 897-902, Oct. 1962.

Powell, R. W., "Experiments Using A Simple Thermal Comparator for Measurements of Thermal Conductivity, Surface Roughness and Thickness of Foils or of Surface Deposits," Journal of Scientific Instruments, Vol. 34, pp. 485-492, Great Britain, 1957.

Putnaerglis, R. A., "A Review of Literature on Heat Transfer Between Metals in Contact and by Means of Liquid Metals," Report No. R. 34, Department of Mechanical Engineering, McGill University, Montreal, 1953.

Rapier, A. C., Jones, T. M. and McIntosh, J. M., "The Thermal Conductance of Uranium Dioxide /Stainless Steel Interfaces," International Journal of Heat and Mass Transfer, Vol. 6, pp. 397-416, May 1963.

Roess, L. C., "Theory of Spreading Conductance," Appendix A of an unpublished report of the Beacon Laboratories of Texas Company, Beacon, New York.

Rogers, G. F. C., "Heat Transfer at the Interface of Dissimilar Metals," Int. J. Heat Mass Transfer, Vol. 2, pp. 150-154, 1961.

Sanderson, P. D., "Heat Transfer From the Uranium Rods to the Magnox in a Gas Cooled Reactor," International Developments in Heat Transfer, ASME, 1961.

Sanokama, Konomo, "Thermal Contact Resistance," (Survey), Journal of JSME, Vol. 64, No. 505, 1961.

Schmidt, E. H. W., and Jung, E., "Measurement of the Thermal Contact Resistance from Stainless Steel to Liquid Sodium," Modern Developments in Heat Transfer, pp. 251-263, Academic Press, New York, 1963.

Schaaf, S. A., "On the Superposition of a Heat Source and Contact Resistance." Quart. Appl. Math., Vol. 5, pp. 107-111, April 1947.

Seide, P., "On One Dimensional Temperature Distribution in Two-Layered Slabs with Contact Resistances at the Plane of Contact," J. Aero/Space Sci., Vol. 25, No. 8, p. 523-524, Aug. 1958

Shlykov, IU. P., and Ganin, E. A., "Thermal Resistance of a Contact," Atom. Energie, Vol. 9, No. 6, pp. 496-498, Dec. 1960. Translation Available.

Shlykov, IU. P., Ganin, E. A., and Demkin, N. B., "Investigation of Contact Heat Exchange," (With Summary in English), TEPLOENERGETIKA, Vol. 7, No. 6, pp. 72-76, Je'60, Redstone Arsenal Translation RSIC-117.

Shlykov, IU. P., and Ganin, E. A., "Experimental Study of Contact Heat Exchange," TEPLOENERGETIKA, Vol. 8, No. 7, pp. 73-76, July 1961. Redstone Arsenal Translation RSIC-128.

Shteinberg, V. M., "New Method For Calculating a Non-Steady State Temperature Field for a Semi-Infinite Inhomogeneous Complex of Bodies in Mutual Thermal Contact," Conference on Heat and Mass Transfer, "MINSK, Jan. 23-27, 1961. (Micro Film).

Shvetsova, E. M., "Determination of Actual Contact Areas of Surfaces By Means of Transparent Models," AKADEMLIA NAUK SSSR, INSTITUT MASHINOVEDENIA, SBORNIK IZNOS V. MASHINAKH, Vol. 7, pp. 12-33, 1953, Being Translated.

Skipper, R. S. G., and Wooton, K. J., "Thermal Resistance Between Uranium and Can," International Conference on Peaceful Uses of Atomic Energy, Proceedings, Vol. 7, pp. 684-690, 1958.



Stoyukhin, B. P., "Instantaneous Temperature at Contact Surfaces Caused by Friction," NAUCH. DOKL. VYS. SHKOLY; MASH. i. PRIB. No. 4, pp. 73-81, 1958. Translation RSIC-142.

Stubstad, W. R., "Measurements of Thermal Contact Conductance in Vacuum," ASME Paper 63-WA-150.

Swann, W. F. G., "Theory of the A. J. Jaffe Method for Rapid Measurement of the Thermal Conductivity of solids," J. Franklin Inst. Vol. 267, No. 5, pp. 363-380, May 1959.

Swann, W. F. G., "Concerning Thermal Junction Resistances in the A. F. Jaffe Method for Measurement of Thermal Conductivity," J. Franklin Inst., V. 268, No. 4, pp. 294-296, Oct. 1959.

Tachibana, F., "Study of Thermal Resistances of Contact Surfaces," Redstone Scientific Information Center Translation RSIC-29, Redstone Arsenal, Alabama. Translated from NIHON KIKAI GAKUKAI SHI, Vol. 55, No. 397, 1952.

Tampico, J., "Measurement of Contact Resistance," Dissertation at Johns Hopkins University, 1941.

Tarasun, L. P., "Relation of Surface-Roughness Readings to Actual Surface Profile," Trans. ASME, Vol. 67, No. 3, April 1945.

"Thermo-Mechanical Analysis of Structural Joint Study," Wright-Patterson Air Force Base Report, WADD IR 61-5, Jan. 1962.

Vernottle, P., "Extension of Fourier's Method to Composite Systems with Resistances to Heat Flow Between Certain Regions," C. R. ACAD. SCI., Vol. 224, pp. 1416-1418, Paris, France, May 19, 1947.

Walther, J. D., "A Study of Transient Thermal Contact Conductance," Masters Thesis Southern Methodist University, School of Engineering, Dallas, Texas. ASTIA No. AD 297-995.

Ward, A. L., "Dependence of Metal-To-Semiconductor Contact Resistance Upon Control Loading," Diamond Ordnance Fuze Laboratory Report TR-731, DDC Report AD 228-744, July 30, 1959.

Weills, N. D., and Ryder, E. A., "Thermal Resistance Measurements of Joints Formed Between Stationary Metal Surfaces," Trans. ASME, Vol. 71, pp. 259-267, 1949.

Wheeler, R. G., "Thermal Conductance of Fuel Element Materials," AEC Report No. HW-60343, 1959.

Wheeler, R. G., "Thermal Contact Conductance," AEC Report No. HW-53598, November 1957.

Wickens, G. W., (Translator), "The Thermal Conductance of Cemented Lap Joints Between AU4G1 Sheets," (Conductance Thermique Des Liaison De Toles D'AU4G1 Collees) Sud-Aviation Test Report No. C. R. 72-003-51, March 1959, Royal Aircraft Establishment, Farnborough, England, Library Translation No. 952, July 1961. ASTIA File Copy AD 262-823.

Wickens, G. W., (Translator), "Thermal Conductance of Lap Joints Between AU4G1 Sheets," (Conductance Thermique Des Liaisons De Toles D'AU4G1), Sud-Aviation Test Report C. R. 72-003-50, Dec. 1957, Royal Aircraft Establishment, Farnborough, England, Library Translations No. 949, June 1961. ASTIA File Copy AD 262-578.

Williams, A., "Comment on Rogers' Paper Heat Transfer at the Interface of Dissimilar Metals," Int. J. Heat Mass Transfer, Vol. 3, p. 159, 1961.

## Additional References

Dugeon, E. H. and Prior, "The Contact Thermal Conductance of Aluminum Sheathed Tubes," National Research Council of Canada, Report MT-24, October 25, 1954.

Dugeon, E. H. and Prior, "The Contact Thermal Conductance of an Aluminum Sheathed Nickel or Tin Plated Uranium Rod, National Research Council of Canada, Report MT-29, September 26, 1955.

Dyban, Kondak, Shvets, "Investigation of Contact Heat Exchange Between Machine Parts," IZV. AKAD. NAUK, USSR ORD. TEKH. NAUK., Vol. 9, pp. 63-79, September 1954. Translation IGRL-T/W-12.

Dyban, E. P. and Shevets, I. T., "Air Cooling of Gas Turbine Rotors," Chapter 10, "Contact Heat Exchange in Turbine Ports," pp. 191-233, IZDATEI'STVO KIEVSKOGO UNIVERSITETA KIEV, 1959, Translation-Technical Documents Liaison Office. MCL-1406/1+2+3+4, July 18, 1962. DDC Copy No. AD-281-848.

Jansson, R. M., "The Heat Transfer Properties of Structural Elements for Space Instruments," M. I. T. Instrumentation Laboratory Reports, E-1173, June 1964.

Kapinos, V. M. and Ilchenko, "Thermal Resistance of Turbine Blade Base Joints," Energomashinostroenie, 5, No. 6, p. 23-26, June 1959.

Kapinos, V. M. and Ilchenko, Title Unknown, (Izvestiya Uysshikh Uchebnykh Zavedenii), Higher Education Information Establishment, Energotika, No. 9, 1958.

Powell, R. W., "The Place of Heat Conduction in the Theory, Practice and Testing of Bonds," Applied Materials Research, 1, 3, pp. 166-169, October 1962.

Ross, A. M. and Stoute, R. L., "Heat Transfer Coefficients Between  $UO_2$  and Zircaloy 2, Report CRFD 1075, Atomic Energy Commission of Canada Limited, 1962.

Shylkov, IU. P., Ganin, E. A., "Heat Exchange by Contact: Heat Transfer Between Contiguous Metal Surfaces," Moskva Gosenergoi Adat, 144 pages, 1963.

Shvets, I. T., "Study of Contact Heat Exchange Between Heat Engine Parts," Proc. of Institute of Power Engineering of AS UKSSSR, No. 12, 1955.

TABLE I

Sample Number	Material	Surface Finish				Hardness Rockwell B	Maximum Flatness Deviation		Remarks
		(RMS)		CLA			micro-meter	10-3 Inches	
		micro-meter	micro-inch	micro-meter	micro-inch				
1	Stainless Steel 304	0.38	15-15	0.38	16-18	B-80	-1.3	-0.05	Ground Finish
2	Stainless Steel 304	0.25	10-10	0.25	6-14	B-80	----	----	Ground Finish
3	Stainless Steel 304	1.3	42-60	1.0	21-60	B-80	-1.3	-0.05	Ground Finish
4	Stainless Steel 304	1.1	43-48	0.63	13-37	B-81	+2.5	+ 0.1	Ground Finish
5&6	Not Tested.								
7	AZ-31B Magnesium	0.30	8-15	0.38	12-17	E-63	-1.3	-0.05	Lathe Cut Finish
8	AZ-31B Magnesium	0.30	8-16	0.43	18-20	E-61	-7.6	-0.3	Lathe Cut Finish
9	AZ-31B Magnesium	1.4	50-50	1.4	50-60	E-62	-5.1	-0.2	Lathe Cut Finish
10	AZ-31B Magnesium	1.4	50-60	1.6	58-68	E-62	-3.8	-0.15	Lathe Cut Finish
11&12	Not Tested.								Lathe cut finish Center, 2 mm dia. depressed
13	6061-T6 Aluminum	0.30	8-16	0.29	11-12	F-88	----	----	
14	6061-T6 Aluminum	0.30	8-16	0.51	20-20	F-87	-1.3	-0.05	Lathe Cut Finish
15	6061-T6 Aluminum	1.4	50-60	0.91	33-38	F-93	+6.4	+0.25	Lathe Cut Finish
16	6061-T6 Aluminum	1.4	50-60	1.4	50-58	F-93	+2.5	+0.1	Lathe Cut Finish
17-24	Not Tested.								
25	Oxygen Free High Cond. Copper	0.20	7-9	0.30	12-12	B-48	+6.4	+0.25	Lathe Cut Finish
26	Oxygen Free High Cond. Copper	0.20	7-9	0.42	16-17	B-48	+1.3	+0.05	Lathe Cut Finish
27	ARMCO Iron		No Test Interface						

TABLE II

Test Run (No.)	Sample Numbers	Material	Interface Temperatures		Pressure (Kilo-Newton/m <sup>2</sup> )	Pressure (PSI)	h <sub>c</sub> (Watts/m <sup>2</sup> -°C)	h <sub>c</sub> (BTU/Hr-Ft <sup>2</sup> -°F)
			T <sub>1</sub> (°C)	T <sub>2</sub> (°C)				
1	3 & 4	304-SS	19.3	29.3	66	9	210	37
2	3 & 4	304-SS	19.5	27.2	220	32	284	50
3	3 & 4	304-SS	21.2	26.6	1164	169	471	83
4	3 & 4	304-SS	22.0	25.9	2225	323	698	123
5	3 & 4	304-SS	22.9	24.6	5973	867	1704	300
6	3 & 4	304-SS	23.0	24.4	7696	1117	2118	373
7	3 & 4	304-SS	22.8	24.9	4795	696	1369	241
8	3 & 4	304-SS	23.2	25.2	4699	682	1448	255
9	3 & 4	304-SS	22.0	25.4	2611	379	829	146
10	3 & 4	304-SS	20.2	27.6	778	113	312	55
11	3 & 4	304-SS	20.2	29.2	220	32	244	43
12	1 & 2	304-SS	26.4	31.4	55	8	318	56
13	1 & 2	304-SS	22.8	25.9	320	32	523	92
14	1 & 2	304-SS	25.6	27.5	1096	159	1312	231
15	1 & 2	304-SS	25.4	26.1	2192	318	3652	643
16	1 & 2	304-SS	—	—	4960	720	8174	1439
17	1 & 2	304-SS	—	—	7517	1091	11418	2010
18	1 & 2	304-SS	—	—	3259	473	6526	1149
19	1 & 2	304-SS	25.9	27.3	1184	172	1755	309
20	1 & 2	304-SS	29.0	33.3	219	32	545	96
21	1 & 2	304-SS	32.8	33.3	4112	597	7474	1316
22	1 & 2	304-SS	32.8	33.2	6304	915	9497	1672
23	13 & 14	6061-T6 Al.	25.7	32.0	70	10	1556	274
24	13 & 14	6061-T6 Al.	16.2	20.0	313	45	3184	557
25	13 & 14	6061-T6 Al.	24.4	27.1	1123	163	4466	776
26	13 & 14	6061-T6 Al.	24.8	27.1	2191	318	5419	954
27	13 & 14	6061-T6 Al.	24.0	25.2	5206	756	15773	2777
28	13 & 14	6061-T6 Al.	32.0	32.7	7696	1117	32314	5689
29	13 & 14	6061-T6 Al.	31.7	32.9	5649	820	20408	3593
30	13 & 14	6061-T6 Al.	31.4	33.7	3761	546	10235	1802
31	13 & 14	6061-T6 Al.	31.6	35.5	2886	419	6065	1066
32	9 & 10	AZ-31B Mag	28.3	37.5	110	16	3666	661
33	9 & 10	AZ-31B Mag	29.4	32.5	220	32	6061	891
34	9 & 10	AZ-31B Mag	28.6	29.9	1195	173	10979	1933
35	9 & 10	AZ-31B Mag	35.2	36.1	2280	331	20607	3628
36	9 & 10	AZ-31B Mag	38.7	39.3	5133	745	34171	6016
37	9 & 10	AZ-31B Mag	43.0	43.7	7696	1117	38596	6795
38	9 & 10	AZ-31B Mag	43.4	44.1	5801	843	35375	6228
39	9 & 10	AZ-31B Mag	42.8	43.5	3582	520	32535	5728
40	9 & 10	AZ-31B Mag	43.3	45.9	627	91	9014	1587
41	25 & 26	Copper	45.7	52.4	65	9	6708	1181
42	25 & 26	Copper	45.5	51.5	220	32	7446	1311
43	25 & 26	Copper	45.2	50.1	1095	159	9279	1632
44	25 & 26	Copper	45.2	50.7	2280	331	10099	1778
45	25 & 26	Copper	44.1	47.7	5560	807	12507	2202
46	25 & 26	Copper	44.3	47.4	7696	1117	14171	2495
47	25 & 26	Copper	44.5	48.3	4285	622	11700	2060
48	25 & 26	Copper	44.2	48.2	3424	497	10990	1935
49	25 & 26	Copper	44.2	49.6	658	95	8270	1456
50	25 & 26	Copper	44.2	49.6	394	57	8201	1444
51	7 & 8	AZ-31 Mag	30.6	44.3	65	9	1073	189
52	7 & 8	AZ-31 Mag	31.7	39.2	219	31	1968	350
53	7 & 8	AZ-31 Mag	30.1	33.8	1096	159	4066	716
54	7 & 8	AZ-31 Mag	41.3	44.3	2116	307	7304	1286
55	7 & 8	AZ-31 Mag	41.5	42.9	5461	792	15069	2653
56	7 & 8	AZ-31 Mag	41.8	42.7	7785	1130	27451	4833
57	7 & 8	AZ-31 Mag	45.5	47.3	4112	596	13722	2416
58	7 & 8	AZ-31 Mag	41.8	45.8	1095	159	5492	967
59	7 & 8	AZ-31 Mag	41.7	42.7	7696	1117	21987	3871
60	—	Armco Iron	—	—	—	—	—	—
61	15 & 16	Al. 6061-T6	32.3	45.1	131	19	1999	352
62	15 & 16	Al. 6061-T6	32.5	39.9	219	31	3431	605
63	15 & 16	Al. 6061-T6	39.5	45.6	1095	159	5282	930
64	15 & 16	Al. 6061-T6	39.9	43.9	2193	318	8071	1421
65	15 & 16	Al. 6061-T6	47.6	49.8	5465	793	17244	3036
66	15 & 16	Al. 6061-T6	47.7	49.0	7873	1142	28712	5055
67	15 & 16	Al. 6061-T6	47.9	50.4	4375	635	15040	2649
68	15 & 16	Al. 6061-T6	48.2	51.2	3340	484	12575	2215
69	15 & 16	Al. 6061-T6	41.1	49.4	658	95	3680	648

TABLE II  
DEFORMED AREA AND HEIGHT OF  
MODELS AS A FUNCTION OF APPLIED LOAD

Model	Load		Area		Height	
	kilonewtons	kilopounds	meters <sup>2</sup> x 10 <sup>30</sup>	Inches	millimeters	inches
All Models	0	0	0	0	12.700	.500
Cone	.445	.100	.107	.002	12.421	.489
Cone	1.335	.300	.324	.005	12.294	.484
Cone	2.224	.500	.636	.010	12.065	.475
Ellipse	2.224	.500	1.140	.018	12.598	.496
Hemisphere	2.224	.500	1.265	.020	12.624	.497
Cone	3.559	.800	1.140	.018	11.938	.470
Cone	5.338	1.200	1.534	.024	11.735	.462
Cone	6.672	1.500	2.027	.031	11.582	.456
Ellipse	6.672	1.500	2.634	.041	12.497	.492
Cone	8.896	2.000	2.588	.040	11.481	.452
Hemisphere	8.896	2.00	3.426	.053	12.497	.492
Ellipse	11.121	2.500	3.973	.062	12.370	.487
Cone	13.345	3.00	3.694	.057	11.024	.434
Ellipse	15.569	3.500	5.451	.084	12.319	.485
Cone	17.793	4.000	4.560	.071	10.693	.421
Hemisphere	17.793	4.000	6.936	.108	12.319	.485
Ellipse	22.241	5.000	7.946	.123	12.090	.476
Hemisphere	26.689	6.000	9.813	.152	12.167	.479
Cone	31.138	7.000	7.240	.112	10.033	.395
Ellipse	33.362	7.500	12.067	.187	11.862	.467

TABLE III  
(cont.)

Model	Load		Area		Height	
	kilonewtons	kilopounds	meters <sup>2</sup> x 10 <sup>-5</sup>	inches	millimeters	inches
Cone	44.482	10.000	9.810	.152	9.601	.378
Ellipse	44.482	10.000	14.234	.221	11.557	.455
Hemisphere	44.482	10.000	15.329	.238	11.887	.468
Ellipse	55.603	12.500	18.241	.283	11.252	.443
Cone	66.723	15.000	15.328	.238	8.560	.337
Ellipse	66.723	15.000	23.430	.363	10.922	.430
Cone	88.964	20.000	23.155	.369	7.595	.299
Ellipse	88.964	20.000	28.199	.437	10.135	.399
Hemisphere	88.964	20.000	31.142	.483	11.125	.438
Cone	111.206	25.000	34.071	.528	6.731	.265
Ellipse	111.206	25.000	37.826	.586	9.347	.368
Hemisphere	111.206	25.000	40.677	.631	10.643	.419
Cone	133.447	30.000	42.888	.665	6.020	.237
Ellipse	133.447	30.000	47.480	.736	8.458	.333
Hemisphere	133.447	30.000	48.071	.745	10.109	.398
Cone	155.688	35.000	54.806	.849	5.385	.212
Ellipse	155.688	35.000	59.981	.930	7.595	.299
Hemisphere	155.688	35.000	58.013	.899	9.550	.376
Ellipse	177.928	40.000	70.077	1.086	6.756	.266
Hemisphere	177.928	40.000	67.477	1.046	8.992	.354
Hemisphere	200.170	45.000	78.413	1.215	8.433	.332
Hemisphere	222.411	50.000	90.174	1.400	7.976	.314
Hemisphere	266.893	60.000	123.948	1.921	7.163	.282



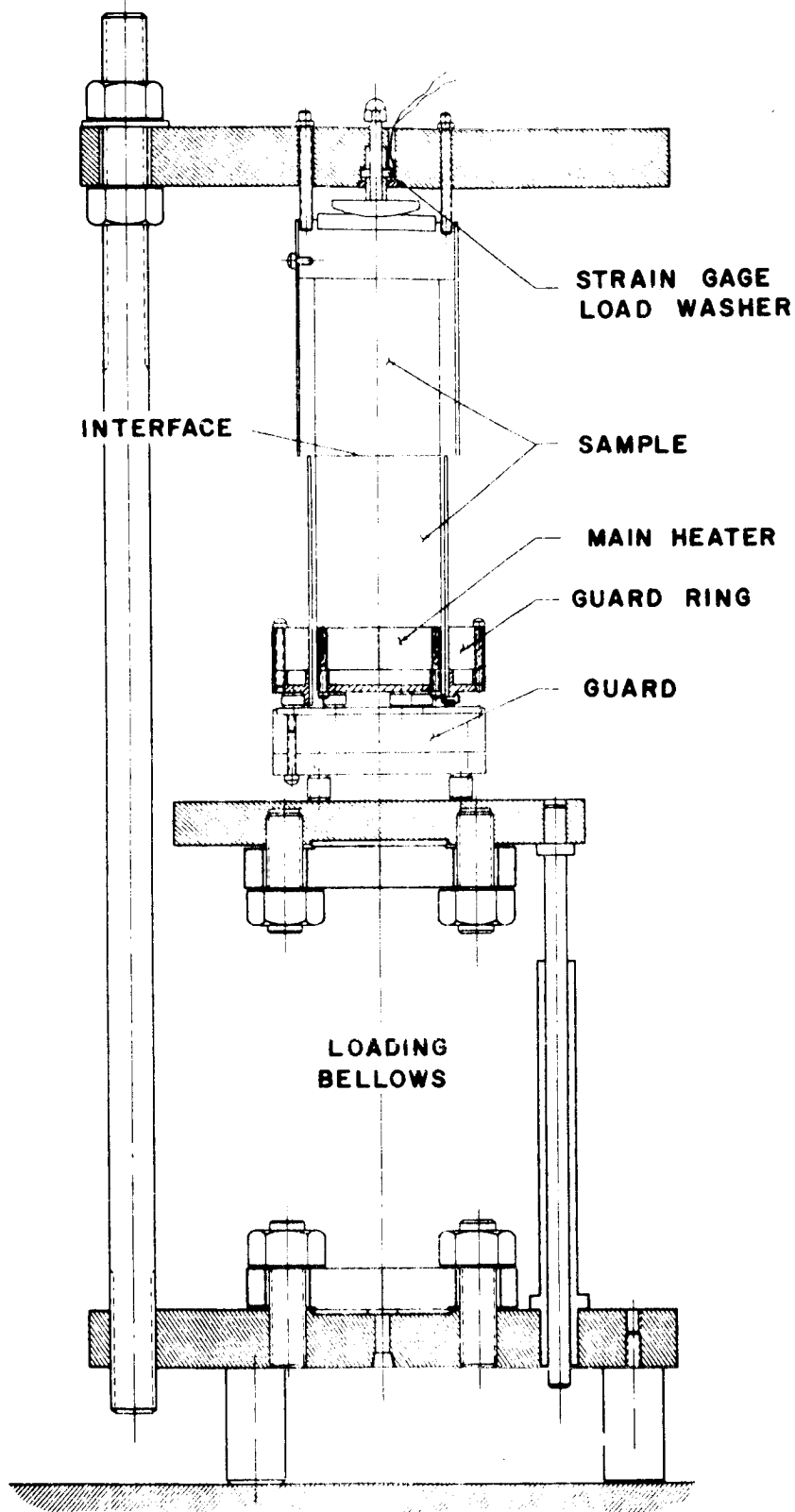


**FIGURE 1. VARIABLE PRESSURE - THERMAL INTERFACE  
CONDUCTANCE APPARATUS**

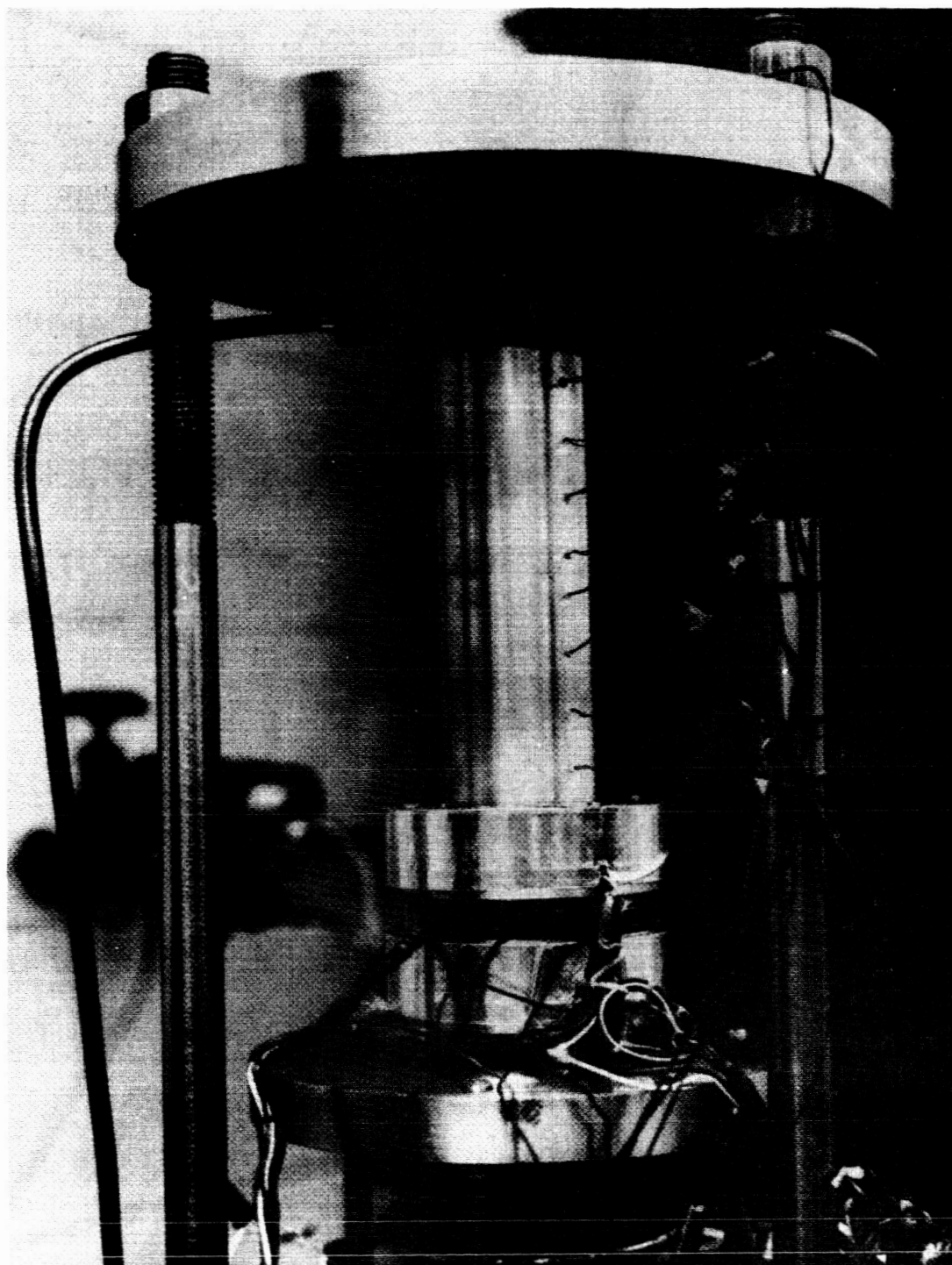


Fig. 2 THERMAL CONDUCTANCE APPARATUS WITH SAMPLE

## REPRESENTATIVE TEMPERATURE GRADIENT

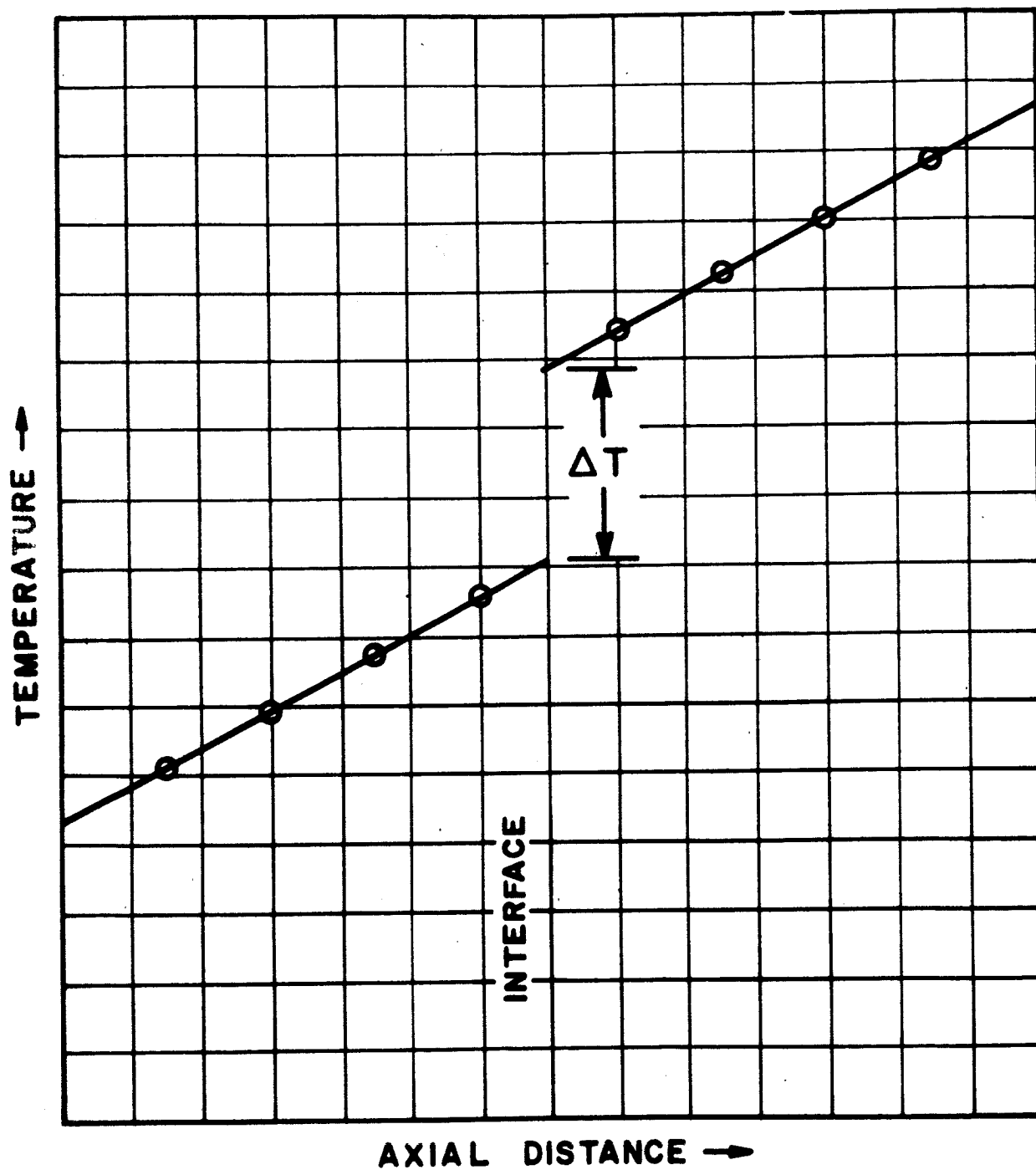
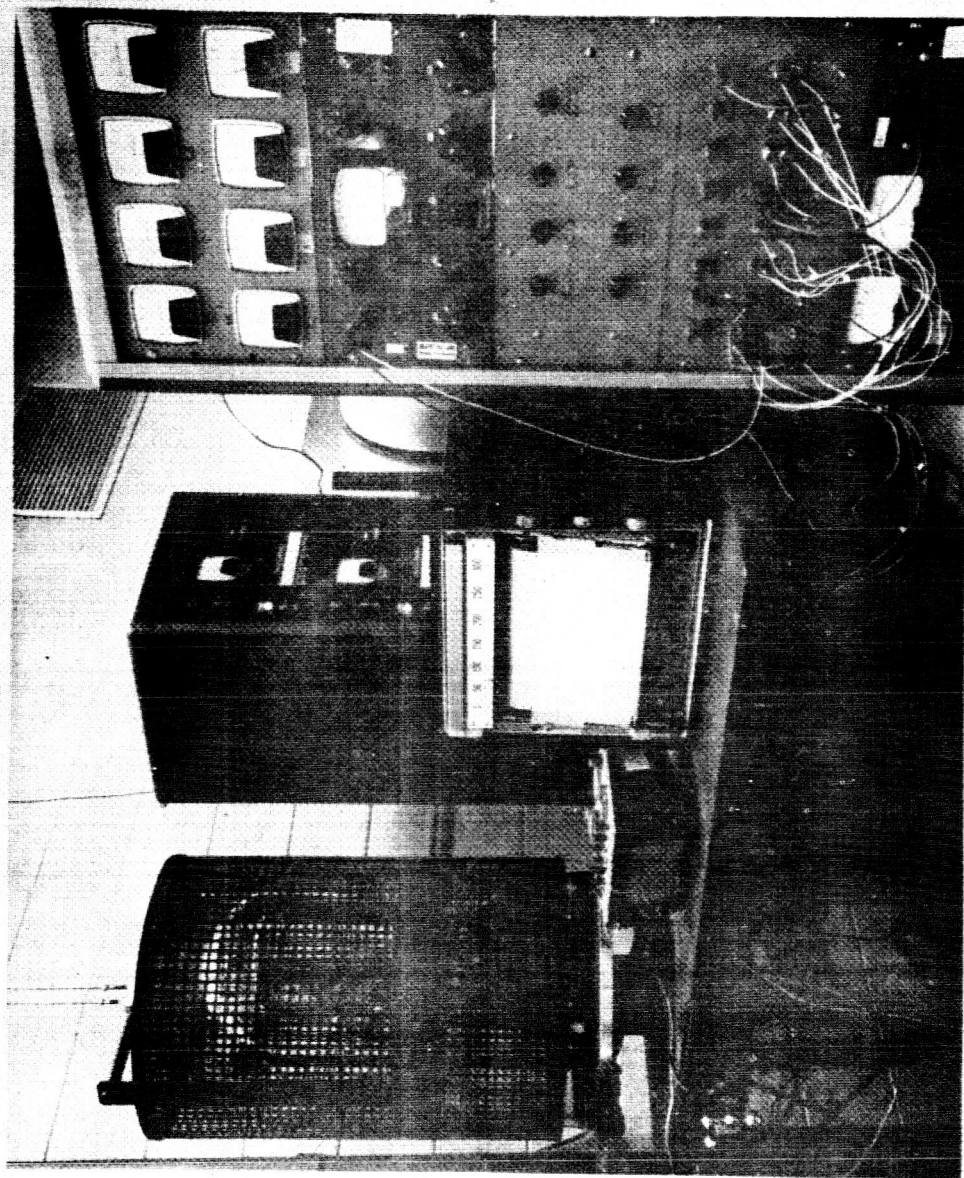


Fig. 3

**TEST APPARATUS AND ASSOCIATED EQUIPMENT**



**Fig. 4**

"TALYSURF" TRACE FOR COPPER SPECIMEN TAKEN THROUGH CENTER

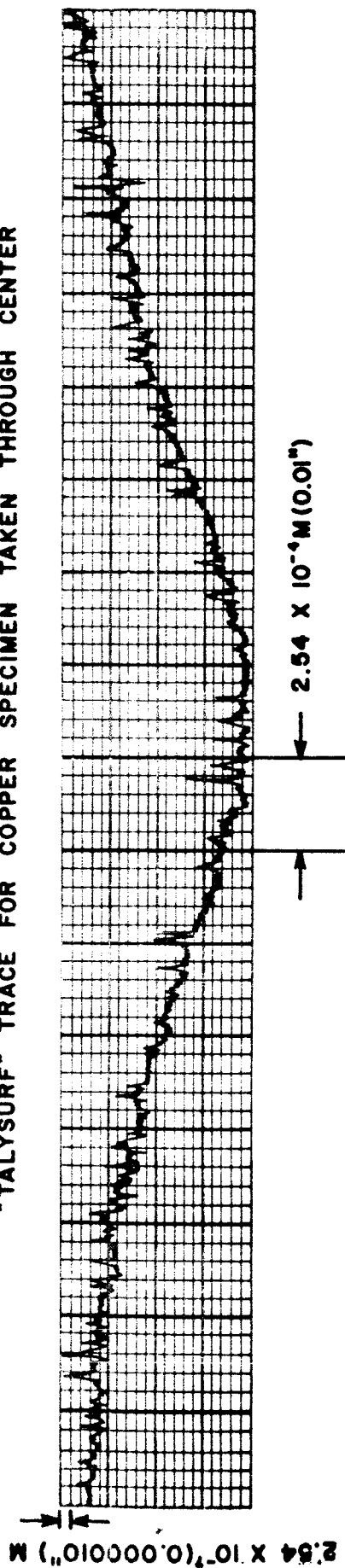


Fig. 5

# THERMAL CONTACT CONDUCTANCE VS. APPLIED PRESSURE

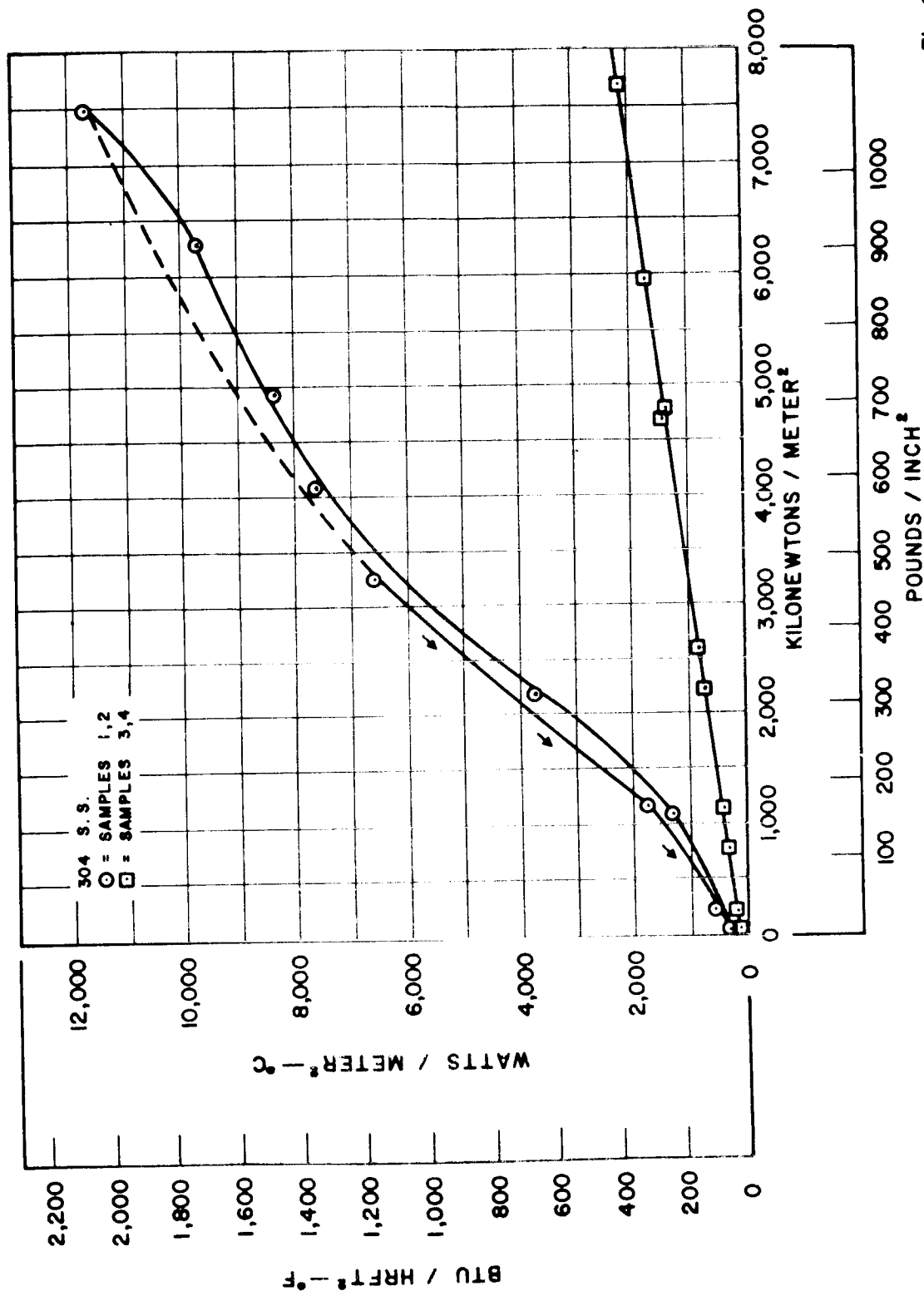


Fig. 6

# THERMAL CONTACT CONDUCTANCE VS. APPLIED PRESSURE

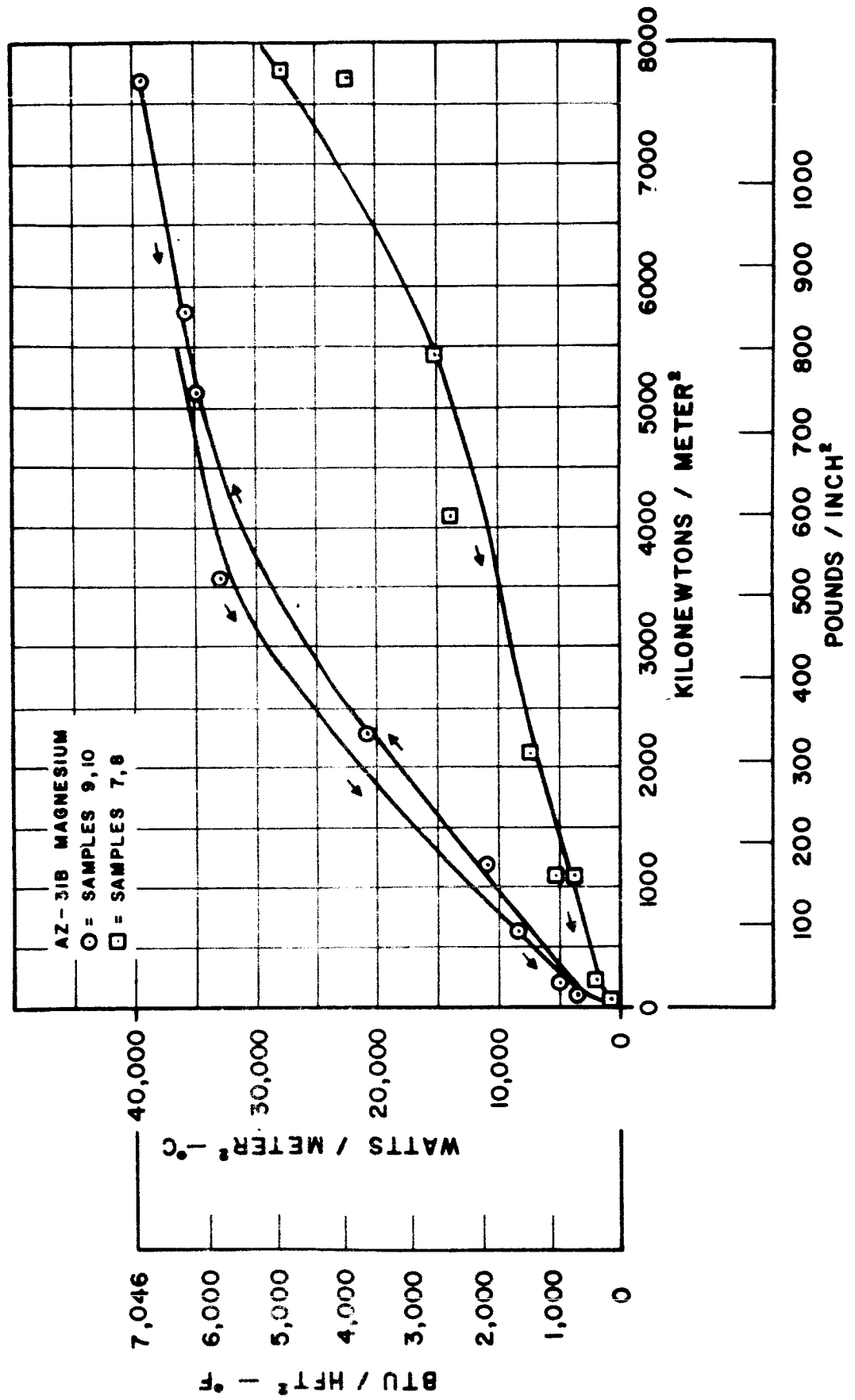


Fig. 7

# THERMAL CONTACT CONDUCTANCE VS. APPLIED PRESSURE

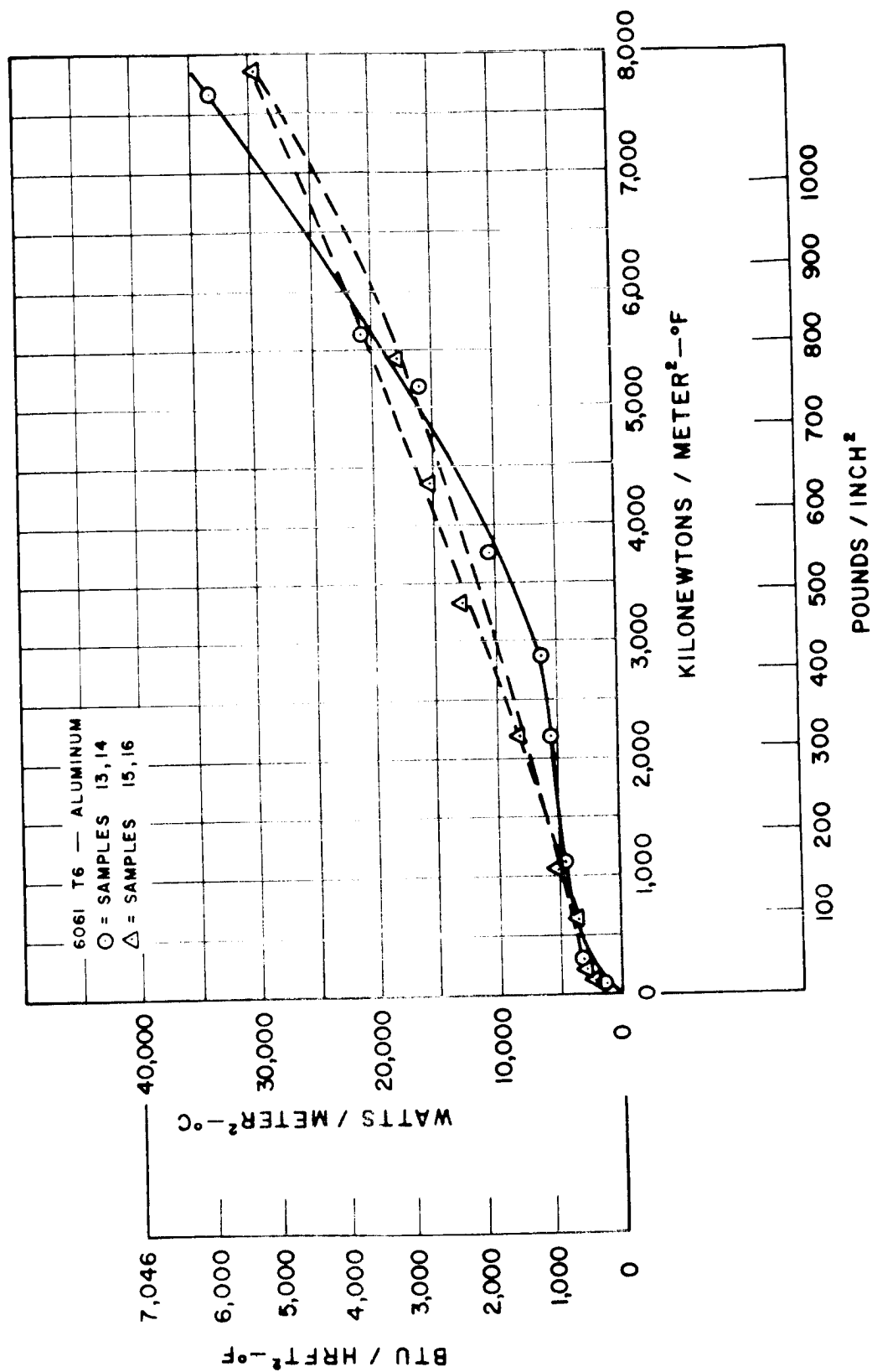


Fig. 8



# THERMAL CONTACT CONDUCTANCE VS. APPLIED PRESSURE

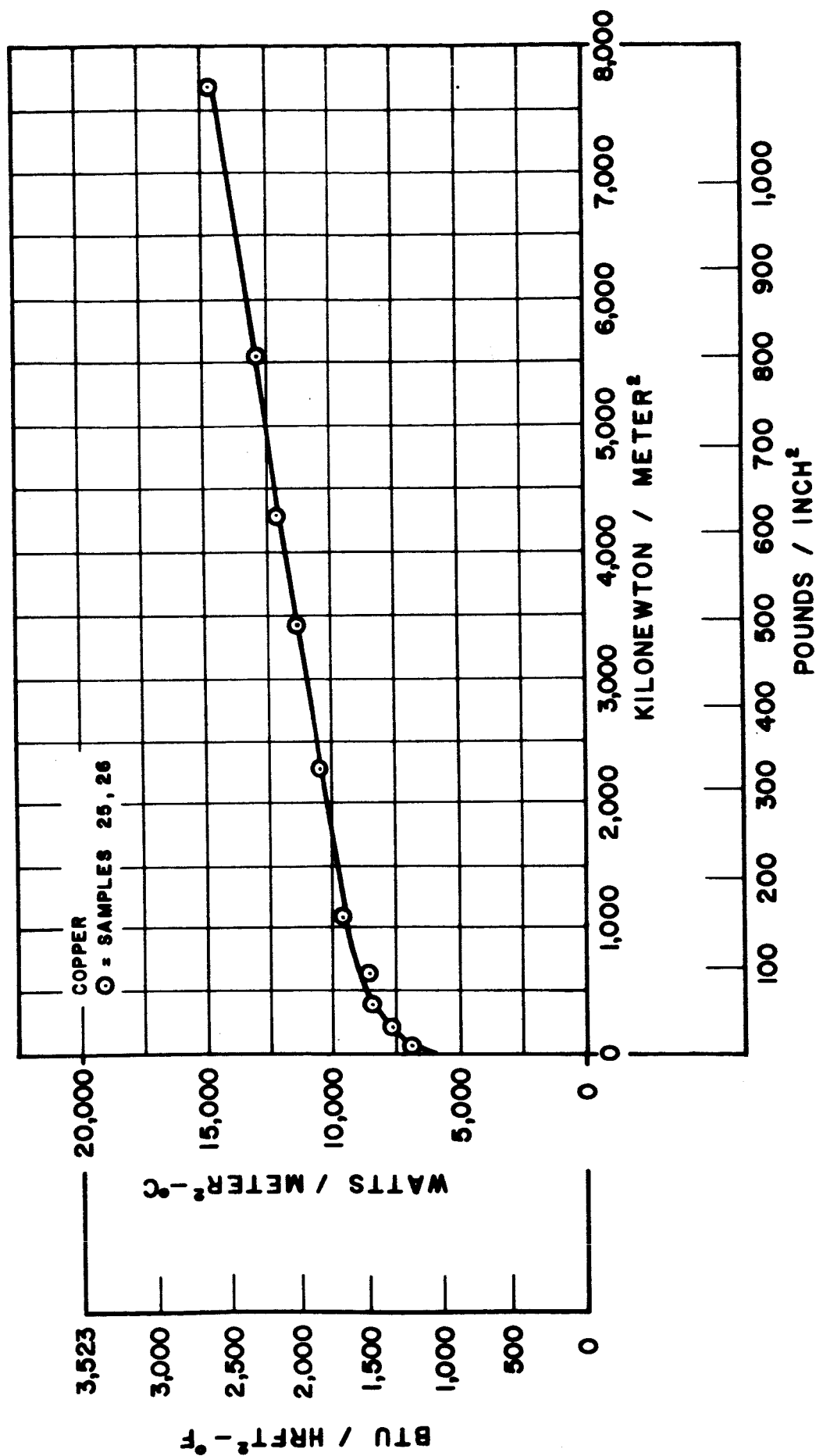


Fig. 9

## DEFORMATION MODELS

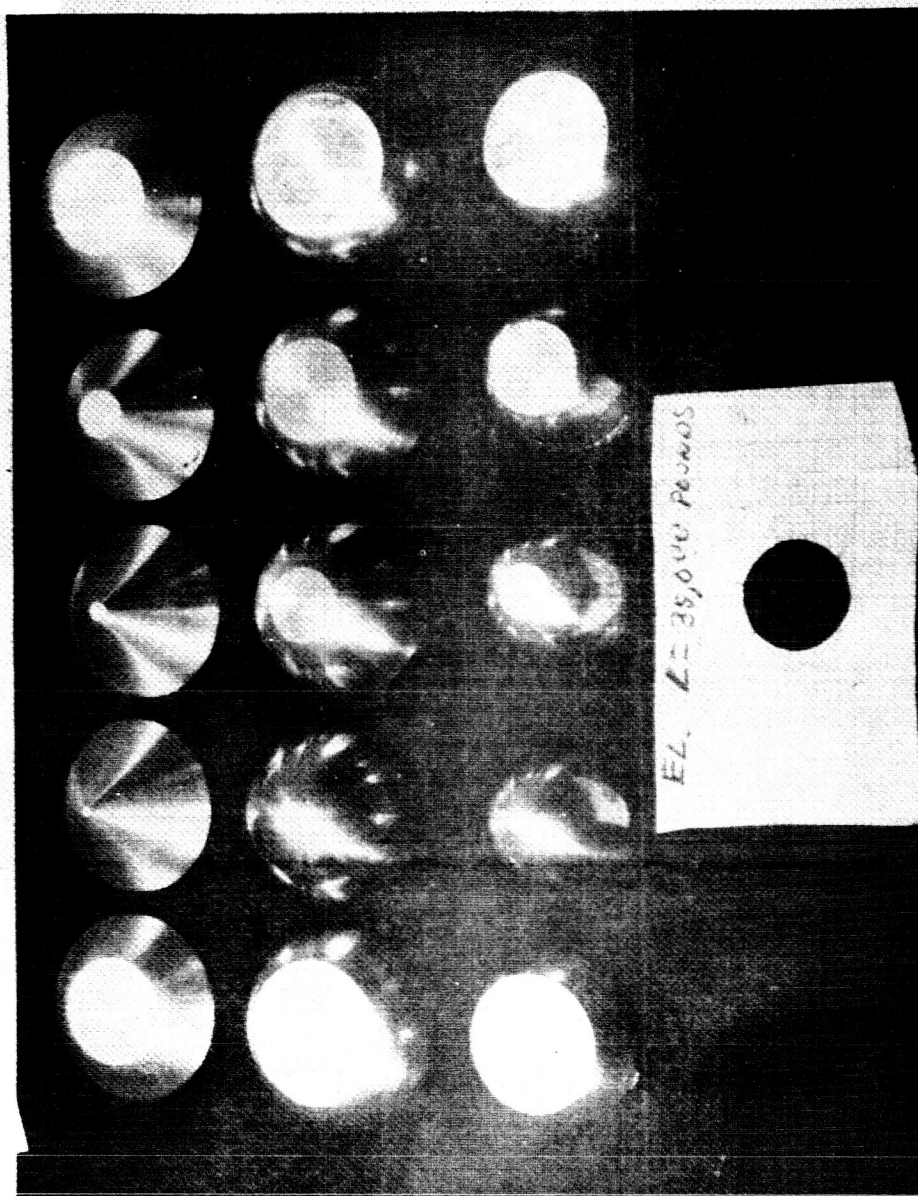


Fig. 10

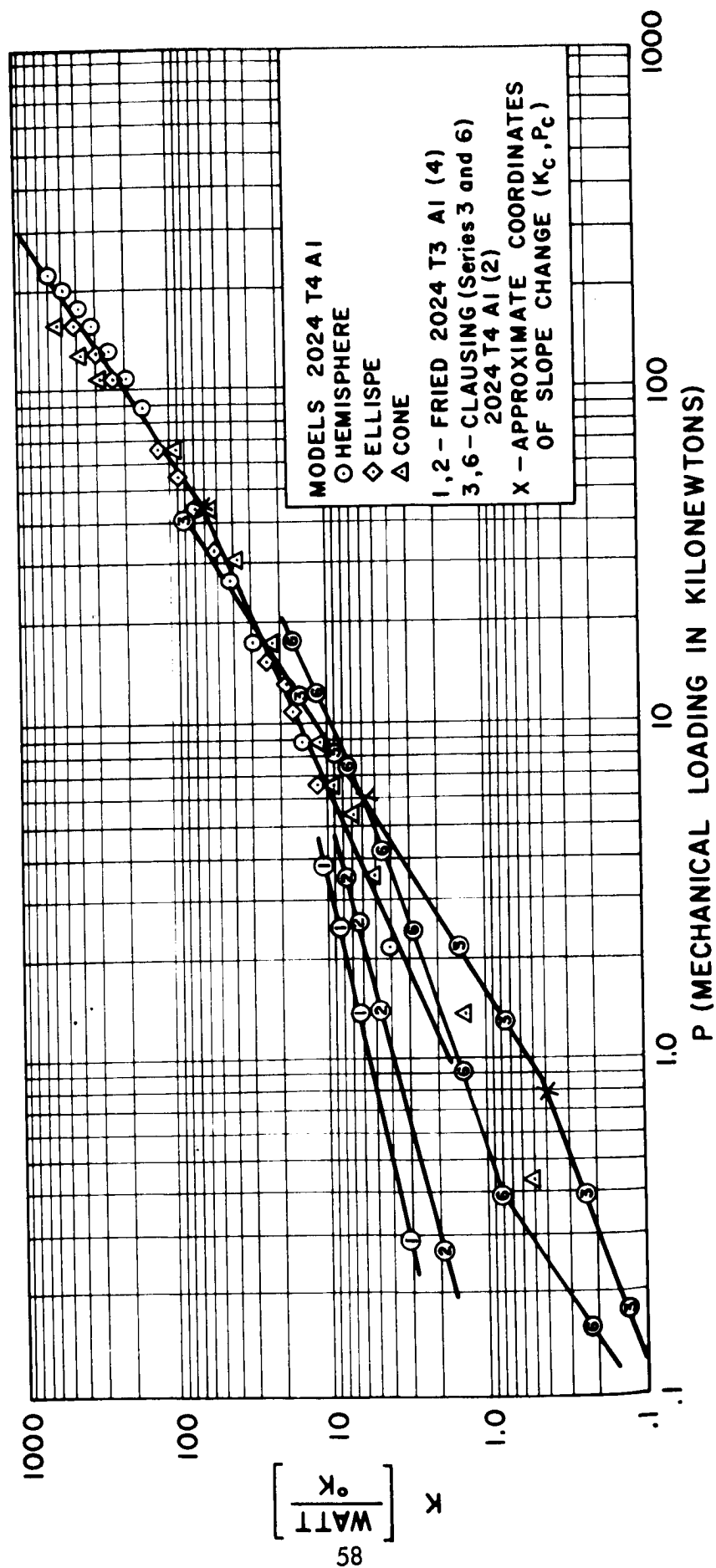


Fig. II COMPARISON OF SLOPE CHANGE OF THERMAL  
 INTERFACE CONDUCTANCE DATA AND MODELS

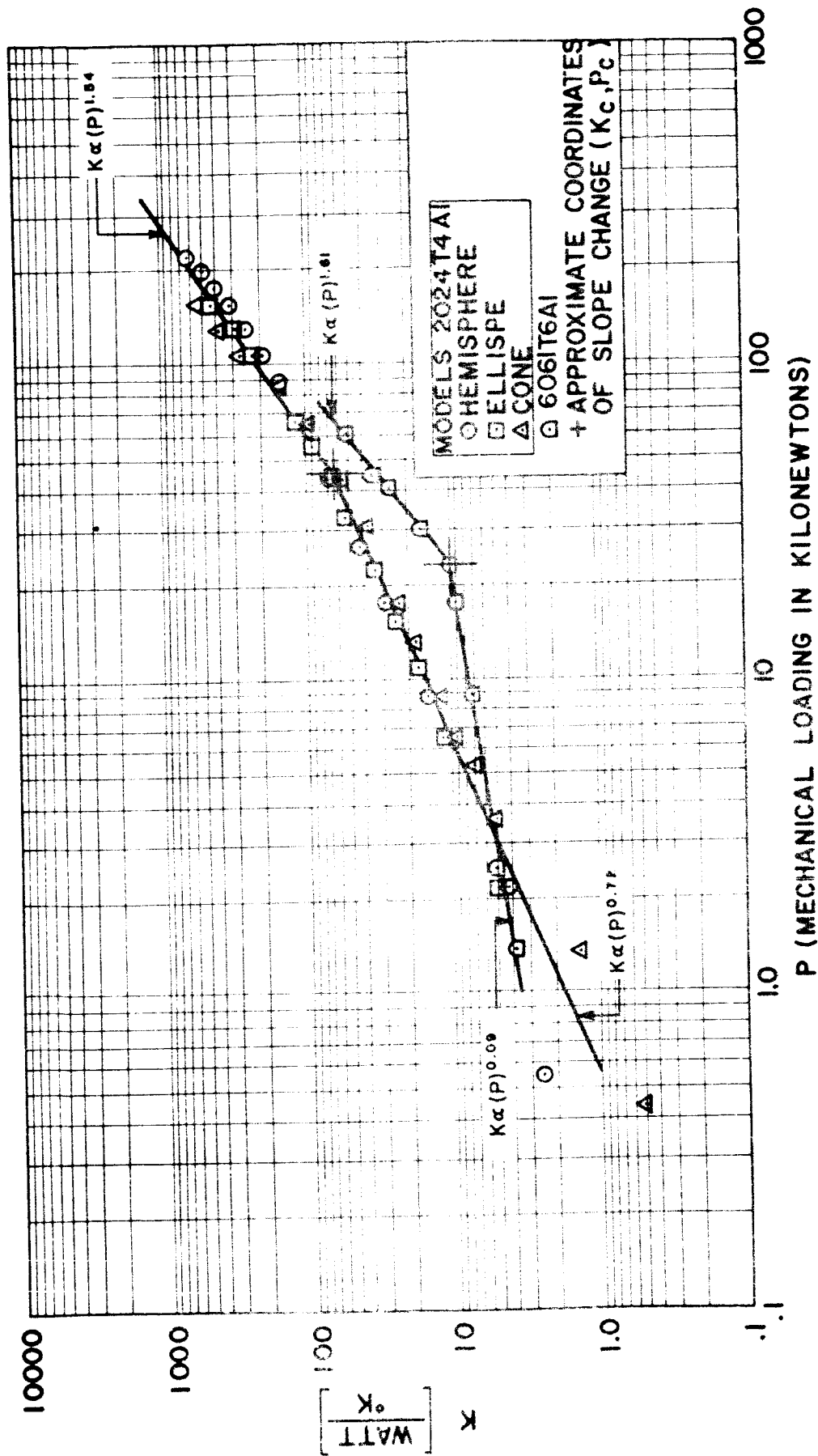


Fig. 12 COMPARISON OF SLOPE CHANGE OF THERMAL INTERFACE CONDUCTANCE DATA AND MODELS

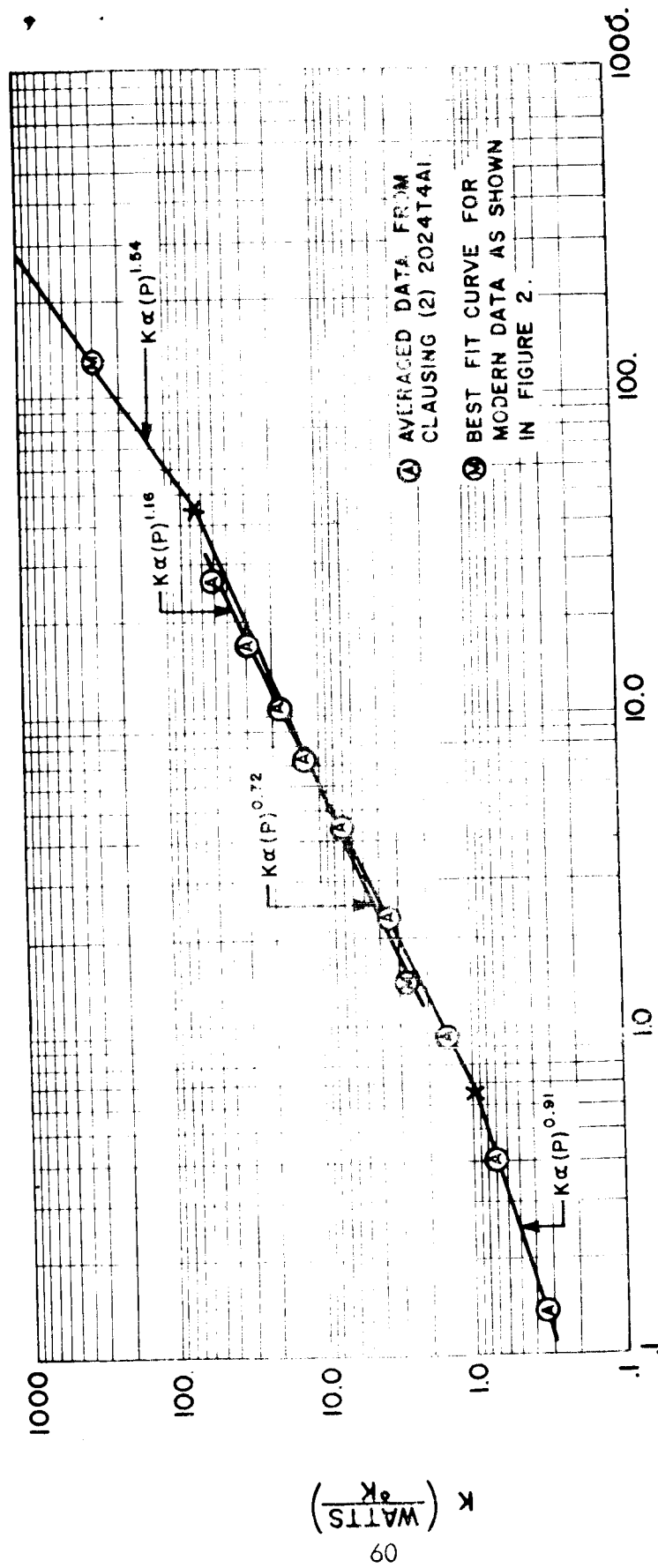



Fig. 13 P (MECHANICAL LOAD IN KILONEWTONS)  
COMPARISON OF SLOPE CHANGES OF  $K_1$  AVERAGED DATA AND MODELS.

N66 37808

MEASUREMENTS OF THERMAL CONTACT  
CONDUCTANCE IN A VACUUM

WALTER E. KASPARECK AND RICHARD M. DAILEY  
ASTRONICS LABORATORY  
MARSHALL SPACE FLIGHT CENTER  
NATIONAL AERONAUTICS AND SPACE ADMINISTRATION  
HUNTSVILLE, ALABAMA



# ABSTRACT

The apparatus used in obtaining experimental results of thermal contact conductance for metallic joints ranging in surface finish from 5 or more than 200 micro-inch CLA (Center Line Average) with contact pressures up to 700 Newton per  $\text{cm}^2$  (1020 psi) is described.

Experimental results for the following materials are presented: 6061 T6 Aluminum, Casting Alloys Magnesium AZ 91C, Almag 35 and Aluminum 256. Combinations of these materials expected in the Saturn program were tested. The addition of an interstitial material, i. e. high vacuum silicone grease, was evaluated and the results are presented.

Detailed descriptions of the provisions made for the avoidance of radiation heat losses and the attempts made to improve measurement accuracies are given.

KUT-1R

## INTRODUCTION

Most of the electronic equipment located in the Saturn IB and V vehicle instrument units will be directly mounted to liquid cooled panels (cold plates) which will serve as sink for the heat generated within the components (Fig. 1). Since the instrument unit is designed for unpressurized operation, there will be no convection cooling of the components during the flight mission.

Although thermal radiation is unaffected by a vacuum environment, the heat removal by radiation is difficult to control because of changing and unpredictable environmental temperatures.

Thus, conduction can be considered the primary cooling mode for the components; i. e., all excessive heat must be transferred across the joint between the bottom of the component-housing and the face of the cold plate.

The described configuration of component mounting creates the problem of determining how much resistance the junction of the component and cold plate, referred to as the joint, will offer to the heat flow from the component to the cold plate.

While the conductivity figures of solids are sufficiently established to predict heat flows within these solids, very little is known about the thermal conductance between two contacting surfaces in a vacuum. A literature survey yielded only a few articles that were close enough to this problem to be considered more carefully.

The papers selected for evaluation (Refs. 1 and 2) \*still lacked the information necessary for Saturn application. Reference 1 included contact pressures to  $24 \text{ N/cm}^2$  (35 psi), while Reference 2 contained information about higher contact pressures but reported only for joints made up by similar metals.

---

\*Numbers in parentheses refer to similarly numbered references in bibliography at end of paper.



In typical Saturn applications however, contact pressures of approximately  $700 \text{ N/cm}^2$  (1020 psi) on dissimilar light metal surfaces with finishes between  $0.7$  and  $5 \mu\text{m}$  ( $30$  and  $200 \mu\text{in.}$ ) CLA are expected. Therefore, it was decided to gather the necessary data for contact conductance by experimental means.

### Basic Considerations

1. Thermal contact conductance in a vacuum is primarily a matter of metallic contact between the surface asperities. To establish a vacuum level that effectively limits the gaseous conduction to an extremely low percentage, molecular gaseous conduction was evaluated at atmospheric pressure and a vacuum pressure of  $1.33 \times 10^{-2} \text{ N/m}^2$  ( $10^{-4}$  torr).

A maximum gap distance of  $0.00025 \text{ cm}$  was assumed, utilizing the proficorder readings shown in Figure 2, to permit evaluation of the molecular mean free path distance. It can be shown (Ref. 3) that at atmospheric pressure and  $288^\circ\text{K}$ , the molecular mean free path is  $6.63 \times 10^{-8}$  meter; at  $1.33 \times 10^{-2} \text{ N/m}^2$  ( $10^{-4}$  torr) and  $288^\circ\text{K}$ , the mean free path is  $50.4 \times 10^{-2}$  meter. With the maximum gap assumed, molecular collisions are very minimal.

Gaseous conduction at atmospheric pressure between two parallel plates was determined as  $998 \text{ watts/cm}^\circ\text{K}$ , whereas at  $1.33 \times 10^{-2} \text{ N/m}^2$  ( $10^{-4}$  torr) the conduction is  $1.63 \times 10^{-6} \text{ watts/cm}^\circ\text{K}$ .

Vacuum thermal conductance values at  $1.33 \times 10^{-2} \text{ N/m}^2$  ( $10^{-4}$  torr) are on the order of  $0.1 \text{ watt/cm}^2\text{K}$ . The effect of air conductance upon the resulting thermal conductance values will be less than 0.002 per cent.

2. The total heat flow, i. e. the amount of heat per unit time flowing across a mounting point, is given by

$$Q_j = h \cdot \Delta t_j \cdot A \text{ (watts)} \quad (1)$$

where

$Q_j$  = heat flow (watts)

$h$  = conductance constant of the joint  $\frac{\text{watts}}{\text{cm}^2 \cdot \text{K}}$

$\Delta t_j$  = temperature, difference across the joint ( $^{\circ}\text{C}$ )

$A$  = cross sectional area of joint ( $\text{cm}^2$ )

For the design of electronic equipment, the temperature rise  $\Delta t_j$  is the primary factor:

$$\Delta t_j = \frac{Q_j}{h \cdot A} \quad (^{\circ}\text{C}) \quad (1a)$$

The only unknown in this equation is the term  $h$ , for  $Q_j$  is assumed to be identical with the power dissipation of the component and  $A$  is the cross sectional area of the joint.

In the term  $h$ , all conditions of the joint, such as surface roughness, flatness, contact pressure, and presence of an interstitial layer, are combined.

Solving equation 1 for  $h$  yields:

$$h = \frac{Q_j}{\Delta t_j \cdot A} \quad \frac{\text{watts}}{\text{cm}^2 \cdot \text{K}} \quad (1b)$$

From Figure 3a and 3b, it can be seen that the temperature drop  $\Delta t_j$  and the surface area  $A$  can be measured directly. The heat flow  $Q_j$  across the joint can be determined by measuring power input (electric) or measuring the temperature drop along a prismatic homogeneous solid with a precisely known conductivity constant  $k$ .

The latter method of measuring temperature difference in a prismatic solid for the determination of  $Q_j$  was used for the following reasons:

1. Calculation of thermal conductance across the interface assumes an even distribution of heat flow. To attain even distribution, it is necessary to insure parallel flux lines in the samples. The fluxmeter is used as a linearizer to insure parallel flux lines as they enter the lower sample.
2. Repeatability from test to test is desirable and will permit a more reasonable comparison of data. With external radiation control, identical temperature differentials in the fluxmeter will result in identical heat flow values.
3. Utilization of the overall testing concept where  $\Delta t_j$  is determined by calculation requires an accurate measurement of heat flow. The fluxmeter method of determining heat flow seemed to be more accurate and desirable because it permits heat flow measurements to be made close to the test joint. For this purpose a second basic term, the conduction within a solid prismatic body, had to be introduced.

$$Q_s = \frac{k \cdot A \cdot \Delta t_s}{L} \quad \text{watts} \quad (2)$$

where  $Q_s$  = heat flow normal to the cross sectional area (watts)

$k$  = conductivity of the solid  $\frac{\text{watts}}{\text{cm}^\circ\text{K}}$

$\Delta t_s$  = temperature differential between two points ( $^\circ\text{K}$ )

$L$  = distance between these points (cm)

Again referring to Figure 3a, it is obvious that basically the mating solids can serve as the "standard" column for determining  $Q_s$ . However, a great variety of materials was planned to be tested with varying and not too well established conductivity values  $k$ , so a standard column was introduced as shown in Figure 3b.

This column was a piece of Armco-iron, chosen because it is a highly pure material with a relatively low conductivity providing a high temperature gradient. A question was raised about the accuracy of the Armco-iron conductivity. Even though published data were used in the calculations, conductivity of the Armco-iron will be verified by test. Both samples and the standard (in the following called fluxmeter) have the same circular cross sectional area. If no lateral heat losses occur, the flow  $Q_j$  must be equal to the flow  $Q_s$ .

$$Q_s = Q_j \text{ (watts)} \quad (3)$$

Substituting  $Q_s$  for  $Q_j$  in equation 1b yields

$$h = \frac{Q_s}{\Delta t_j \cdot A} \quad \frac{\text{watts}}{\text{cm}^2 \cdot \text{K}} \quad (4)$$

This equation presents the basis for the construction of the test apparatus.

### Test Apparatus

The three main parts of the test apparatus are the test fixture, instrumentation, and vacuum system, as shown in Figure 4.

#### A. Test Fixture

The test fixture as shown in Figure 5 was constructed of two flat plates held together by three steel rods, a pressure bellows mounted to the bottom plate, and an adjusting screw in the top plate. The use of a bellows

was recommended by E. Fried (Ref. 1) for convenient changing of the contact load without disturbing the vacuum. Going from bottom to top (in the direction of the heat flow), the central or actual measuring column consisted of the main heater, the fluxmeter, lower sample, upper sample, cooler, and load cell.

All contacts, where a low heat resistance was desired, were lapped and filled with high vacuum silicon grease; these were the joints between (1) heater and fluxmeter, (2) fluxmeter and lower sample, and (3) upper sample and cooler.

To reduce the lateral heat transfer from or to the center column by radiation, an improved radiation shielding device was provided. The tendency has been for other experimenters to use a single shield with an encompassing heater. This limits the vertical temperature matching or nulling characteristics of the radiation shield.

The radiation shielding device is unique because of its ability to reduce the radiation losses in six discrete levels of the test column. Gold plated, aluminum rings bonded with graphite cloth heating elements were each controllable so that mating the temperatures of the rings with those of the column would reduce radiation to an insignificant minimum.

It was learned from previous tests that the rings influence each other by a "mirror" effect on the column; therefore, separating disks of fiberglass were introduced to serve as "radiation heat baffles." The diameter of the cylindrical column was 3.8 cm (1.5 in.), the length of the fluxmeter was 8.2 cm (3.25 in.), and the length of the samples was 1.90 cm (0.75 in.).

#### B. Instrumentation

As previously shown, temperature measurements throughout the test fixture were very critical. The problems associated with accurate temperature measurement became apparent as the test apparatus design progressed.

Noting Figures 5 and 6 will give some insight as to the complexity of the thermocouple instrumentation. Several of the more important factors considered during instrumentation of the test fixture are described and the basic reason given for careful consideration:

1. Thermocouple instrumentation was considered the most critical factor in the test fixture design. The calculation of  $Q_s$  (equation 2) utilizes a  $\Delta t_s$  measured at two specific levels shown in Figure 5. In addition to providing the basis for determining  $h$ , i.e. with the calculated  $Q_s = Q_j$  (equation 3), those thermocouples located concentrically around the test column vertical center line were utilized to assist in monitoring and reducing lateral heat losses.

2. The lateral heat losses were reduced to a negligible quantity by the use of the guard rings (Fig. 5). The temperatures of the guard rings were continuously monitored during tests and adjusted to insure that the temperature difference between the test column surface and the inner surface of the guard rings was held to less than 40 microvolts or approximately  $1^\circ\text{K}$ . Controlling the temperature differential to  $1^\circ\text{K}$  or less will reduce the radiation losses from the test column to a value of approximately 0.002 watts or 0.007 per cent of the input electrical power. This is believed to be a negligible quantity since the effect upon the calculated conductance will be minimal. To further insure compatible temperature readings, thermocouples on the test column and the guard ring surfaces were cemented in place; i.e. identical mounting techniques were used,

Monitoring and adjusting the guard rings will be eliminated when the automatic guard ring controller is fabricated. An electronic circuit has been designed to compare the outputs of two heat sensors (one on the test column and one on the guard ring) and then to adjust the power input to the guard ring to null the readings to less than  $1^\circ\text{K}$  difference.

3. The initial group of thermocouples used in the test program were calibrated and found to deviate less than  $0.1^{\circ}\text{K}$  from NBS standards. All thermocouples to date have been from the same manufacturer and, to the best of the authors knowledge, from the same material batch; therefore, their accuracy is considered to be adequate. All reasonable precautions have been taken to insure temperature measurement accuracy.

4. Determination of the temperature differential ( $\Delta t_j$ ) across the joint, i. e. between the mating surfaces of the test samples, was accomplished in the following manner.

Thermocouples were inserted in the samples in the same pattern shown in Figure 7, an average measured distance of 0.16 cm from the test surface. This average was obtained by X-ray and measurement under a microscope.

A temperature differential from the thermocouple to the test surface could be computed with the previously calculated heat flow (watts), the measured distance  $L$  from the thermocouple to the surface, the known cross sectional area, and the published conductivity of the test sample. This value was then either subtracted from the measured temperature for the lower sample or added for the upper sample to obtain the surface temperatures.

A question was raised concerning the placement of thermocouples so close to the sample test surface. A statement by the author of Reference 2 indicated that the thermocouples could be within the area of constriction resistance. That is where the heat flow lines in the material are being directly affected by the metallic contacts.

To verify or disprove the procedure being used as described above, two samples as shown in Figure 3a will be prepared. After completion of the test, temperature measurements will be graphically plotted as shown in Figure 3a, and the  $\Delta t_j$  obtained from this plot will be used to calculate  $h$ . The variation of the  $h$  with that calculated from using the short samples will be indicative of the error introduced by thermocouple location.

For ease in fixture maintenance and changing of samples, a rotary vacuum feed-through switch is utilized (Fig. 7). Thermocouples from the column were soldered to the switch points inside the vacuum chamber. A single thermocouple was used to reference the switch to an ice-bath junction outside the vacuum jar. This technique permitted a complete thermocouple circuit to exist between the measuring point and the potentiometer.

These four points are considered to be the most significant in the instrumentation of the test column.

### Experimental Program

An experimental program was set up according to the design concept of cold plates to be used in Saturn application (Table I).

At the inception of the testing program, the prime material under consideration for the cold plate mounting surface was 6061-T6 Aluminum; therefore, the colder (upper) samples were made of this material in an attempt to simulate cold plate operation.

Cast alloys such as Almag 35, Mag AZ91C, and Aluminum 356 were chosen for the hot (lower) samples due to their extensive use in Saturn IU electronic components.

Table I shows test run 6 with an interstitial layer. A more elaborate testing with interstitial layers will be carried on as shown in Table II. Also the behavior of soft foils, such as indium (Run 14), will be studied separately.



## Test Results

The primary purpose of this experimental program has been to obtain values of thermal contact conductance between mating metallic surfaces in a vacuum environment. This data will be utilized in Saturn Instrument Unit electronic component design and evaluation. The testing program as outlined in Table 1 & 2 was scheduled to obtain data on representative materials currently being used in the design of Saturn I.U. components.

It was necessary to verify the operational accuracy of the test apparatus before an extensive testing program was undertaken. The first test runs, presented in figures 8, 9 and 10, were performed with careful monitoring of the internal temperature measurement points. Test Run 1, performed on lapped samples, was run to evaluate the control capabilities in terms of maintaining parallel heat flux lines throughout the test column.

To assist in the evaluation of apparatus accuracy, a computerized data reduction program was employed. The solution of Equation 4 was programmed permitting timely review of test data. Placement of thermocouples as shown in Figure 7 permitted a number of contact conductance values to be obtained utilizing the computer program.

Reviewing these results showed a spread in the calculated conductance of  $\pm 5\%$  at low pressure and  $\pm 2.5\%$  at high pressures.

Lower contact pressures, on the test samples, result in larger temperature differentials (i.e. lower contact conductance) across the test joint. In the case of flat samples, this is an indication of the minimum microscopic contact area. Where the samples are not flat, greater differentials will occur, indicating a minimum of macroscopic contact area.

It must be noted that the spread in contact conductance was reduced as the pressure was increased. This is an indication that the test apparatus has the inherent capability of permitting parallel heat flux lines to be established in the test column.

The constriction resistance is influenced by three main factors: contact pressure (number of microscopic points of contact), the flatness and the type and finish of samples.

At low contact pressures, the constriction resistance is higher than at high contact pressures. Due to the higher constriction resistance, greater temperature differences will occur across the measuring plane at the joint.

For higher contact pressure, the constriction resistance will be smaller, due to more microscopic points of contact. This will result in increased uniformity at the temperature measuring plane, thus a smaller spread in contact conductance.

Repeatability has been shown in figure 9 to be within 1-2% of two successive runs. This also is an indication that operational accuracy, i.e., evaluation of machined surfaces for design application, is satisfactory.

Data presented in figures 8, 9 & 10 was obtained from samples, (RUNS 1-5), which had not been mated until assembled in the test fixture. Samples were machined, wrapped and stored for periods up to four months. Oxide coatings which may have formed during this time period were not disturbed. This was intentional due to the possible storage times for Saturn Components.

To obtain a base for evaluation of test results, samples for Run 1 were lapped to less than 0.07 mCLA. Lapped samples provided the close simulation to optically flat surfaces which will generally provide the greatest macroscopic contact area, hence the highest contact conductance.

Results from test run 1, with hysteresis points, are shown in figure 8. Compared to the results shown from the Reference 2 report, it can only be stated that the values are greater in magnitude. This difference could possibly be traced to difference in materials, surface finish measurement technique and even to the testing method used for obtaining these results. Those items indicate the difficulty to be experienced in comparison of data from other experimenters and even the data obtained in different runs from the same test apparatus.

The data from test run 2 ran contrary to published data which showed the finer the surface finish, the greater the contact conductance. To support the validity of the data, profilometer readings (Figure 2) taken prior to application of pressure indicated

- - -

an apparent flatness deviation of 0.002 cm. Macroscopic contact areas show in only three points in figure 2.

Measurements taken after the application of contact pressure exceeding  $700 \text{ N/cm}^2$  indicated that the overall flatness deviation of .002 cm in a diameter of 3.8 cm was not affected. Some minor microscopic changes were noted, i.e., asperities were reduced in overall height indicating the application of pressure.

Results for Runs 3 & 4 presented in figure 9 represent data taken on samples with a better relative flatness than the samples from Run 2. Proficorder measurements on these samples showed no appreciable flatness deviation even though the surface roughness was near twice that of Run 2 Samples.

It is a generally accepted fact after reviewing published data that the greater the surface roughness the less the conductance. This assumes the surface finish as the sole parameter of comparison. However reviewing the results from the Run 2 - 3 & 4, surface flatness has a greater apparent affect than does the surface finish. Sufficient experimentation has not been done to determine the magnitude of the effect of surface flatness upon the contact conductance.

- -

Runs 3 & 4 were made utilizing identical materials, finishing processes and relative flatness. These runs were made to verify repeatability characteristics of the test apparatus. As indicated by the results shown in figure 9, a variation of less than 5% was found to exist between Runs 3 & 4.

Run 5 was performed primarily to determine the change in contact conductance with repeated cycling of pressure. This was intended to simulate the removal and remounting of R-ASTR components on the IU conditioning panel. To ideally simulate the above, the samples should have been physically separated, rotated 1-2 degrees and pressure reapplied.

Mounting bolt area characteristics are such that the macroscopic contact should remain the same however the microscopic contact area cannot be repeated with a removal and subsequent remounting to the same location. In this case the conductance will not vary from the initial value shown in figure 10.

#### Conclusions:

The explanation of the physical nature of the thermal contact conductance is beyond the scope of this report. Since the primary purpose of this experimental program was the determination of design data for Saturn vehicle components, review of microscopic effects upon contact conductance will be suggested for a future program.

Test data shown in Figures 9 & 10 have indicated that the magnitude of thermal contact conductance attainable with normal machined surfaces in the Saturn program will not create excessive temperature differentials between the conditioning panel and the component mounting surface. For design purposes,

a heat load of 10 watt per mounting bolt area (5 x 5 cm) has been assumed. Under this condition, utilizing the contact conductance from Run 2 @  $350 \text{ N/cm}^2$  of  $0.7 \text{ watt/cm}^2\text{-}^\circ\text{K}$ , a temperature differential of less than  $1^\circ \text{K}$  would exist. For component thermal design purposes, this differential can be neglected in most cases.

Due to the discrepancies noted for the Run 2 data, application of these results cannot be used for design purposes. A valid evaluation of surface flatness must be undertaken with a well defined program to determine the relationship of flatness deviation to contact conductance. A program of this nature will require a review of the methods used for measuring temperature differentials across the test joint.

Data obtained from this experimental program cannot be utilized to determine an average temperature differential over the entire component mounting surface. This is due to the lack of knowledge concerning the average contact pressure. It is to be assumed that the only definable contact pressure is directly adjacent to the mounting bolt.

Prior to Runs 2 & 3 profilometer readings were taken (figure 2, shows Run 2) to obtain some insight into the macroscopic and microscopic characteristics of the test surfaces. Measurements made after a test cycle did not indicate major changes in the surface characteristics.

It was concluded that surface changes could not be evaluated with profilometer measurements. This conclusion is supported by

the work of Fenech and Rohsenow in Reference 4.

Test runs to date (1-5) and the remainder scheduled in Tables 1 and 2 will not permit full comprehension of the microscopic affects of the surface upon thermal contact conductance. Many parameters cannot be properly evaluated with the relatively few test runs scheduled.

A greatly expanded program coordinated with other experimenters is necessary to fully evaluate the mechanics of thermal contact conductance in a vacuum environment.

The following items are considered the major areas of interest to be studied in a future program:

1. The relationship between surface characteristics, (i.e., flatness deviation, surface finish) and contact conductance. To properly compare test data, a common basis for defining surface characteristics must be agreed upon. To evaluate flatness deviation and surface finish, each must be taken separately and then combined in a closely controlled test.

2. Investigation of the problems involving the standardization of test samples, i.e., diameter, length, surface measurement technique and material thermal properties (thermal conductivity). Ideally, a single source to supply samples would be a good solution to the problem of discrepancies in materials and methods of surface measurements.

3. Temperature measurement techniques and data evaluation procedures should be stanradrized to the greatest extent practicable.

4. Evaluation of the affect of non-metallic interstitial materials upon the conductance should be thoroughly investigated.

5. Variation of conductance when mating similar materials and dissimilar materials must be determined.



### ACKNOWLEDGMENT

The authors wish to give acknowledgment to Mr. J. Boehm, Chief of Electro Mechanical Engineering Branch, for the initiation and the support of the experimental program.

They also thank Messrs. H. Burk and R. Rathbun from IBM for their valuable theoretical and practical contributions, Mr. J. B. Stanley from Applied Research Branch, who provided and maintained the fine, reliable vacuum system for the experiment, and Mr. J. Castner from Computation Lab for his assistance in preparing the computer program for data reduction and evaluation.

## REFERENCES:

1. Erwin Fried and Frederick A. Costello, "Interface Thermal Contact Resistance Problem in Space Vehicles," ARS Journal, February 1962, pp. 237 - 243.
2. A. M. Clausing and B. T. Chao, "Thermal Contact Resistance in a Vacuum Environment," University of Illinois, Engineering Experiment Station, Report ME-TN-242-1 NASA Research Grant NsG-242-62
3. Prepared under sponsorship of National Aeronautics and Space Administration, United States Air Force, and United States Weather Bureau, "U.S. Standard Atmosphere, 1962," U.S. Government Printing Office, Washington, D.C., December 1962, p. 13.
4. H. Fenech and W. M. Rohsenow, "Thermal Conductance of Metallic Surfaces in Contact," Massachusetts Institute of Technology, U.S. Atomic Energy Commission, Contract AT(30-1)2079, May 1959.

TABLE I

## THERMAL CONTACT CONDUCTANCE TESTING PROGRAM

Run #	Lower Sample		Upper Sample		Remarks
	Material	Finish*	Material	Finish	
1	Almag 35	Lapped	6061-T6	Lapped	
2	Almag 35	0.81-1.60	6061-T6	0.81-1.60	
3	Almag 35	2.54-5.08	6061-T6	2.54-5.08	
4	Almag 35	2.54-5.08	6061-T6	2.54-5.08	
5	Mag AZ91C	0.81-1.60	6061-T6	0.81-1.60	Hysteresis Testing Silicone grease Interstitial layer
6	Almag 35	2.54-5.08	6061-T6	2.54-5.08	
7	Mag AZ91C	0.81-1.60	6061-T6	0.81-1.60	
8	Alu 356	0.81-1.60	6061-T6	0.81-1.60	
9	Mag AZ91C	0.81-1.60 Black Anod	6061-T6	0.81-1.60	
10	Almag 35	0.81-1.60	Mag AZ91C	0.81-1.60	

## NOTE \*

The finish refers to micro-meters CLA machined with flycutter except for Run #1.

Run #5 increasing and decreasing contact pressure until variation in conductance is negligible.

TABLE II

## THERMAL CONTACT CONDUCTANCE TESTING PROGRAM (con't)

Run #	Lower Sample		Upper Sample		Remarks
	Material	Finish *	Material	Finish	
11	Alu 356	0.81-1.60 Fly	Mag AZ91C	0.81-1.60 Endmill	
12	Almag 35	0.81-1.60 Shaper	6061-T6	0.81-1.60 Shaper	
13	Almag 35	0.81-1.60 Fly	6061-T6	0.81-1.60 Fly	Foil Investigation
14	Almag 35	0.81-1.60 Lapped	6061-T6	0.81-1.60 Lapped	Indium
15	Almag 35	Black Anod.	6061-T6	Black Anod.	
16	Almag 35	Lapped	Mag AZ91C	Lapped	Hysteresis Test
17	Al2024T3	Lapped	Mag AZ91C	Lapped	
18	Al Mag 35	0.81-1.60 Shaper	Mag AZ91C	0.81-1.60 Fly	Foil Investigation
19	Al Mag 35	0.81-1.60 Endmill	6061-T6	0.81-1.60 Fly	Aluminum
20	Al 356	0.81-1.60 Fly	Mag AZ91C	0.81-1.60 Fly	Silicone grease
					Interstitial layer

## NOTE \*

Finish as indicated by process and micro-meter CLA

Fly = Flycutter

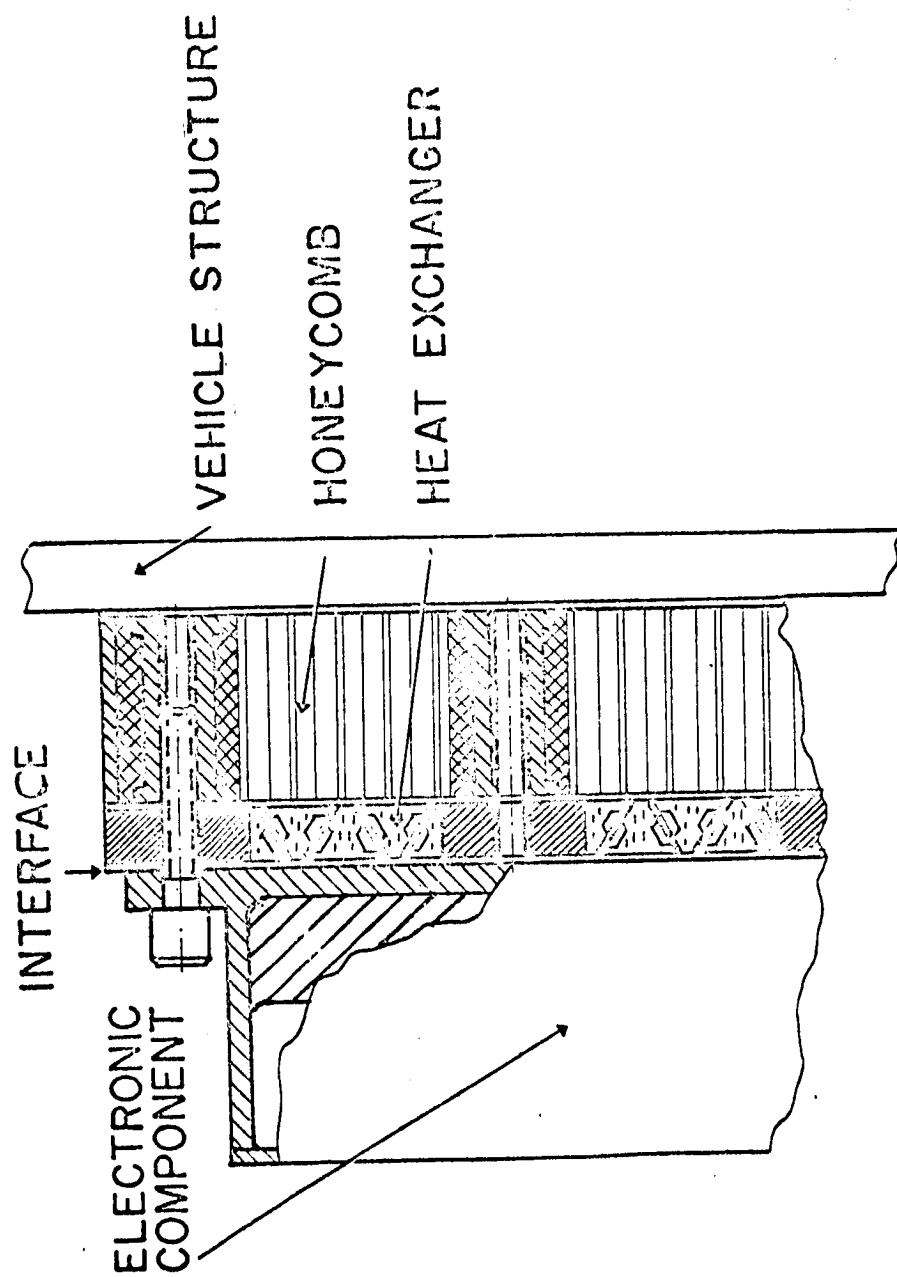
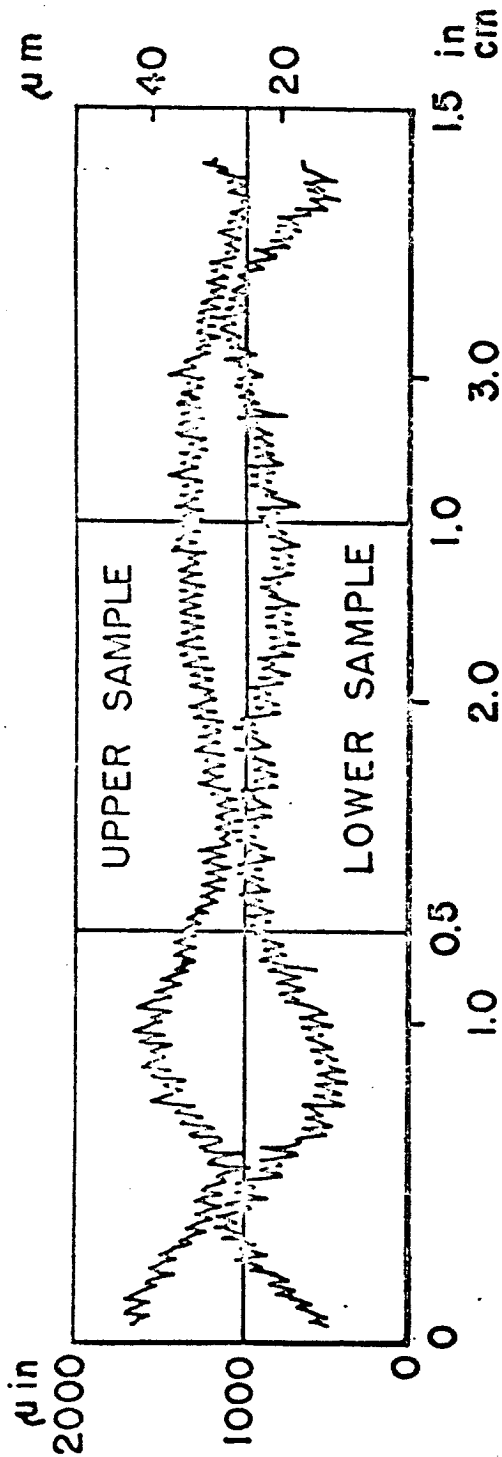
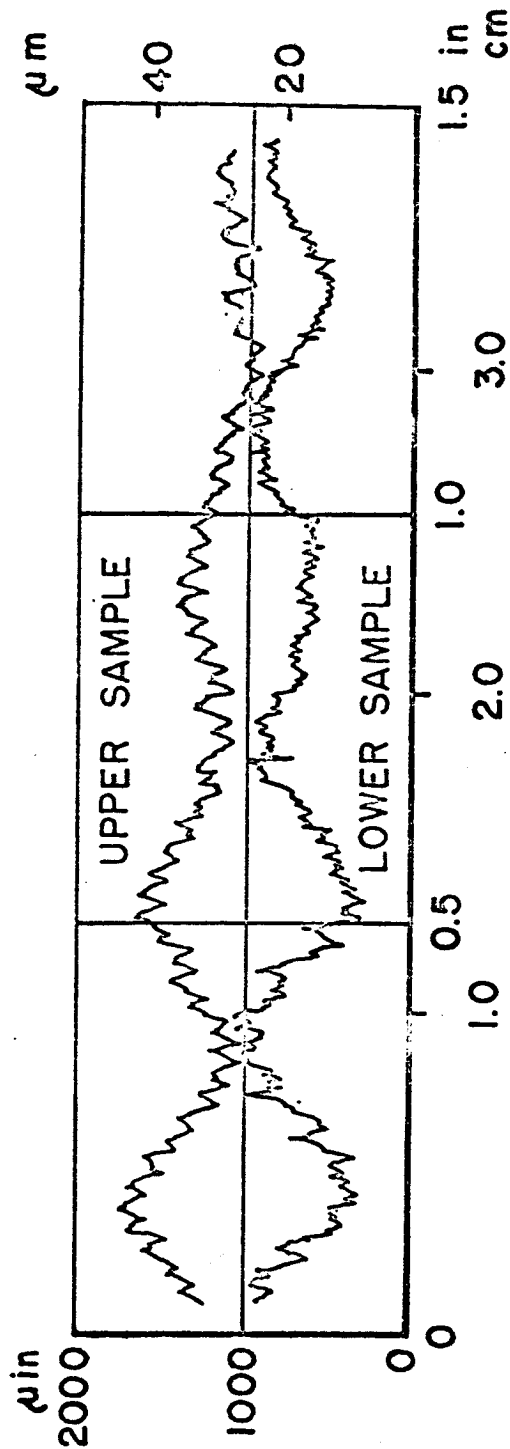


Fig. 1: Cold Plate Configuration in Saturn Application

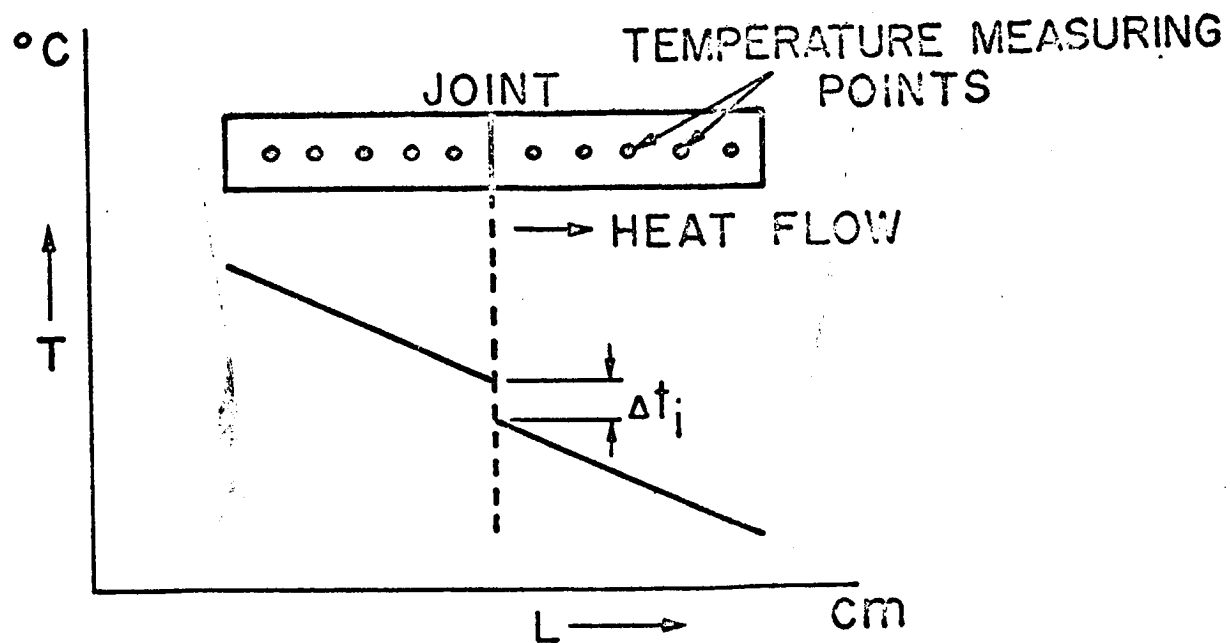


a. READINGS TAKEN PERPENDICULAR TO FINISHING MARKS

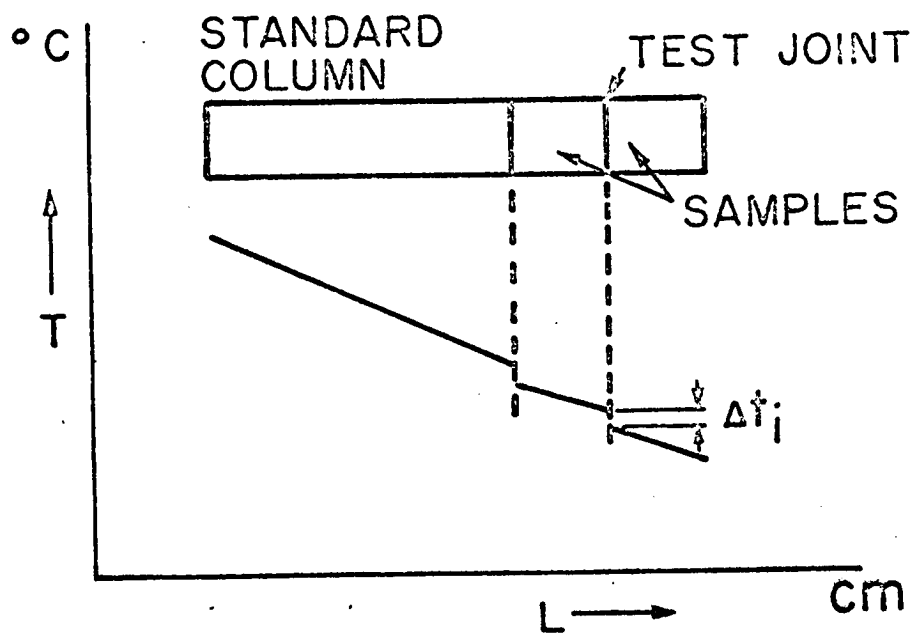


b. READINGS TAKEN NEAR PARALLEL WITH FINISHING MARKS

Fig. 2: Profilometer Readings on Samples of Test Run 2. Upper Sample: Alu 6061 T6 Lower Sample: Alu 6061 T6  
 Almap 25 Flatness Deviation: Approx 0.002 cm Surface Finish: 1.6  $\mu$ m CLA



a.



b.

Fig. 2: Temperature Gradient due to a Steady Heat Flow  
 a. In two samples of the same material.  
 b. In a Standard Column and two samples.

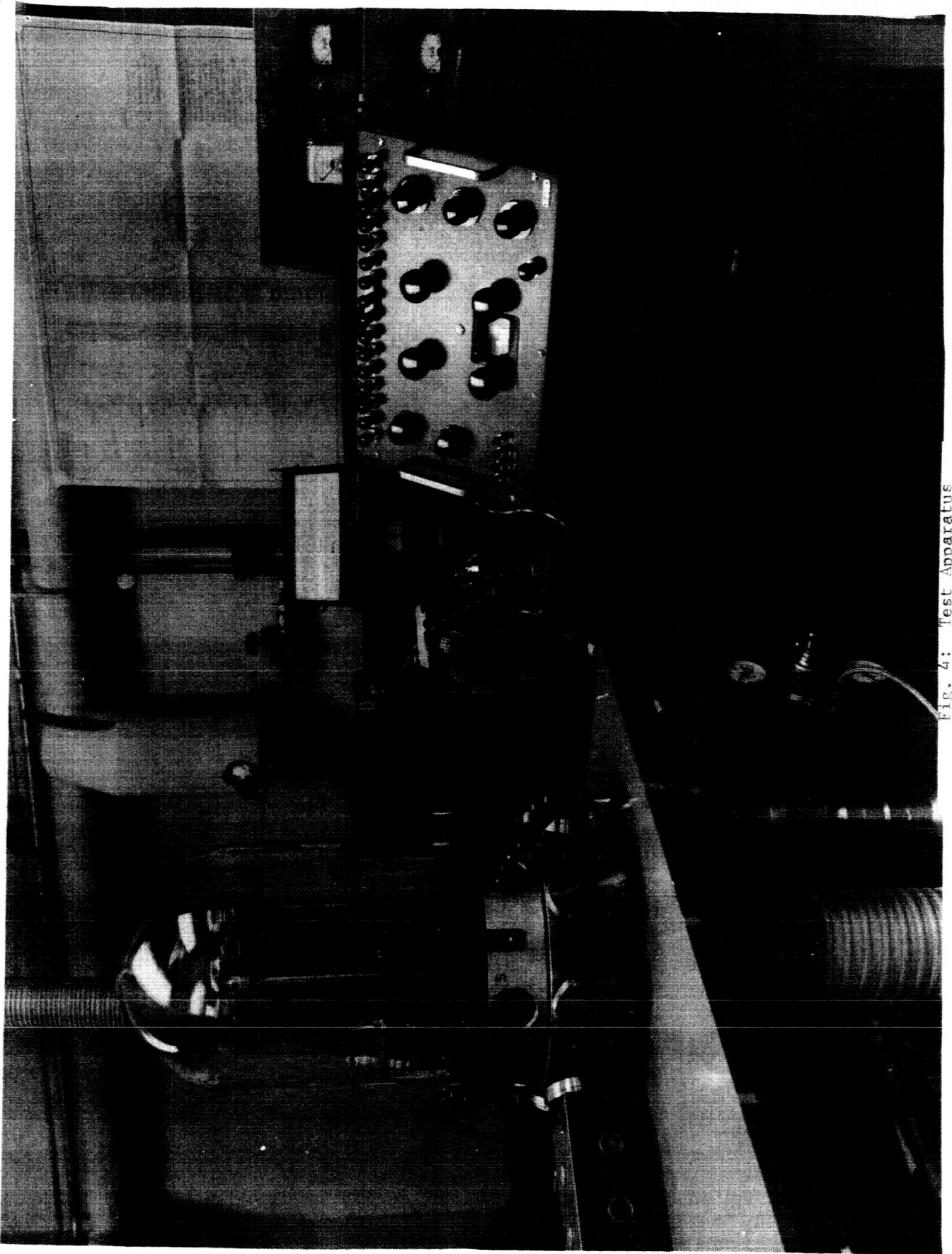


Fig. 4: Test Apparatus



Fig. 5

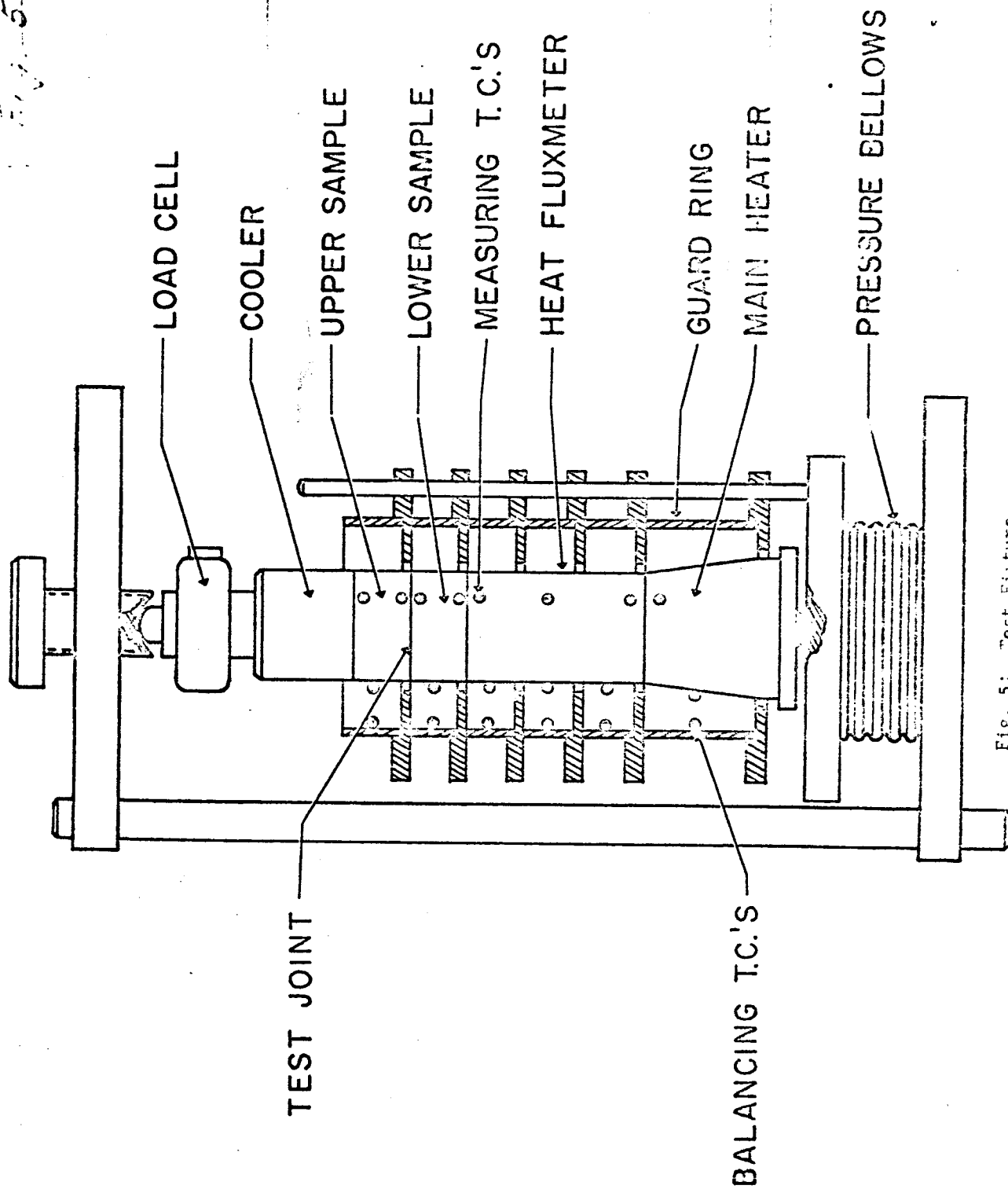


Fig. 5: Test Fixture

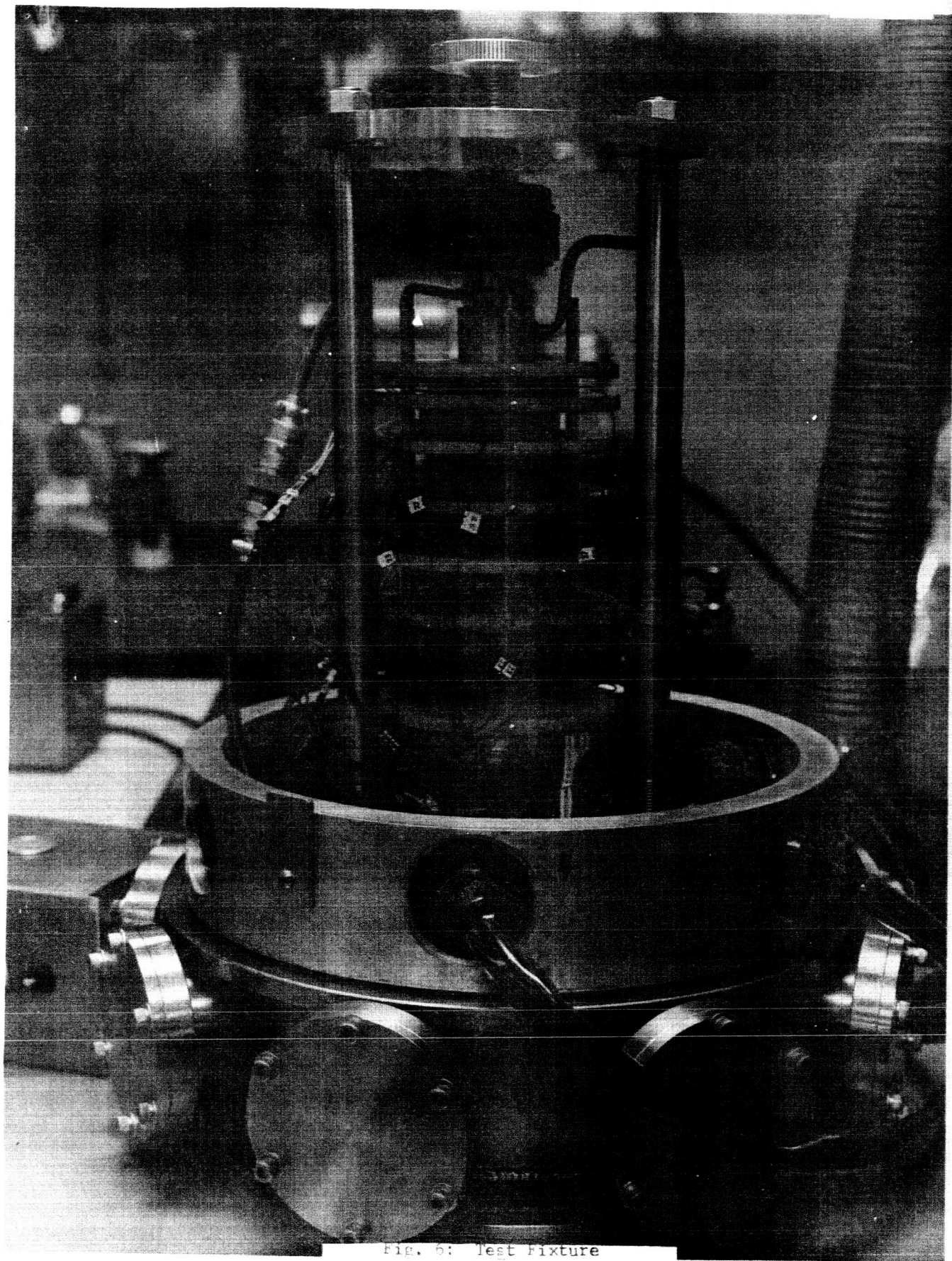


Fig. 6: Test fixture

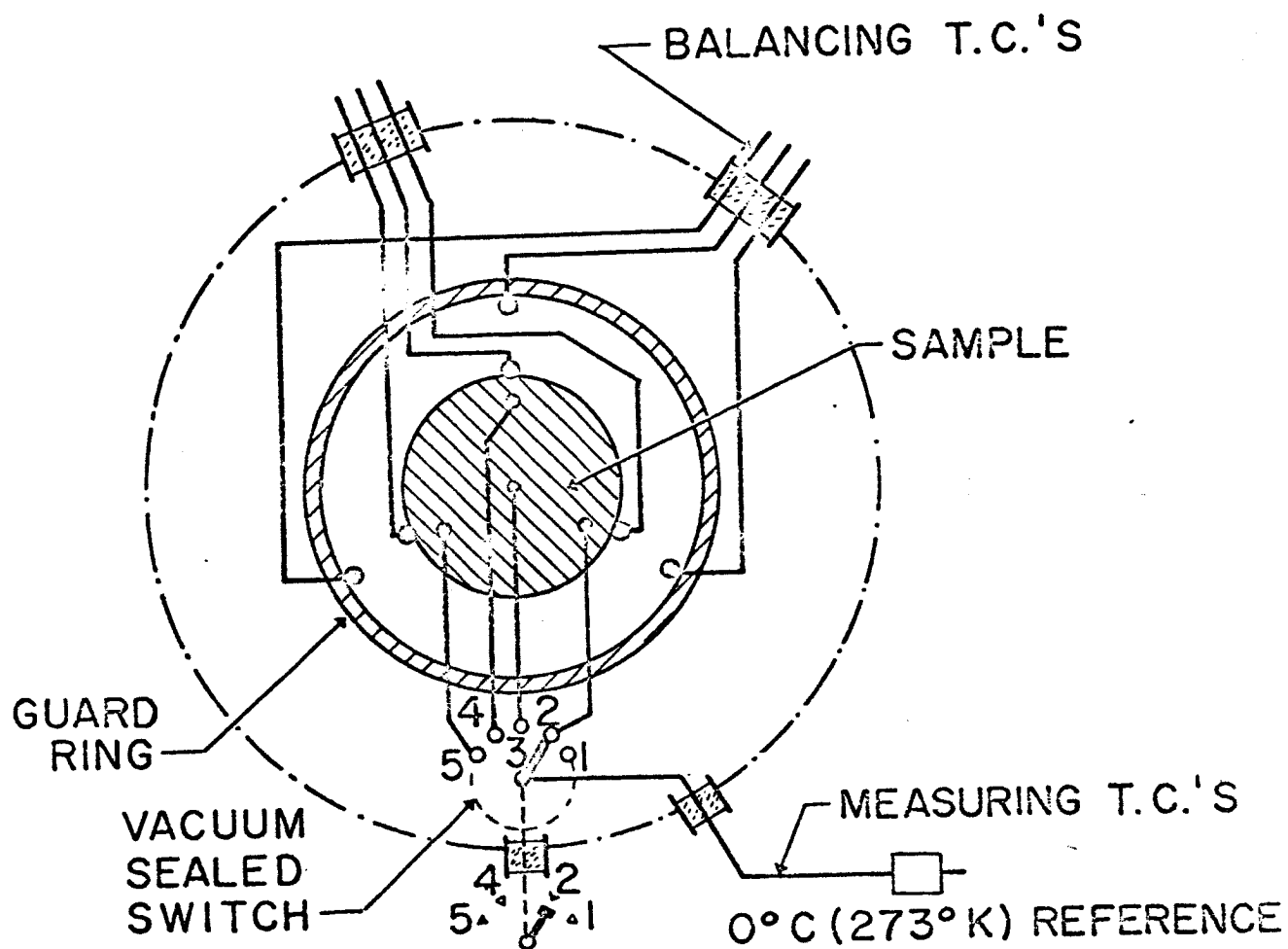
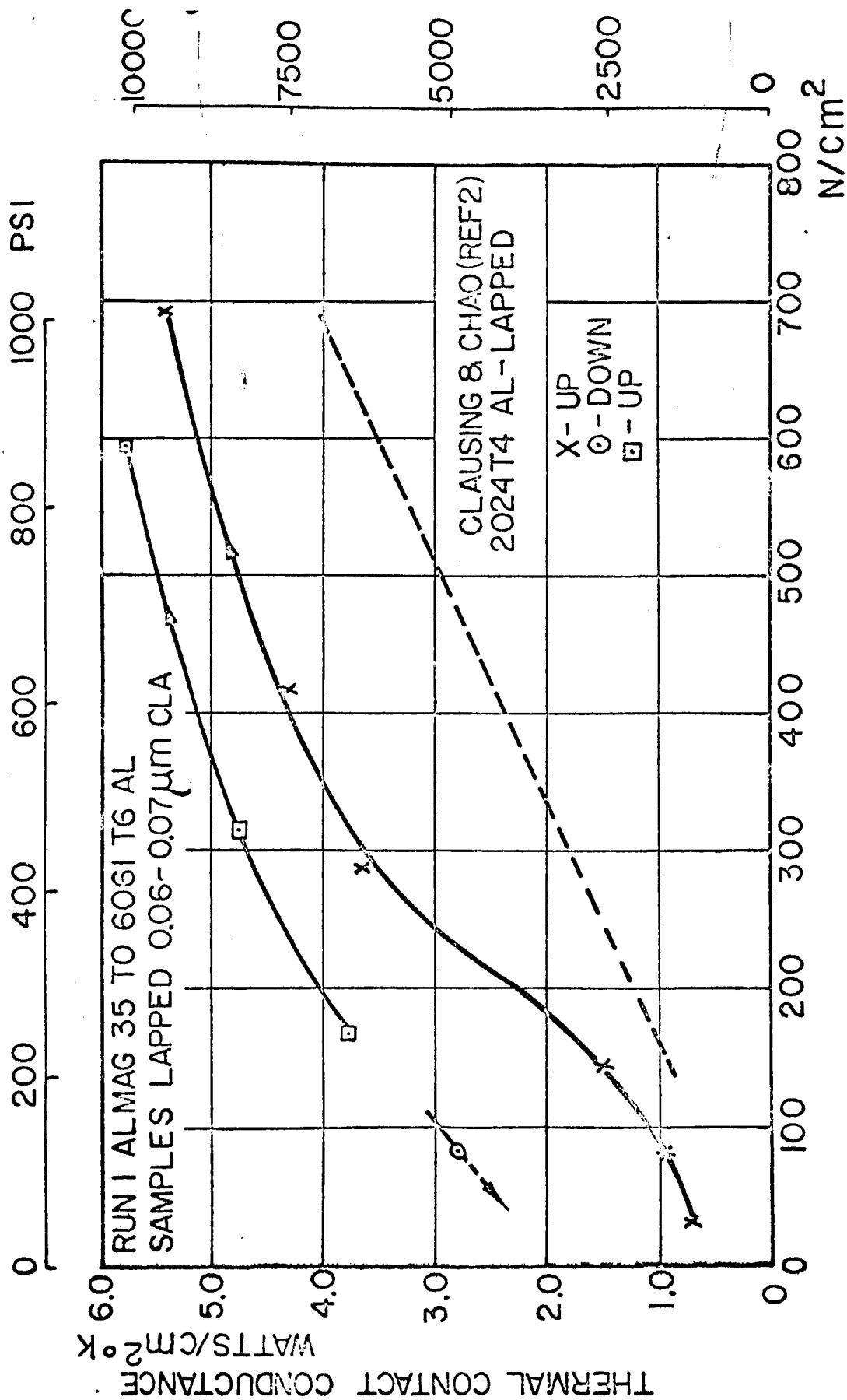
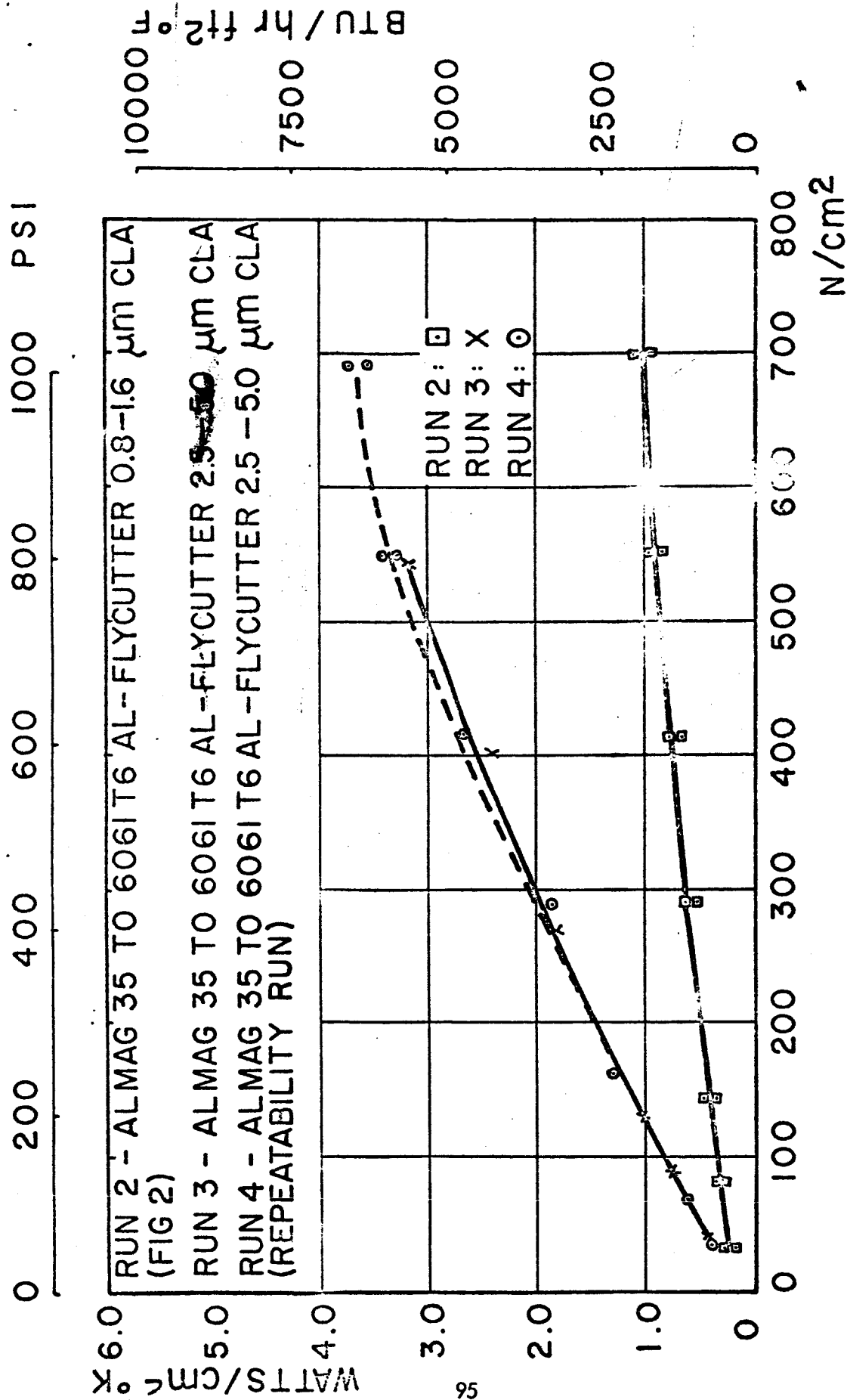


Fig. 7: Arrangement of Thermo Couples

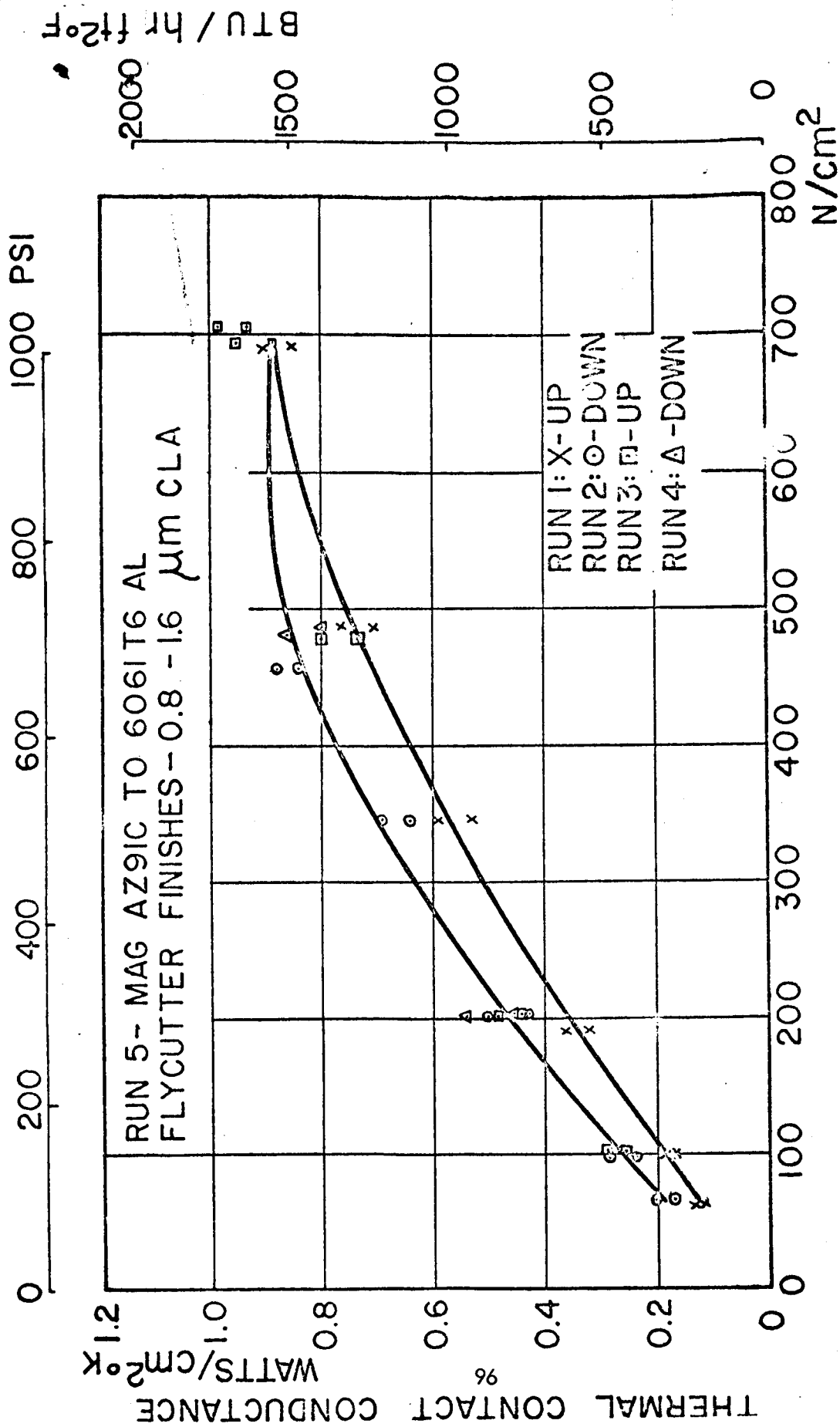


CONTACT PRESSURE  
 Fig. 8: Contact Conductance vs Contact Pressure, Run # 1



## CONTACT PRESSURE

Fig. 9: Contact Conductance vs Contact Pressure, Runs 2, 3 & 4



CONTACT PRESSURE

Fig. 10: Contact Conductance vs Contact Pressure, Run #5

Thermal Joint Conductance Research

N66 37809

Review and Planning Conference

February 19, 1964

Thermal Joint Conductance

Dr. J. Michael F. Vickers  
Research Specialist  
Engineering Research Section  
Jet Propulsion Laboratory



## Thermal Joint Conductance

J.M.F. Vickers

1. This work is proceeding in several areas with which the Jet Propulsion Laboratory has direct contact:
  - i. Research at the University of Illinois where the author has been the technical monitor for NASA on the grant.
  - ii. Work in-house and with consultants on the theoretical analysis of actual joints.
  - iii. Experimental work in-house which is still in the stage of development of equipment.
  - iv. Work in-house on the correlation of available information.
2. The work at the University of Illinois was initiated by the Section during the summer of 1961, when Arthur Clausing was a summer employee. He did a literature search during this period, and when he returned to University of Illinois persuaded his advisor, Professor B. T. Chao, that he should work in this area for his Doctoral Thesis. This has been sponsored by NASA on a research grant for two years. During this period, Dr. Clausing has completed his Ph.D., and a report has been issued by University of Illinois.(1)

This work has been entirely concerned with the determination of the variation of the joint conductance with nominally uniform contact pressure for various materials; that is, a columnar apparatus has been used, with contact pressures up to about 1,000 psi. The most important finding has been that the joint conductance is more dependent upon the variation of the surface flatness than the surface roughness for thick or columnar specimens and that, using the Hertz equation to calculate the contact areas involved, it was possible to correlate the data very well. The metals used initially were brass, (Anaconda Alloy 271, a leaded brass, 35.5 Zn, 3% Pb.), magnesium AZ 31B, stainless steel 303, and aluminum 2024 T4. A representative drawing of the test equipment is shown in Figure 1, and the plots from the raw data for a low contact pressure and a high contact pressure for lapped aluminum specimens in Figure 2. The results obtained for lapped aluminum for various contact pressures is shown in Figure 3. Figure 4 shows some results for brass; here  $d_t$  is the total equivalent flatness deviation and  $b_L$  the radius of the constriction regions. It will be noted that there is a considerable difference in the curves, increasing for increasing mean interface temperature, but not directly affected by the flatness deviation to constriction radius ratio  $\frac{d_t}{b_L}$  which is not varying directly with the increase



in joint conductance. The reason for the significant change associated with  $T_m$  is that the change in interface temperature involves a significant change in the value of the mean thermal conductivity of the material, and of the modulus of elasticity. When these are taken into account a remarkable collapse of the data points is obtained. The collapsed data for aluminum is shown, rather than brass, but the curves have similar shape and degree of conformity, Figure 5. The first thing to note is that the curve drawn is not the best curve through the points, but is the theoretical prediction for the material concerned. Actually what is plotted is the ratio of the mean thermal conductivity of the material  $k_m$  to the interface conductance,  $h$ , that is,  $\Delta L$ , divided by the radius of the macroscopic constriction regions ( $b_c$ ) against  $\zeta = (R/E_m)(\epsilon_c/d_c)$  the ratio of the product of the contact pressure and the radius of the macroscopic constriction regions to the product of the modulus of elasticity and the total equivalent flatness deviation. In the ordinate,  $\Delta L_m$  may be considered as the additional length of the contact members which would produce the same resistance as the existing interface. Since

$$h = \frac{Q}{A \cdot \Delta T}, \quad \therefore \frac{k_m}{h} = \frac{k_m A \Delta T}{Q}$$

$$\text{But } Q = \frac{k_m A \Delta T}{\Delta L}, \text{ where } \Delta L = \text{length.}$$

$$\text{Therefore } \frac{k_m}{h} = \frac{k_m A \Delta T}{Q} = \Delta L = \text{length}$$

The reduced results for all the materials tested is shown in Figure 6, where it will be seen that good conformity is obtained with the theoretical curve over most of the range for all materials. It should be noted that while there are some bad points for stainless steel and aluminum at low pressure, and that these two materials also lie off the curve periodically at higher pressures, that points also exist for these two materials in all regions which lie exactly on the theoretical curve.

Work is still continuing on this project to attempt to find the reasons for the discrepancies which exist, and also to investigate the reported directional effects when two dissimilar metals are in contact. A recent progress report in this area indicates that for aluminum-stainless steel contacts there is a strong directional effect, that the contact resistance is a function of the flux involved, and that the dependence, that is whether the contact resistance goes up or down with flux, is also directionally dependent, and, naturally, as the flux goes to zero, so does the directional effect.

Some related work, under Professor Boresi of the Department of Theoretical and Applied Mechanics, University of Illinois, (under the same contract), relates to the effect of thermal strain produced by the temperature gradients caused by the macroscopic constriction. This work was initially undertaken as a three-dimensional, axisymmetric problem in thermoelasticity, but has proved intractable to date. More success is presently being obtained in the plane problem, which is mentioned in the progress report as proceeding hopefully towards the elimination of truncation and roundoff errors. The plane case should be applicable, at least qualitatively, to the axisymmetric case.

3. It is felt that much of the available information, except for that of Barzelay et al (2) at Syracuse, and one or two papers in vacuo (3), is not directly applicable to real joints. Almost all of the work has been done with a "nominally uniform" contact pressure, that is with columnar type apparatus, between maxima of 35 psi contact pressure in one case, Fried and Costello (4), and 3000 psi in the highest case, Cordier (5). In actual practice what is needed is the behavior of actual bolted joints, where the contact pressure varies from a maximum under the bolt head, out to zero (or even separation) between the bolts.

Some theoretical analyses have therefore been carried out at JPL to try to connect up the type of work done by Chao and Clausing with the type of problem encountered in a spacecraft.

The first item was done by Professor Keith Newhouse, (6) while spending a summer with JPL from the University of Nebraska. He analyzed the effect of sources of heat of finite size distributed on one side of a thin plate which was radiating, on the other side, to space. This indicates the relative importance of joint conductance to plate resistance in the case of a module attached directly to its radiating surface. The converse type case, of the plate receiving radiation and feeding into a finite sink is also of interest, but has not been studied as yet by Newhouse.

The second area studied was by Dr. T. J. Lardner, previously serving his Army duty at JPL, and now a consultant to JPL while an instructor at MIT (7). He took the case of two cylinders, Figure 7, with a constant input heat flux, and a constant heat rejection temperature. The joint conductance was considered to have a fixed value at the axis of the cylinders, and to fall off linearly to zero, or to a fixed value, at the periphery, the extreme case of this being the constant joint conductance out to the periphery.

The results for various slopes of joint conductance vs. radius are shown in Figure 8, where it can be seen that as the slope increases from zero, (i.e. constant joint conductance), the temperature discontinuity at the interface increases. This is also shown in Figure 9 as a function of the slope.

The ratios of the temperature discontinuity at the interface on the axis to that for a constant joint conductance are shown in Figure 10, as a function of the ratio of the product of the flux and the axial length of the cylinders to the product of the thermal conductivity and the rejection temperature. In Figure 11 the same ratio is plotted against the ratio of the flux to the product of the maximum joint conductance and the rejection temperature. It will be noted that in the case of the temperature discontinuity for  $C = 1$ , (that is the joint conductance falling to zero at the periphery), the temperature discontinuity is at least twice that for constant joint conductance, and for smaller values of  $C$  this is reduced. It should be noted that the total joint conductance varies in this analysis, as  $C$  is reduced in magnitude.

Other work, performed by Lardner and another consultant, Dr. H. E. Williams of Harvey Mudd College, involved the solution of the problem of the contact pressure distribution for two plates in contact. The only work from the literature which appeared to be helpful was that of Sneddon (8), and some later work by Fernlund (9) and by Nelson (10).

Sneddon had taken the two dimensional case of an infinite plate loaded by a strip of constant width, and had worked out the midplane stresses. These are a good first approximation to the contact pressure between two infinite plates under similar loading. Williams elaborated on this for a greater variety of load width to plate thickness ratios for multiple strip combinations (11). Lardner then took Nelson's results for the axisymmetric case, and elaborated them, using the principle of superposition to produce the results for annular loading (12). The first of these cases is shown in Figure 12, together with the axisymmetric loading configuration. For plates which are thick relative to the diameter of the load it will be noted that the maximum stress is small compared to the loading, but that the contact load is spread over a radius about three times that of the imposed loading. For thinner plates the maximum stress increases, and the spreading out of the contact load relative to the imposed loading is reduced. When one examines the axisymmetric case for annular loading, Figure 13, one sees, on moving from the inner edge of the loading outwards, that the contact pressure first increases and then begins to decrease. It is felt that while these trends are approximately true for the actual loading under consideration that, for a real bolt where there exists a hole through the plate, this will be modified to have a maximum either very close to, or coinciding with, the inner edge of the loading. This particular plot is for the case of a load hole of the same diameter as the total plate thickness; that is, the radius is equal in thickness to one of the two plates in contact. It is apparent that, for a thin annulus, the spreading action is large, while as the annular width increases the additional radius involved decreases.

This work is continuing, with difficulties. A problem developed with the computer program when one tried to put a hole in the plate. Fernlund overcame the problem by making an assumption which is not felt to be justified; when one does not make this assumption, the computer memory is overloaded. However an approach has just been reached which should not lead to the computer overloading, but no actual runs have yet been made.

Other work to be undertaken is to determine edge effects, that is how the stress patterns are modified by the presence of one, two or three plate edges in the neighborhood of the loading; also to work away from the midplane so that one can have solutions for a thin plate bolted to a thicker plate.

4. The work described above, that is the effect of uniform pressure on the joint conductance, can be combined with the variation of pressure from Lardner and Williams to predict the actual variation of the joint conductance in the vicinity of a bolt. This can then be used in conjunction with Lardner's work on the effect of variable joint conductance on the heat flow to predict actual fluxes through a bolted joint, and further combined with the work of Newhouse to predict behavior when an item is bolted to a radiating surface.

It is proposed to check some of this theoretical work with the apparatus shown in Figure 14. Here one can check, for either circular or annular loading, the net heat flow between plates which are either solid or have a hole bored through them. The results can be compared with those predicted as indicated above. This apparatus will have a dead weight loading system capable of applying up to 10,000 psi at the interface, which is known to be the actual interface pressure existing under bolts in JPL spacecraft. It will, further, be capable of holding this loading for a very considerable period of time (7 days) so that one can check out thoroughly the results reported by Cordier. Cordier reported that the joint conductance is a function of time of application of the load as well as time of outgassing and the net load and that this effect is further complicated by the net thermal and stressing history of the specimen.

5. Some work has recently been completed in-house at JPL, in trying to correlate all the existing data from the literature. It is hoped to produce a report in the near future, and this will list i. the references, ii. all the information on the materials and test conditions which can be obtained or inferred from the papers and iii. the data obtained, plotted in consistent units throughout. It is hoped also to list the names of people working in the field who have data on various materials which they have not yet published, so that those who are interested can contact these people directly. It is hoped that this report can be up-dated periodically (possibly once per year), and that through it JPL can act as a

reasonable clearing house for information. It is hoped that people will draw the attention of JPL to those papers which exist, and have been omitted, and also that they will draw attention to their own papers, and those of others, as they appear.

6. This completes the description of the work currently under way at JPL. There are obviously many areas which are not touched on at all, but it is felt that a coordinated attack is being developed on one of the major problems on joint conductance, the production of a system of analysis which will allow the experimental results to be applied to actual bolts.

# REFERENCES

1. Thermal Contact Resistance in a Vacuum Environment, Clausing, A. M., and Chao, B. T., Engineering Experiment Station, Department of Mechanical and Industrial Engineering, ME-TN-242-1, University of Illinois, August 1963
2. Barzelay, M. E., et al, NACA TN-3167, March 1954  
NACA TN-3295, May 1955  
NACA TN-3824, April 1957  
NACA TN-3991, July 1957  
NACA TN D-426, May 1960
3. Controlling Factors of Thermal Conductance Across Bolted Joints in a Vacuum, Aaron, W. K., and Colombo, G., ASME Paper 63-W-196, 1963. John, J.E.A., and Hilliard, J.M., NASA TN D-1753, July 1963
4. Interface Thermal Contact Resistance Problem in Space Vehicles, Fried, E. and Costello, F. A., ARS Journal, Vol. 32, pp. 237-243, 1962
5. Experimental Studies of the Influence of Pressure on Thermal Contact Resistance, Cordier, H., Annales de Physique, 13 Serie, 1-6, 1961 (Redstone Scientific Information Center, Translation RSIC-116, Redstone Arsenal, Alabama).  
Experimental Study of the Influence of Pressures on Thermal Contact Resistance, Cordier, H. and Maimi, R., Seance, Academie des Sciences, Comptes Rendus 250, pp. 2853-2855, April 1960, (SIA Translation 63-10777)
6. Newhouse, K. N., Personal Communication, August 1963. This work is written up for presentation to ASME, and it is hoped will be published shortly.
7. Effect of a Variable Thermal Joint Conductance, Lardner, T. J., JPL Space Programs Summary No. 37-21, Vol. IV, pp. 53-55, June, 1963
8. Fourier Transforms, Sneddon, I. N., p. 479, McGraw-Hill Book Co., New York, 1951; also Proceedings of the Cambridge Philosophical Society, Vol. 42, pp. 260-271, 1946.
9. A Method to Calculate the Pressure Between Bolted or Riveted Plates, Fernlund, Ingemar, Report No. 245, Transactions Chalmers University of Technology, Gothenburg, Sweden, 1961.
10. Further Consideration of the Thick-Plate Problem with Axially Symmetric Loading, Nelson, C. W., Journal of Applied Mechanics, Vol. 29, ASME Transactions Series E, No. 1, pp. 91-98, March 1962
11. Personal Communication, March 1963
12. Thermal Joint Conductance: Midplane Stress Distribution, Lardner, T. J., JPL Space Programs Summary No. 37-19, Vol. IV, pp. 83-85, Feb. 1963

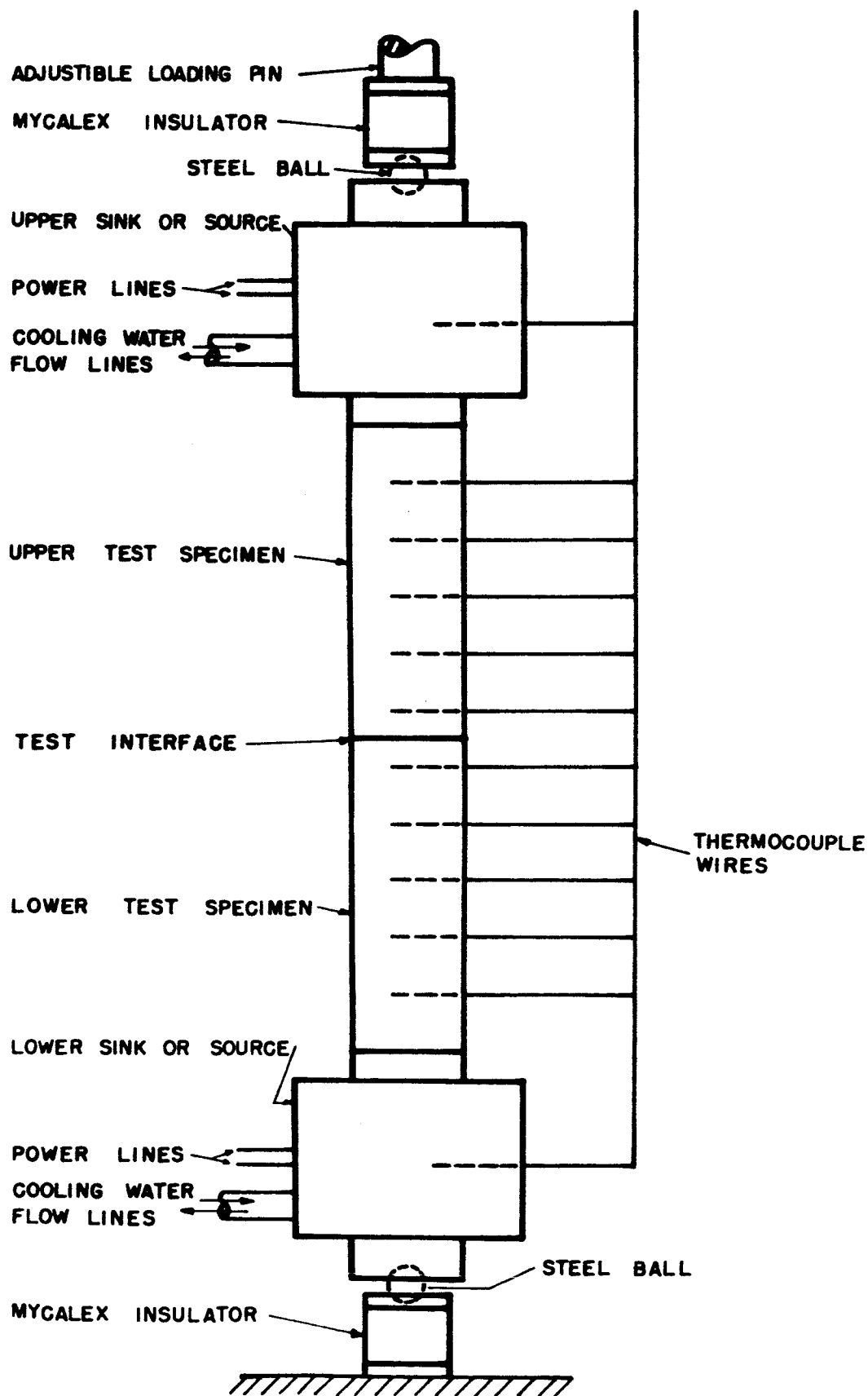


Fig. 1.

Apparatus used by Clausing  
and Chao

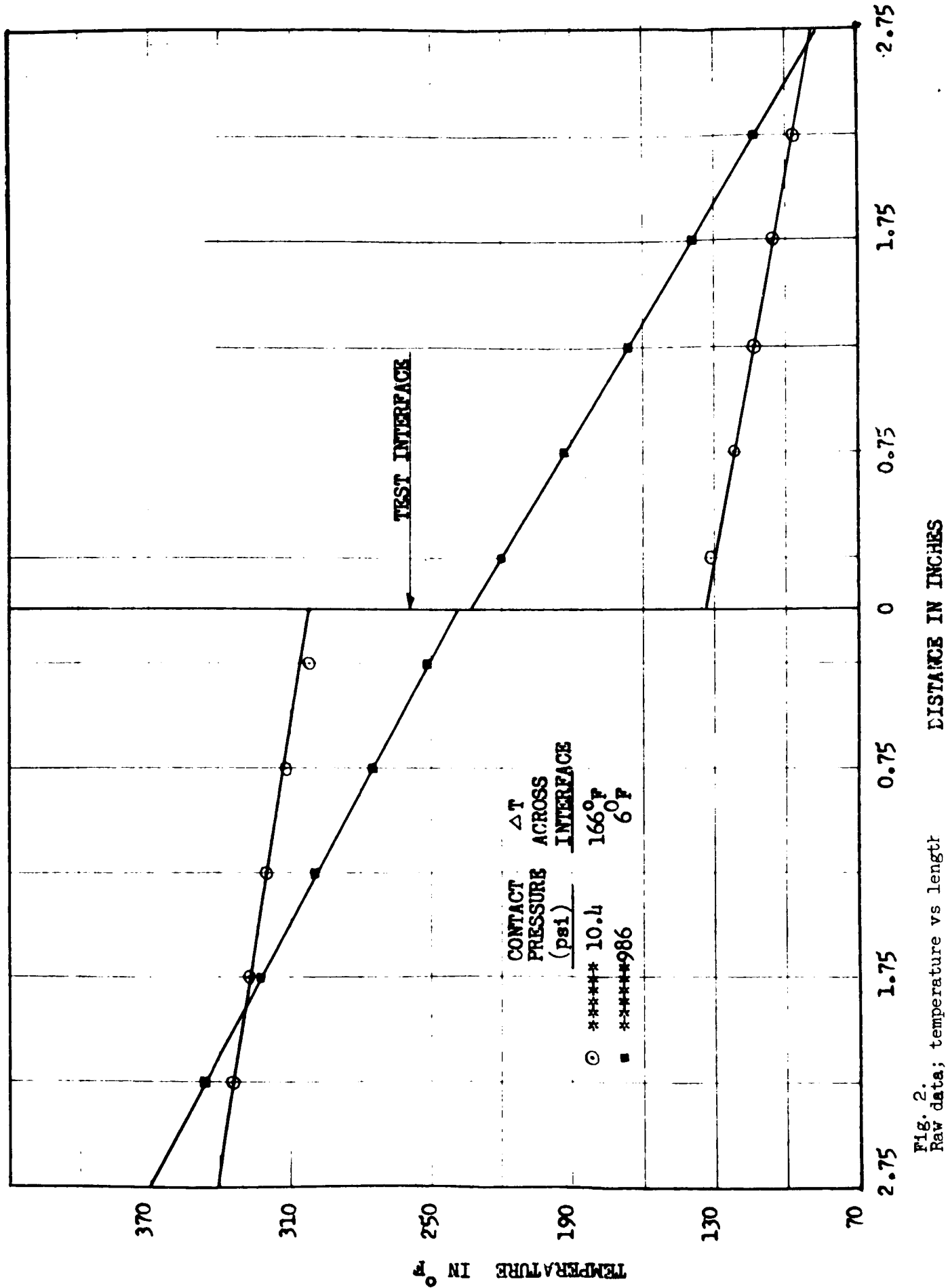


Fig. 2. Raw data; temperature vs length for two contact pressures. Aluminum specimen



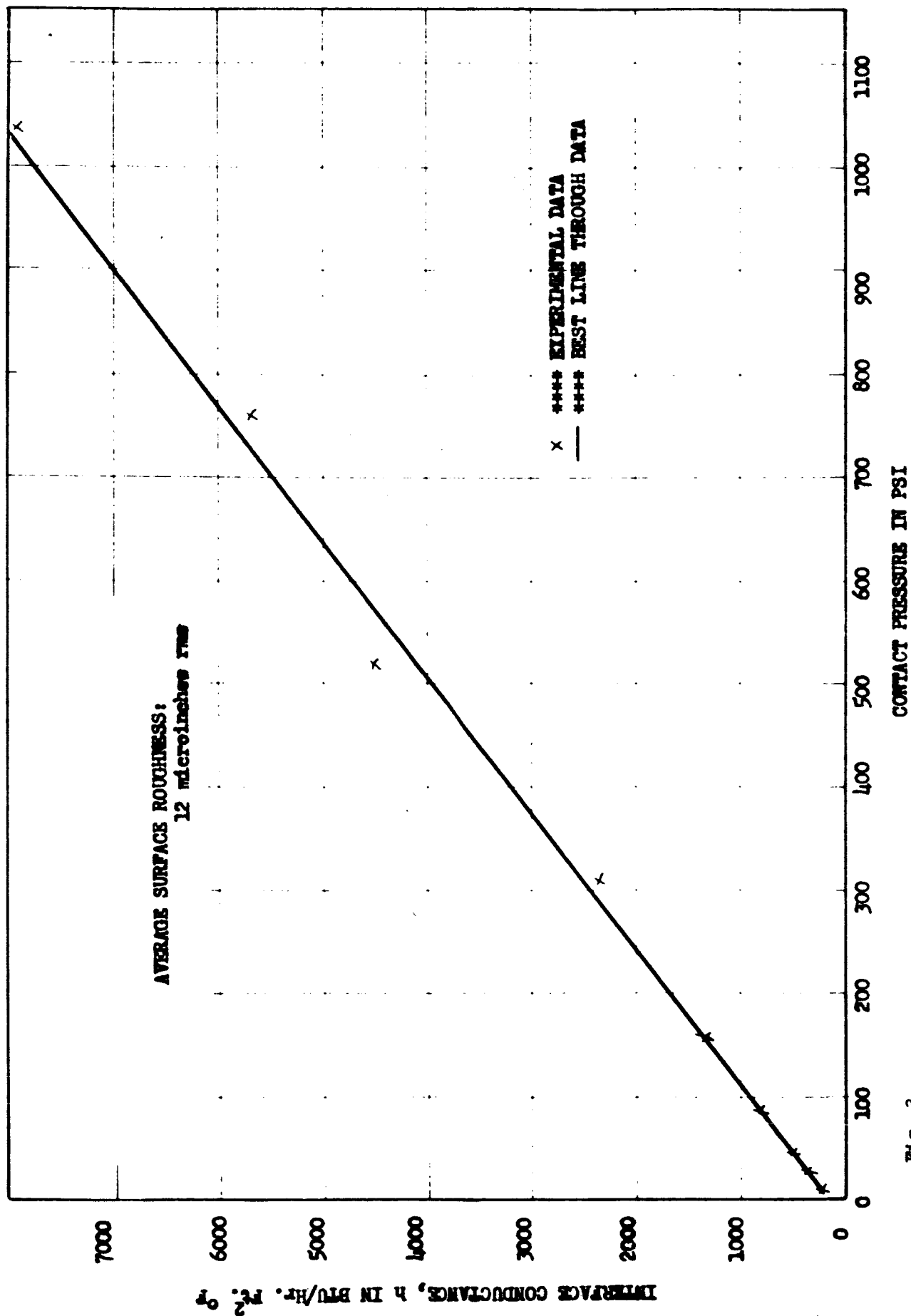


Fig. 3.  
Interface conductance vs  
pressure.  
Lapped aluminum specimens

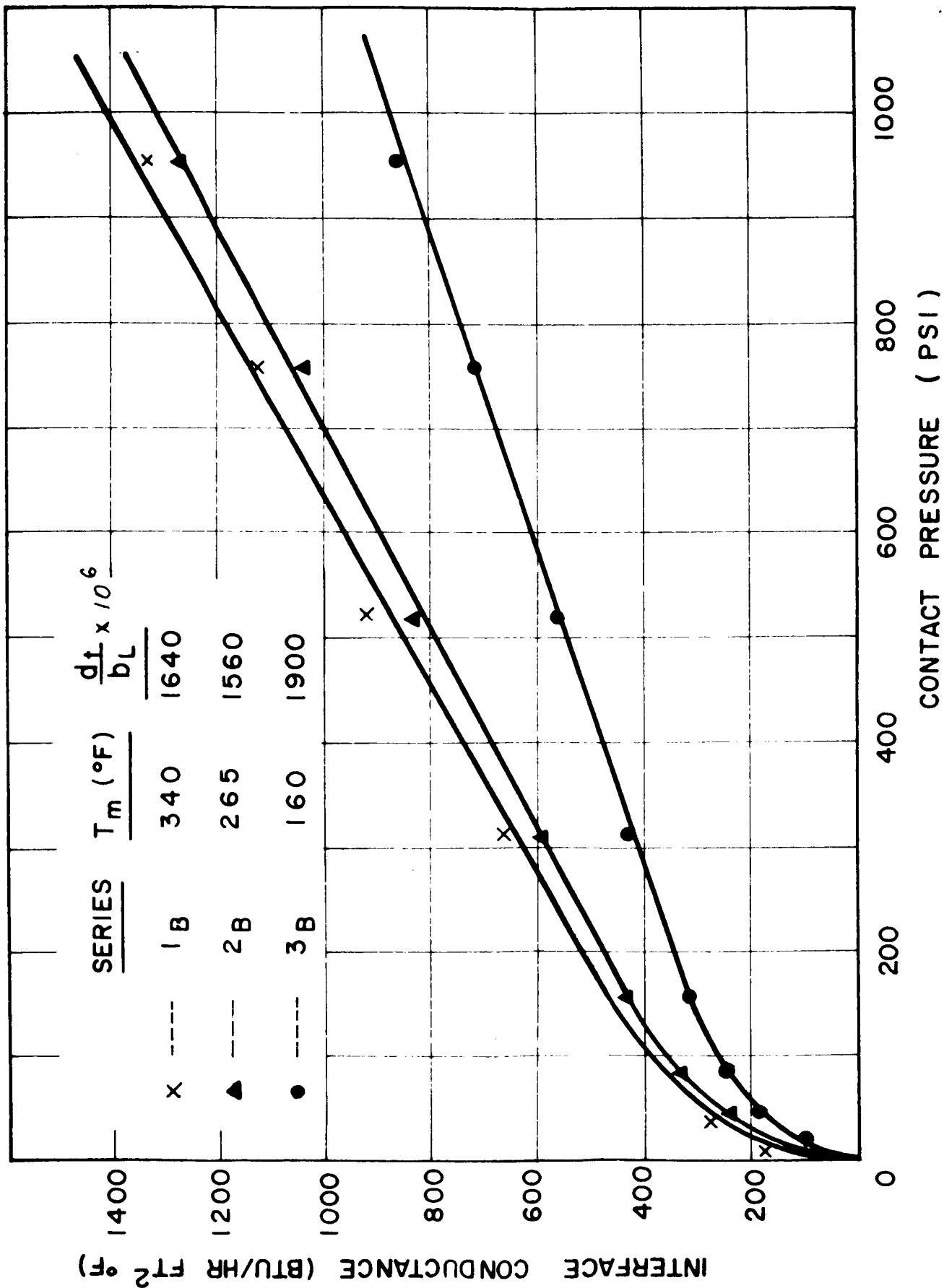


Fig. 4.  
The influence of  $T_m$  and  $d_1/b_L$  on variation of interface conductance with pressure. Brass specimens.

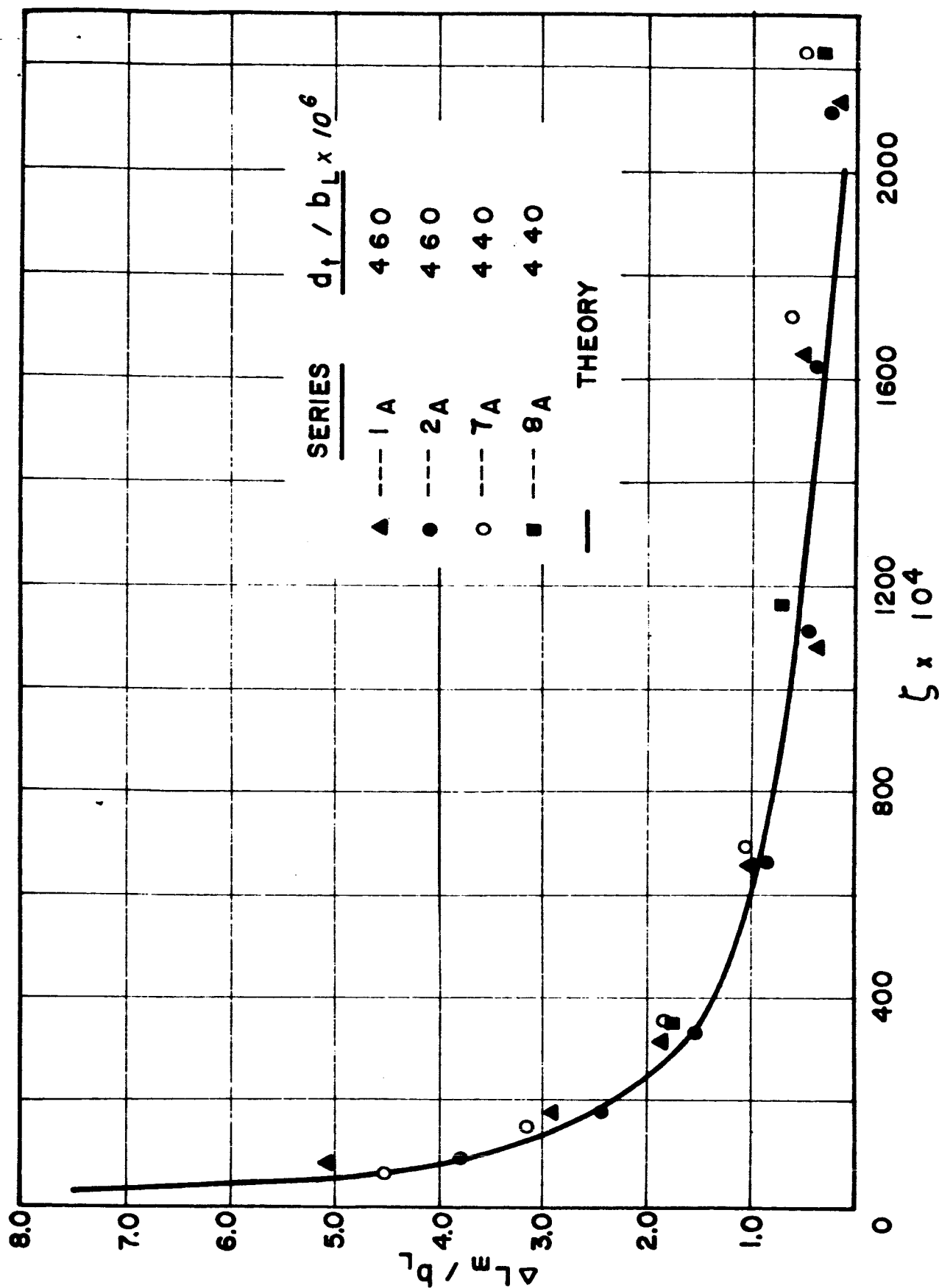


Fig. 5.  
Comparison between data and  
theory for rough aluminum  
specimens

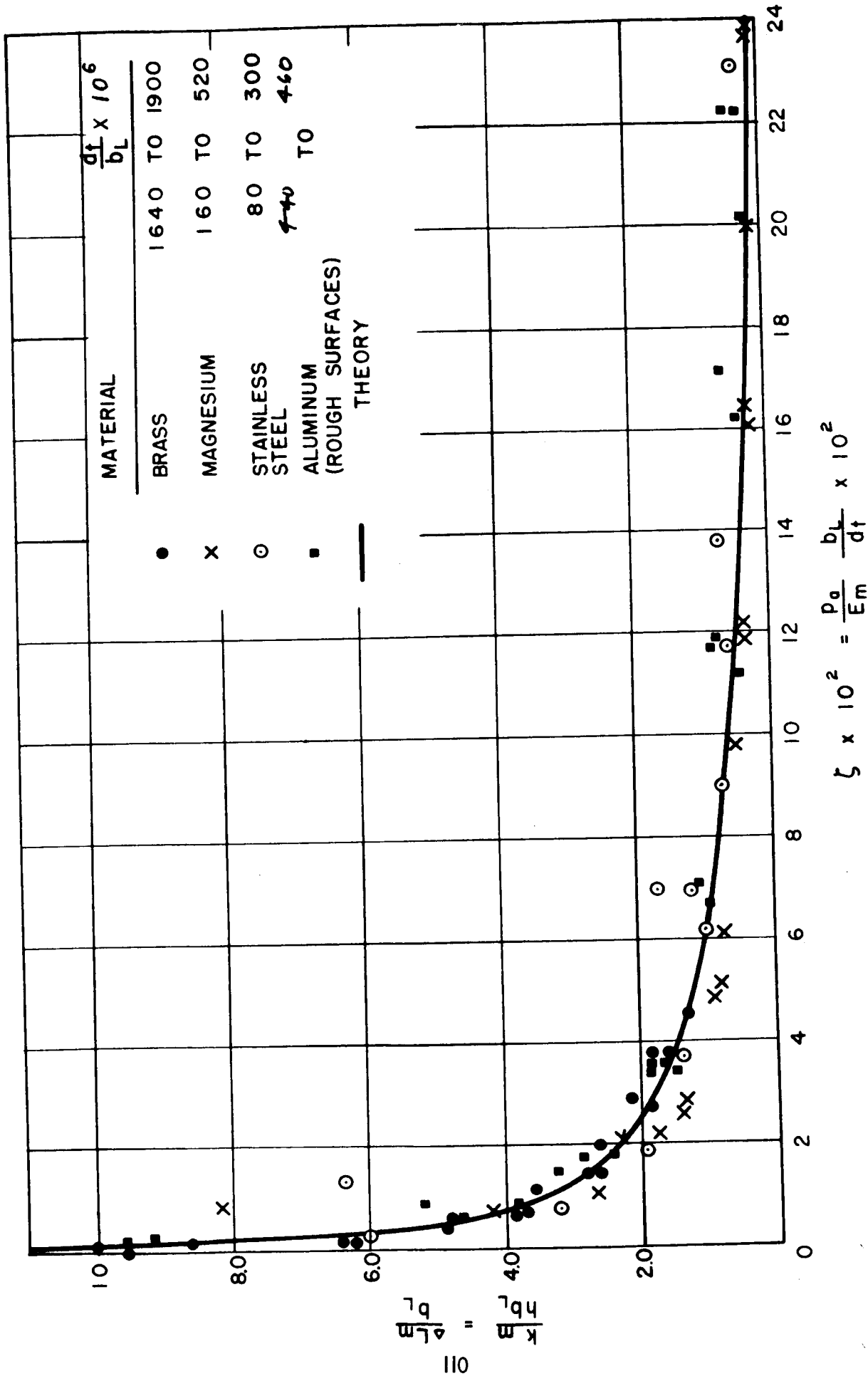
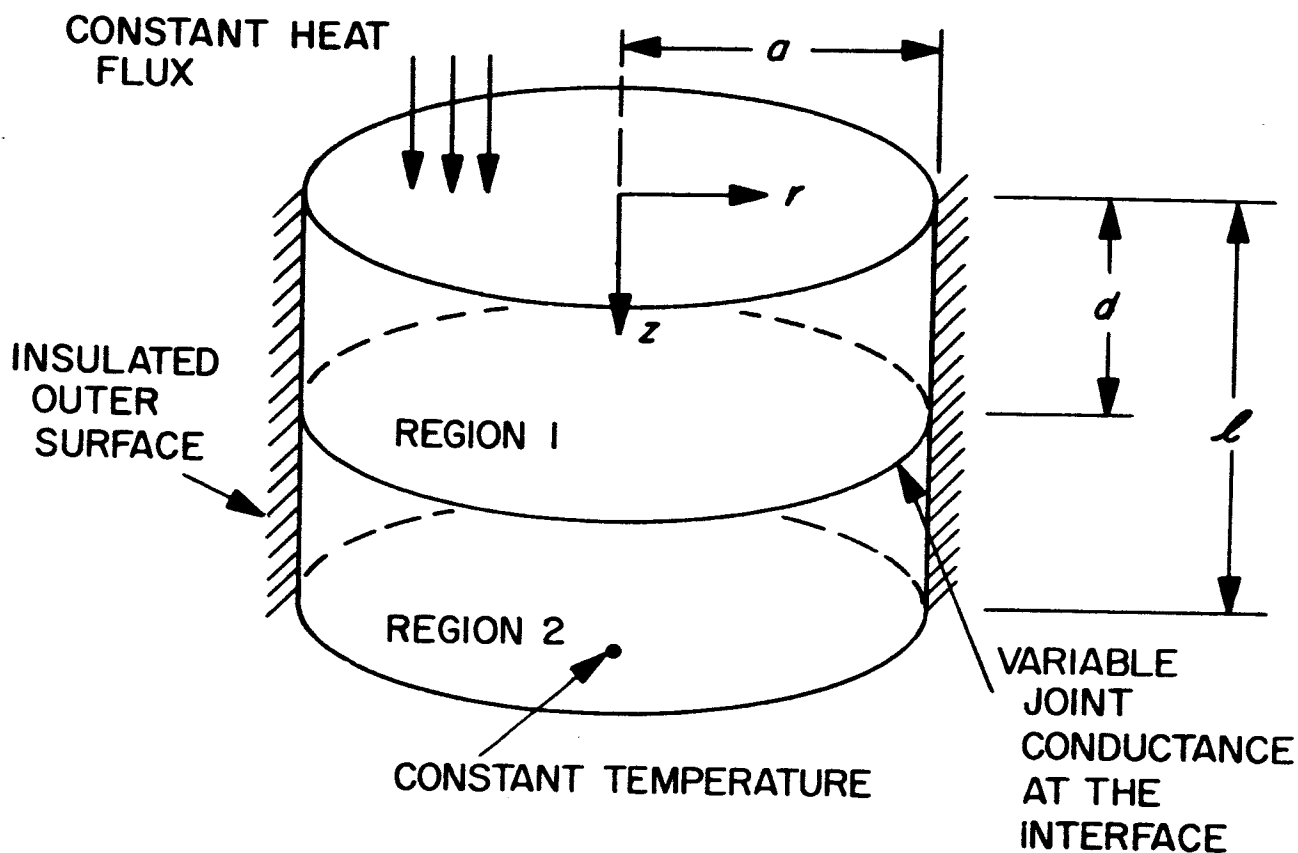
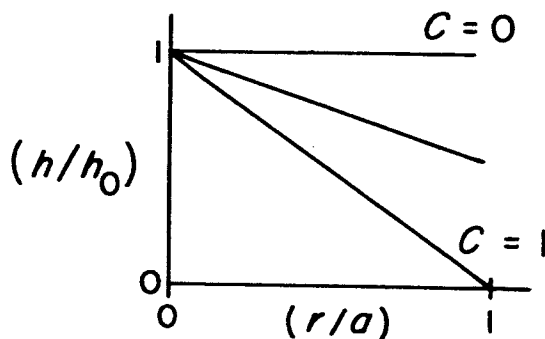


Fig. 6.  
Comparison of results from  
all materials investigated  
with theory



(a) GEOMETRY AND ASSUMPTIONS OF MODEL



(b) VARIATION OF JOINT CONDUCTANCE AT THE INTERFACE,  
 $(h/h_0) = 1 - C(r/a)$

Fig. 7.  
 Mathematical model for effect  
 of variable joint conductance

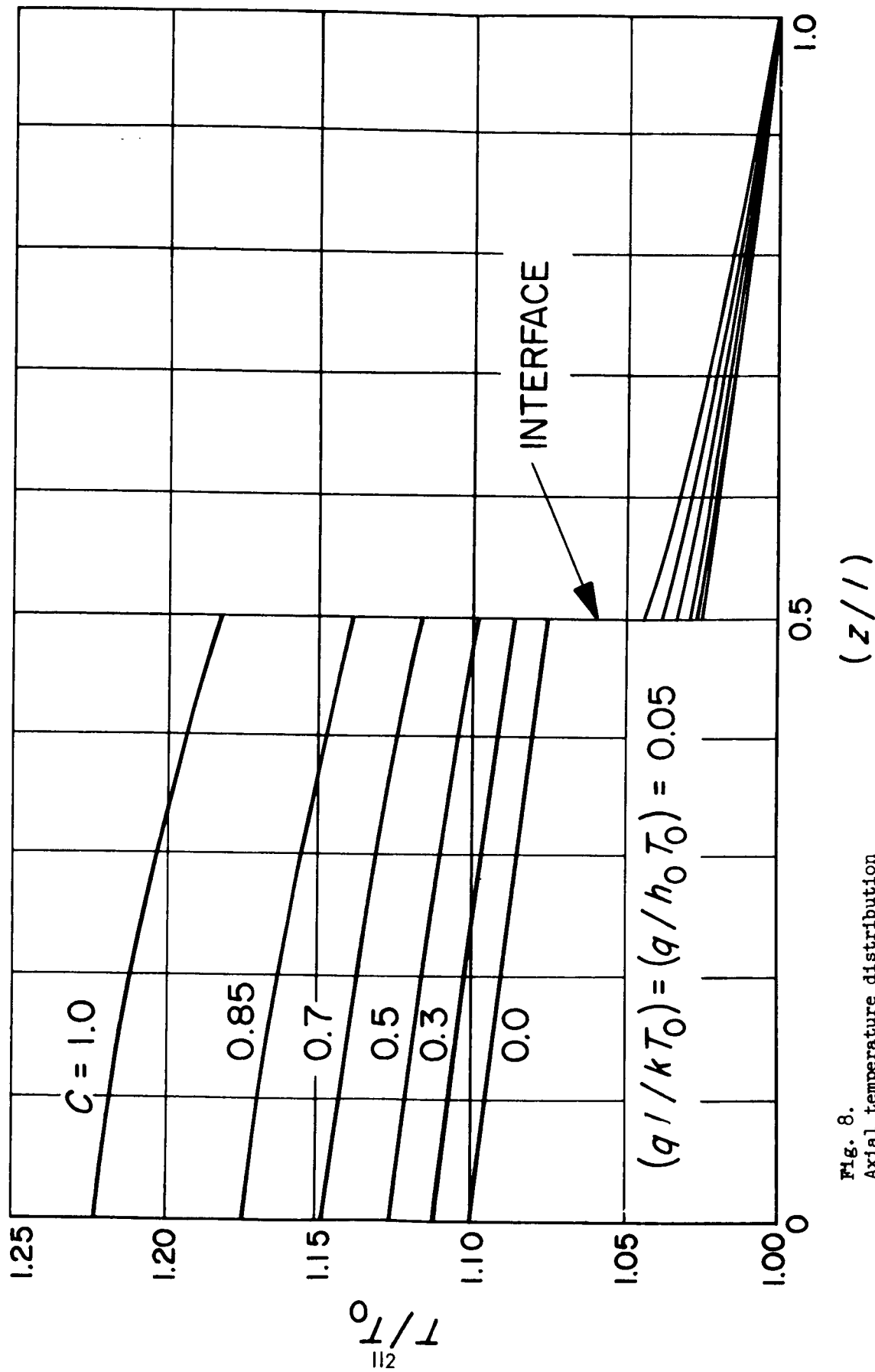


Fig. 8.  
Axial temperature distribution  
for different values of the  
constant  $C$

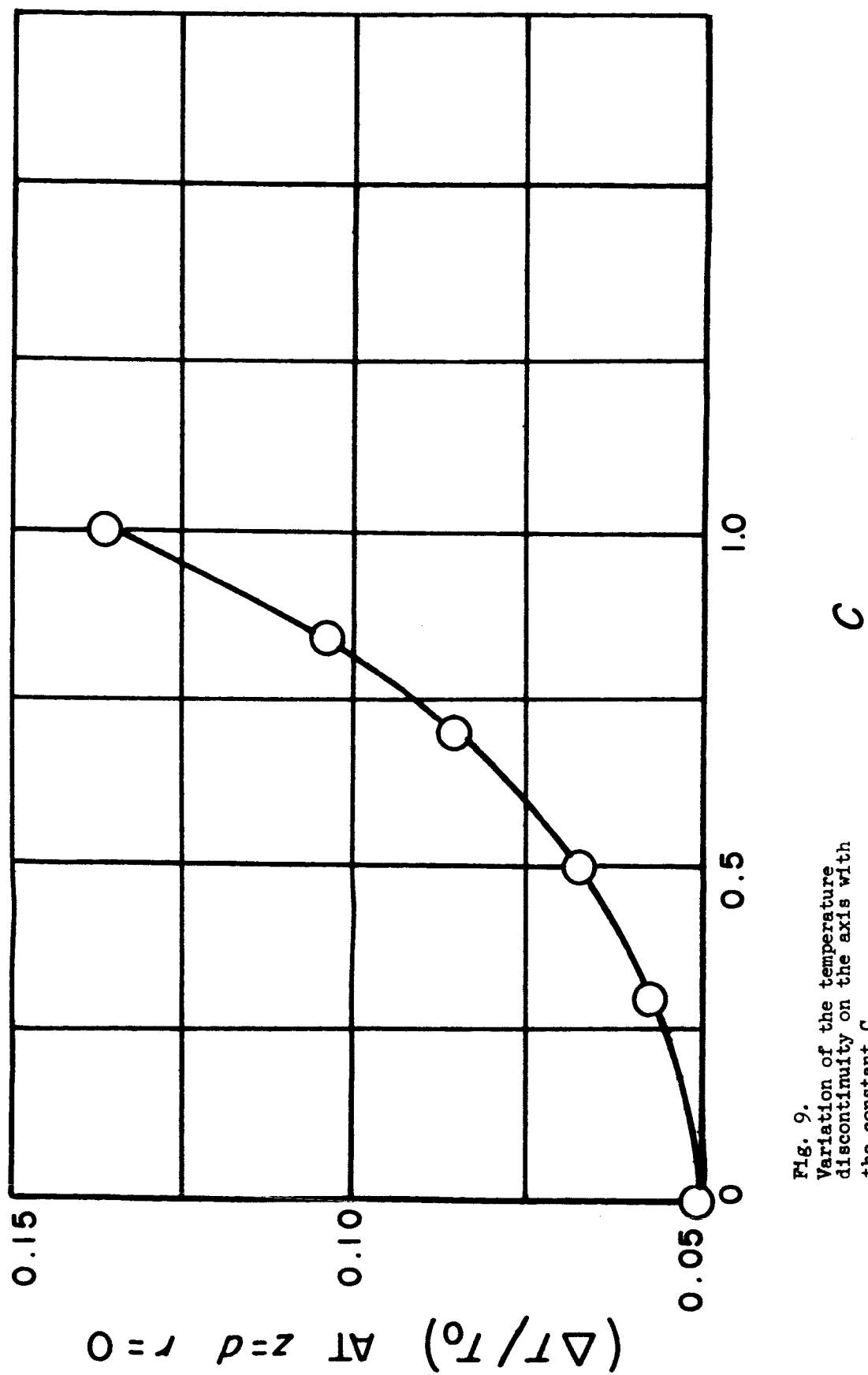


Fig. 9.  
Variation of the temperature  
discontinuity on the axis with  
the constant  $C$

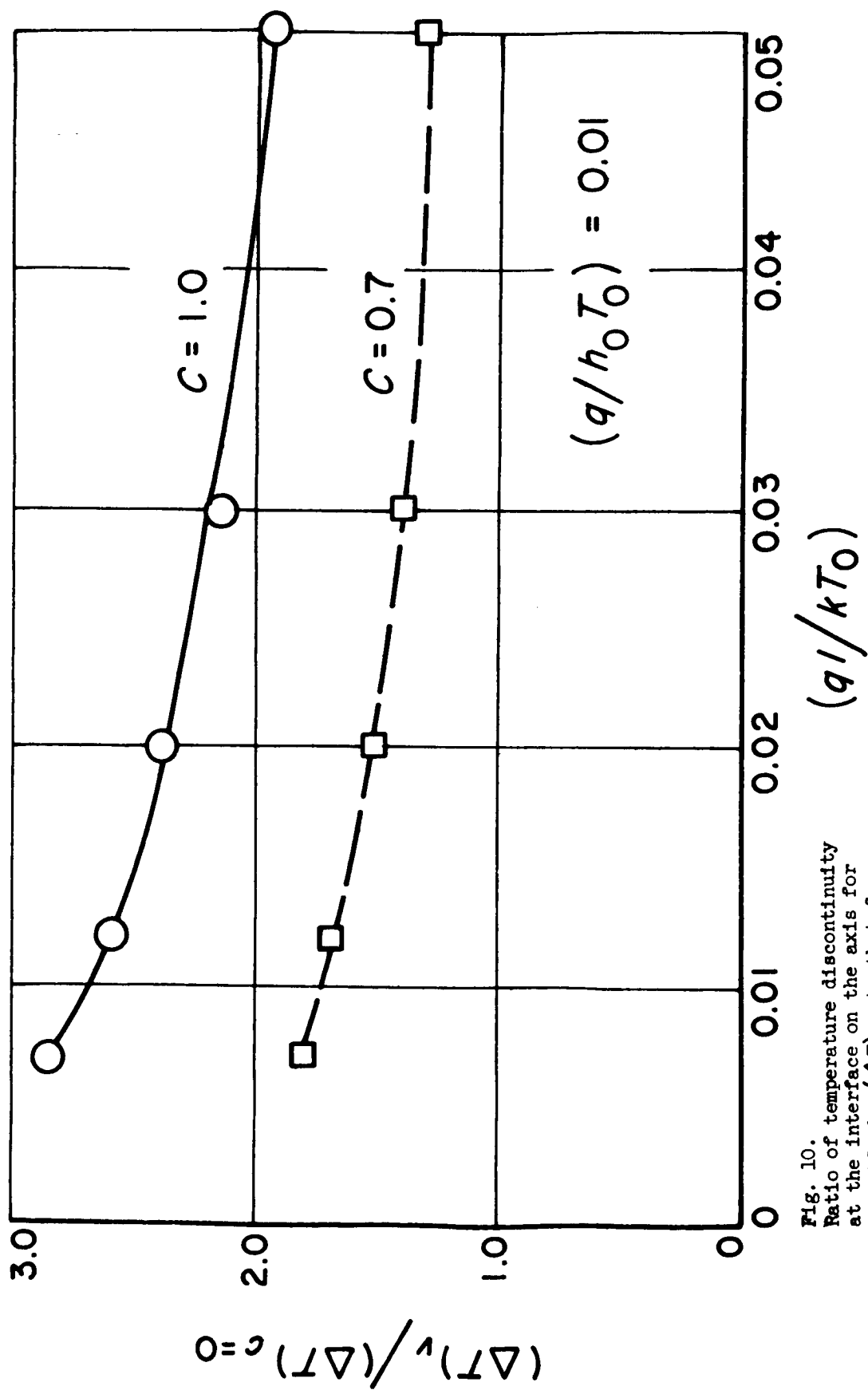


Fig. 10.  
Ratio of temperature discontinuity  
at the interface on the axis for  
variable  $h$ ,  $(\Delta T)_{C=0}$ , to that for  
constant  $h$ ,  $(\Delta T)_{C=0}$ , vs  $(q_l/kT_0)$



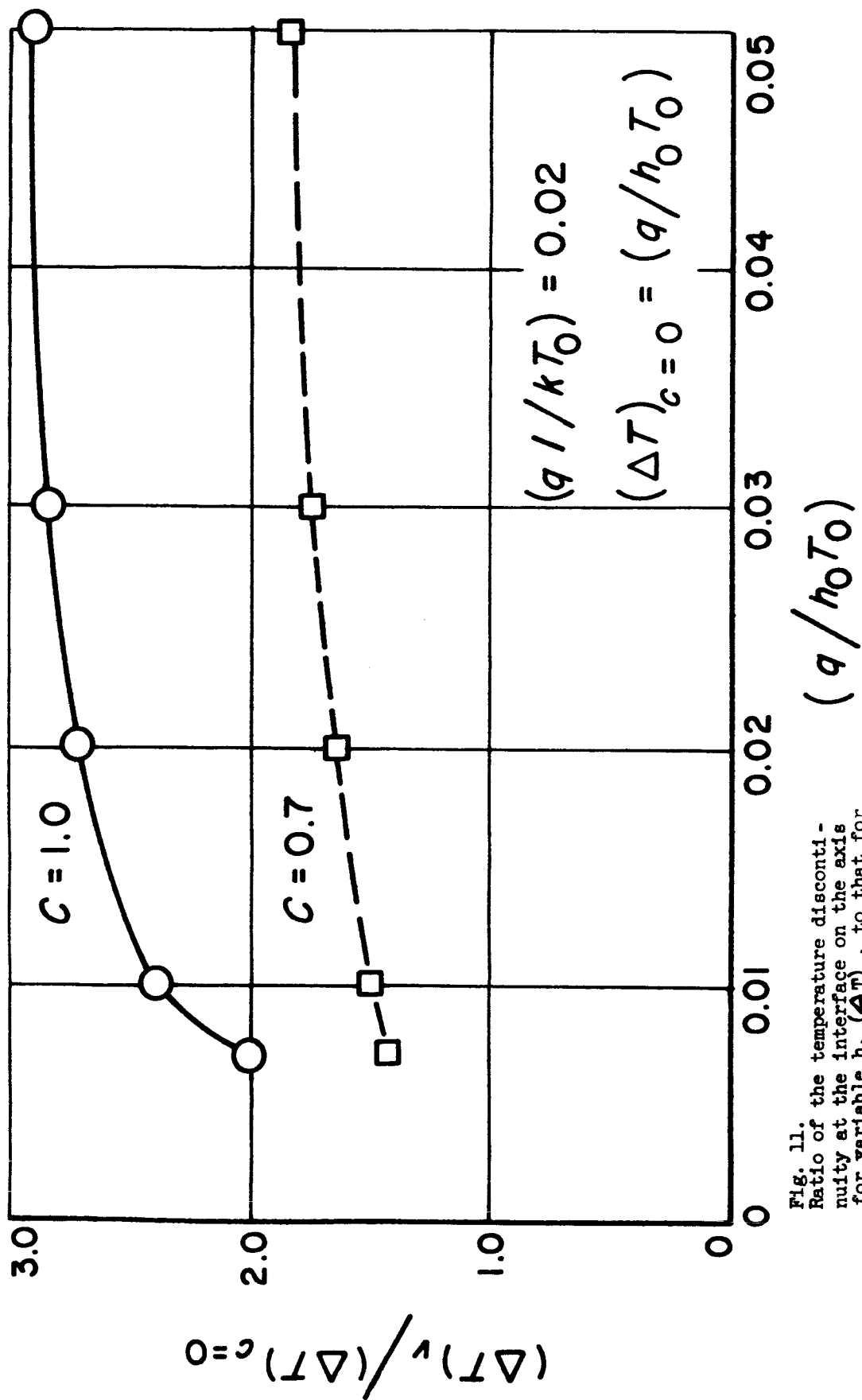


Fig. 11.  
 Ratio of the temperature discontinuity at the interface on the axis for variable  $h$ ,  $(\Delta T)_{C=0}$  to that for constant  $h$ ,  $(\Delta T)_{C=0, \sqrt{h}(q/h_0 T_0)}$

# CIRCULAR LOADING

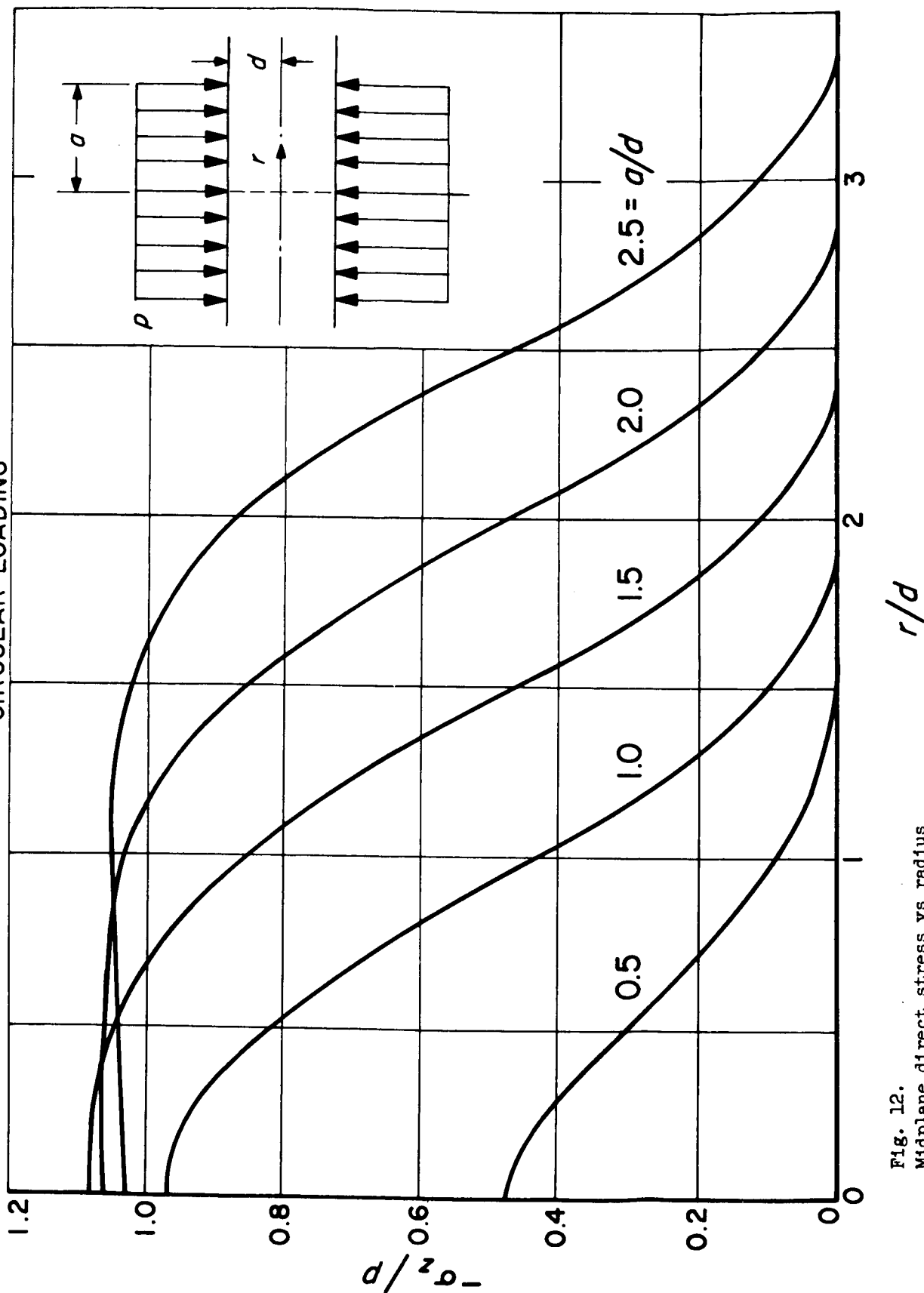


Fig. 12.  
Midplane direct stress vs radius  
for different values of loading  
ratio  $a/d$ . Circular loading.

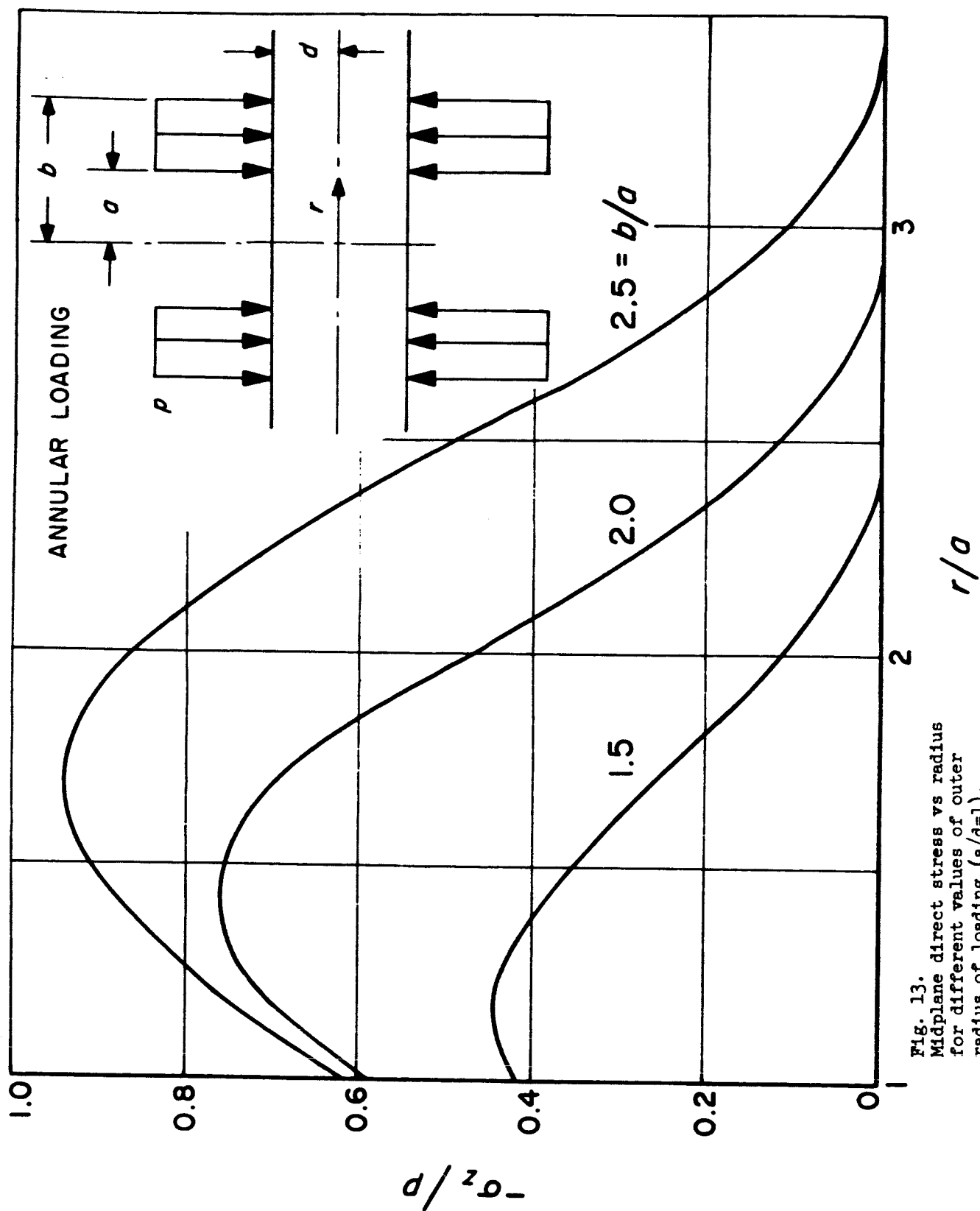


Fig. 13.  
Midplane direct stress vs radius  
for different values of outer  
radius of loading ( $a/d=1$ ).  
Annular loading



N66 37810

THERMAL CONDUCTANCE OF MOLYBDENUM AND STAINLESS-  
STEEL INTERFACES IN A VACUUM ENVIRONMENT

by R. D. Sommers and W. D. Coles

Lewis Research Center  
National Aeronautics and Space Administration  
Cleveland, Ohio

We will assume an awareness of the general nature of the problem of joint conductance and an overall understanding of the qualitative interaction of various parameters such as surface roughness, contact pressure, interface temperature, etc. The purpose of this paper is to report a series of thermal conductance measurements taken on SS 304 and molybdenum joints in a vacuum environment.


Figure 1 shows what the situation is at a joint of two metals. Due to the microscopic irregularity of the surfaces, the pieces do not make intimate contact across the entire apparent contact area. Based on the temperature profile as measured along the pieces, there exists a fairly large temperature drop across the interface. The quantity of interest is the thermal conductance  $h$  defined as the ratio of heat flow per apparent area of contact to the temperature drop across the interface.

Figure 2 presents a schematic of the apparatus. The vacuum chamber is formed by a steel bell jar in which the pressure is maintained at  $10^{-6}$  torr or lower. Variable contact pressure is obtained through an air cylinder loading system external to the vacuum chamber. The load is measured by means of a Baldwin load cell as shown in the schematic. The friction reliever was a small solenoid-activated hammer that applied two sharp raps a minute to the loading shaft. This was an expedient that proved necessary to relieve frictional forces encountered in the "O" ring seals around the loading shaft.

Inductive heating was utilized as a heating source. Excitation was of 10,000-kc frequency supplied by a 30-kw machine built commercially by Tocco, Inc.

The heat flow was determined by measuring the axial temperature gradient along a piece of high purity copper and utilizing a known thermal conductivity (ref. 1) in the one-dimensional Fourier heat conduction equation.

Figure 3 is a photograph of the test shaft with the specimens in place. The thermocouples used were chromel-alumel, 32 gage, peened into the surfaces  $1/8$  inch. The thermocouple leads were wrapped three fourths of the way around the shaft before passing through any temperature gradients. Thermocouple outputs were measured with a Rubicon Portable Potentiometer (Model 2732). One point might be made here: the general configuration is such that an auxiliary measurement could be made of the thermal conductivity of the test specimens. Such measurements were generally in good agreement with reported values for these materials, indicating that the instrumentation technique is satisfactory.



Our measurements were all made in a vacuum environment. In order to provide some basis for comparison with values determined under atmospheric conditions, figure 4 presents some thermal conductances measured by Barzelay, et al. (ref. 2) at Syracuse University. The values shown are for a joint of stainless steel. The curves show the typical dependence on contact pressure and average interface temperature - increasing with both. For reference purposes note that the values of  $h$  average around  $1500 \text{ Btu}/(\text{hr})(\text{sq ft})(^\circ\text{F})$ .

Figure 5 shows the thermal conductance of a SS 304 joint in vacuum. The curves have the same dependence on contact pressure and interface temperature but are about an order of magnitude lower than the values of the preceding figure. The difference is attributed to a loss of gas from within the interface and the consequent elimination of gaseous conduction. The heat transfer now proceeds via metallic conduction and thermal radiation. The lowest curve of figure 5 presents the conductance for radiation only, and we are left with the evident conclusion that the principal mode of heat transfer is metallic conduction.

Figure 6 presents the data for a molybdenum joint in a vacuum. These values are about a factor of five higher than those for the SS 304 joint. This is in good agreement with the relation between the thermal conductivities of these two materials and indicates that the extent of real contact is comparable in the two cases. Figure 7 shows the thermal conductance of a mixed joint composed of molybdenum and SS 304. The one unusual characteristic that is immediately obvious is that the conductance decreases with increasing interface temperature. At the moment this is unexplained. One might say that this is a reflection of the temperature dependence of the thermal conductivity of molybdenum, which decreases with increasing temperature. However, why did the curves for the molybdenum-molybdenum joint not show this trend?

Barzelay (ref. 2) observed such a dependence for a stainless-steel - aluminum joint and advanced the idea that it was due to warping of the surfaces. He also found that the conductance was a function of the direction of heat flow for the stainless-steel - aluminum joint.

Figure 8 presents the thermal conductance for a molybdenum-SS 304 joint with the heat flow reversed. There is a marked decrease in the conductance values. In all fairness, it should be pointed out that the two molybdenum-SS 304 joints under discussion are composed of different surfaces, so that not all of the difference may be due to the change in heat flow direction. One interesting point is the reversal of the decreasing trend when the heat flow is from the molybdenum to the SS 304. Furthermore, this reversal occurs when the molybdenum surface attains  $\sim 900^\circ \text{F}$ . In the test of figure 7, despite an average interface temperature of  $1000^\circ \text{F}$ , the molybdenum surface did not rise much above  $700^\circ \text{F}$ . Therefore it is entirely possible that a reversal would have been noticed if the test had been extended to higher temperatures.

The data for the mixed joints at the moment is lacking clearcut interpretation, but the results of Barzelay for SS-Al and our results for molybdenum and SS 304 reveal some coincidences that are interesting. For example, the conductance is higher when the heat flows from the softer material to the

harder. Since in this case the softer material reaches a higher temperature, this may be an indication of a greater tendency to flow and improve the extent of real contact. Tables 1 to 5 present details of the test surfaces and experimental measurements and are included as a supplement to the figures.

In any event our present studies are centering around these materials and others that may form joints composed of materials of widely varying properties. We are also planning to extend the vacuum environment into the  $10^{-13}$  Torr range.

#### REFERENCES

1. Charles F. Lucks, and Hubert W. Deem; Thermal Properties of 13 Metals.  
ASTM Special Tech. Pub. 227, 1958.
2. Martin E. Barzelay, Kin Nee Tong, George F. Holloway; Effect of Pressure on  
Thermal Conductance of Contact Joints. NACA TN 3295, 1955.



$$h = \frac{\dot{q}/A}{\Delta T_i}$$

BASIC FUNCTION OF

$$\left( \frac{A_{\text{REAL}}}{A_{\text{APPARENT}}} \right)$$

SUBSIDIARY FACTORS

1. MATERIAL OF JUNCTION
2. SURFACE ROUGHNESS
3. MATERIAL IN VOIDS
4. CONTACT PRESSURE
5. SURFACE TEMPERATURES

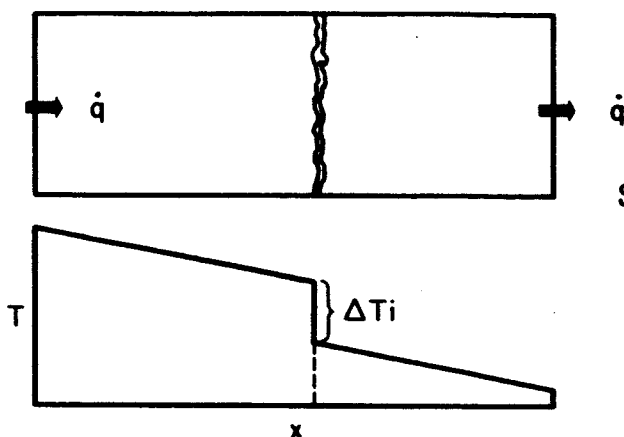
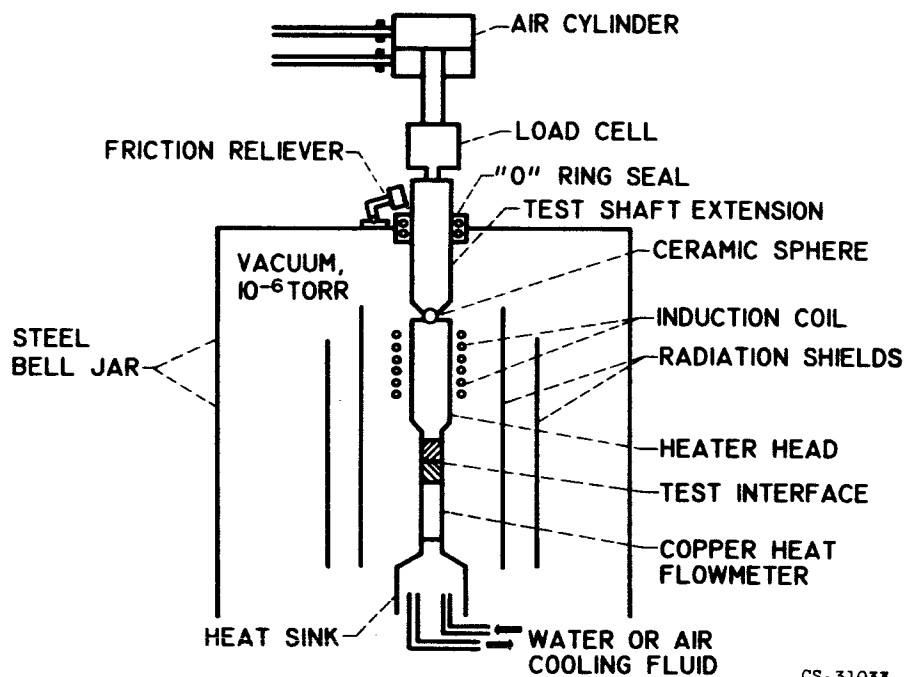


Fig. 1. - Interface conductance.

CS-26277



CS-31033

Fig. 2. - Thermal conductance apparatus.

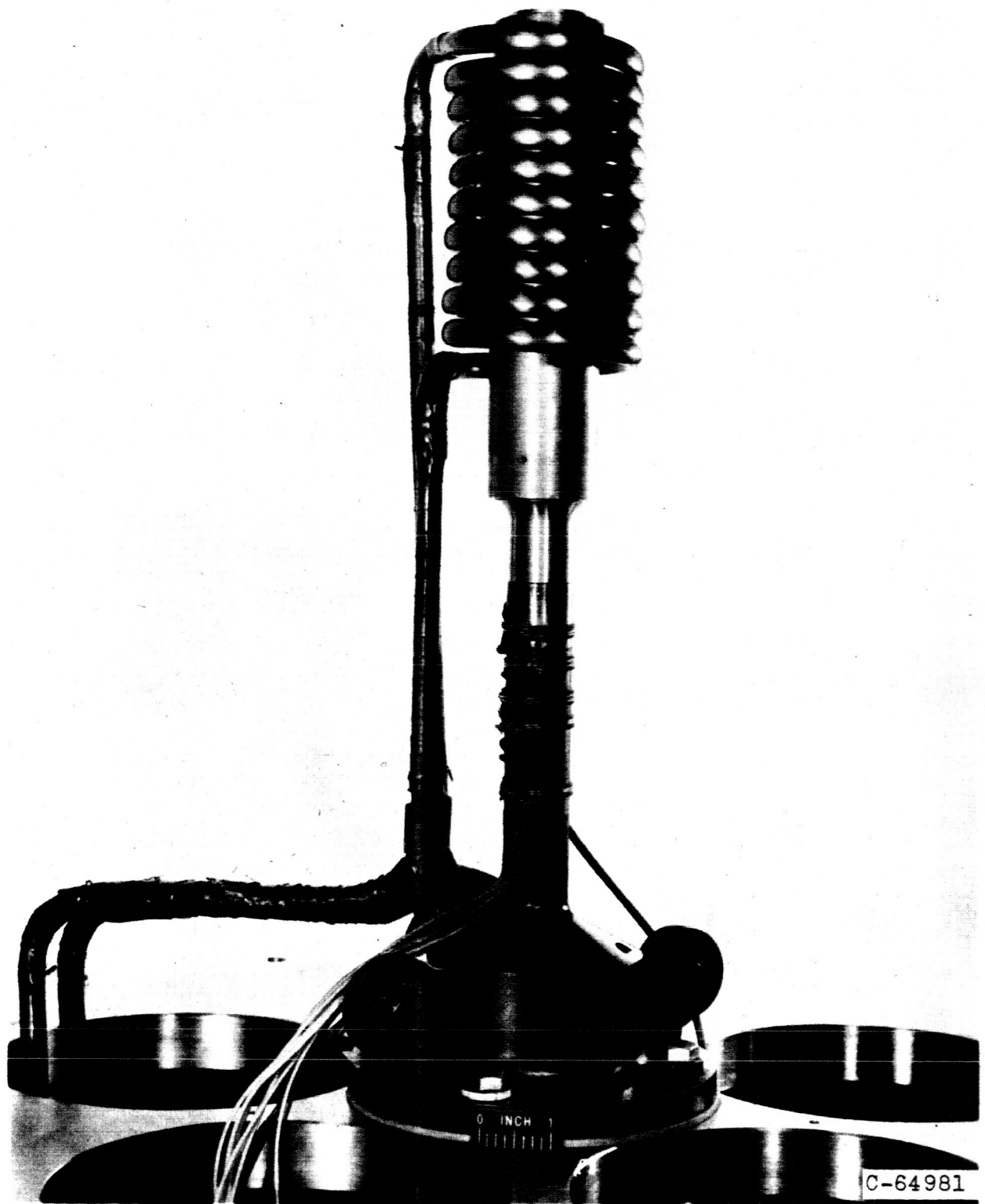


Fig. 3. - Thermal conductance apparatus view of test section.

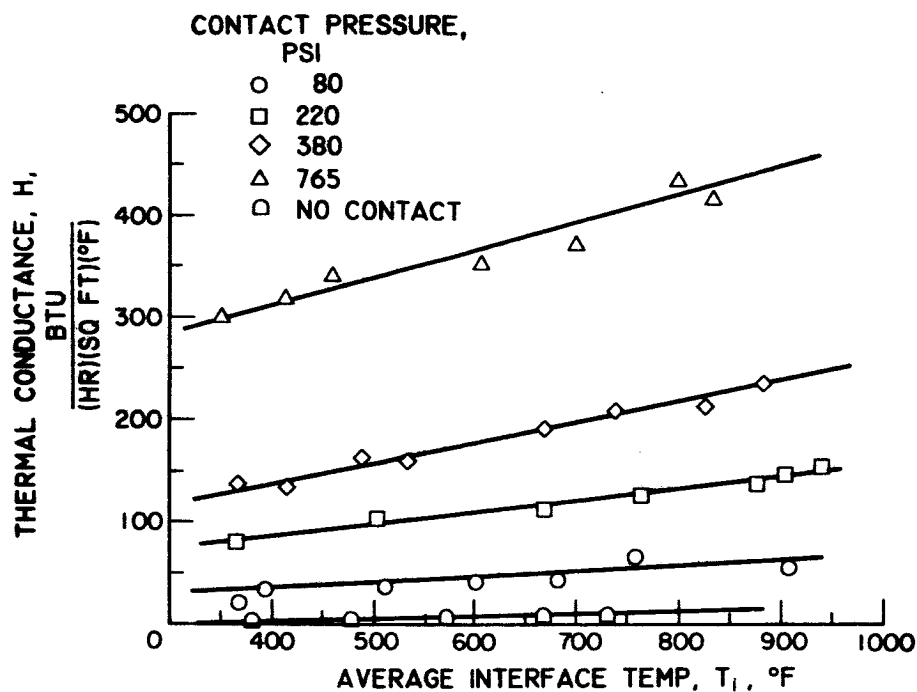


Fig. 5. - Thermal conductance of stainless steel 304-stainless steel 304. Ambient pressure,  $10^{-6}$  Torr; surface roughness, 16  $\mu\text{in}$ .

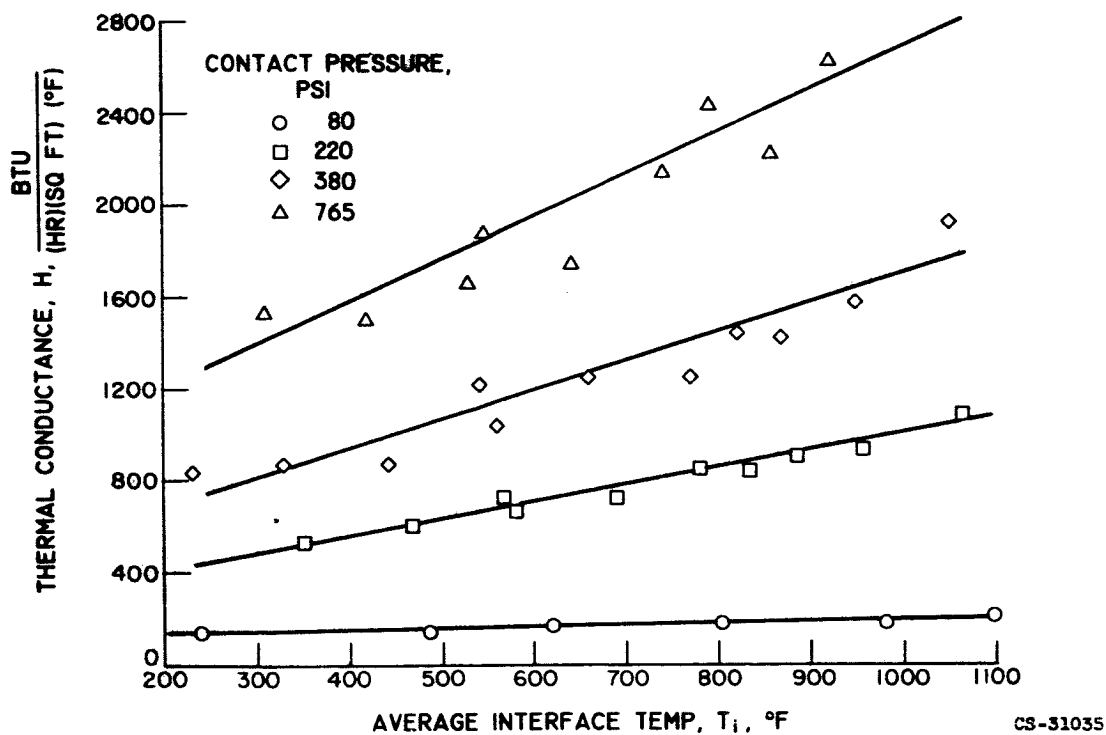


Fig. 6. - Thermal conductance of molybdenum-molybdenum. Ambient pressure,  $10^{-6}$  Torr; surface roughness, 16  $\mu\text{in}$ .

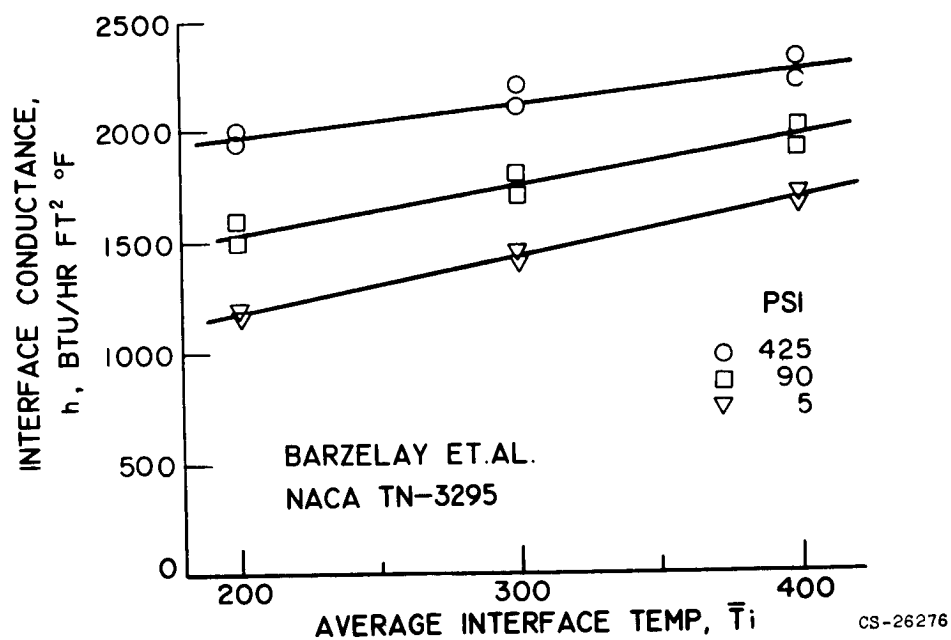


Fig. 4. - Interface conductance stainless steel to stainless steel, surface roughness 30  $\mu$ in.

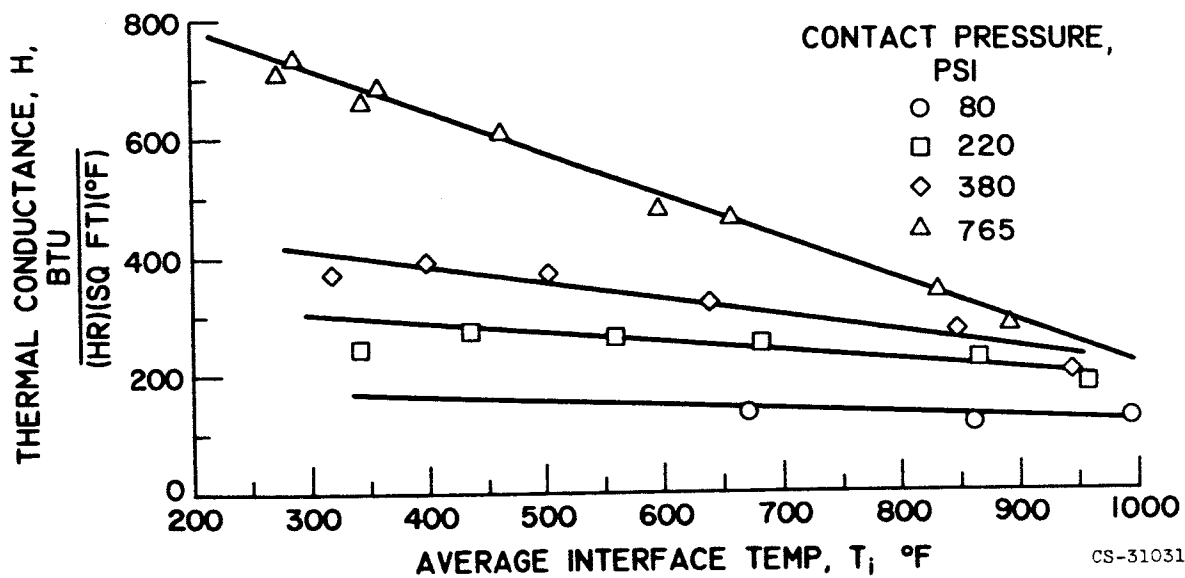


Fig. 7. - Thermal conductance of molybdenum-stainless steel 304 (heat flow from stainless steel 304 to molybdenum). Ambient pressure,  $10^{-6}$  Torr; surface roughness, 16  $\mu$ in.

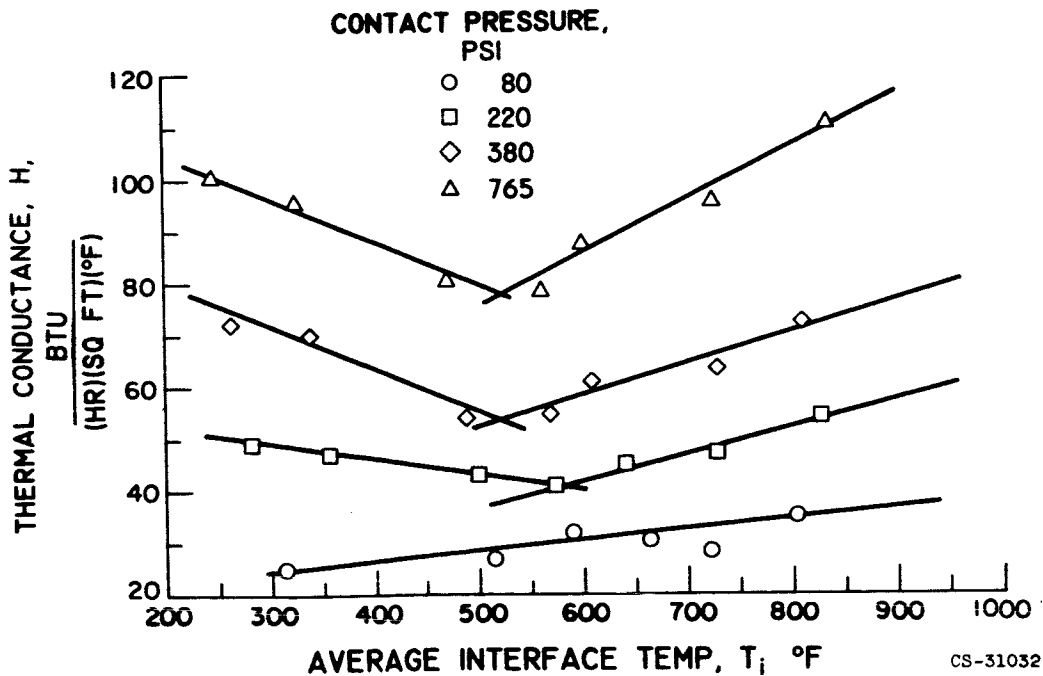


Fig. 8. - Thermal conductance of stainless steel 304 and molybdenum heat flow from SS 304 to molybdenum surface roughness 16 $\mu$ in.; ambient pressure  $10^{-6}$  Torr.

TABLE 1. - SURFACE AND INTERFACE

CHARACTERISTICS

(a) Surface characteristics

Surface	Material	Surface roughness, $\mu$ in.	Surface area, sq in.
Mo <sub>1</sub>	Molybdenum	16 ↓	0.6207
Mo <sub>2</sub>	Molybdenum		.8012
SS <sub>1</sub>	SS 304		.6940
SS <sub>2</sub>	SS 304		.7850

(b) Interface characteristics

Configuration	Heat-flow direction	Apparent contact area, sq in.
SS <sub>1</sub> -SS <sub>2</sub>	SS <sub>1</sub> to SS <sub>2</sub>	0.6940
SS <sub>1</sub> -Mo <sub>2</sub>	SS <sub>1</sub> to Mo <sub>2</sub>	.7353
Mo <sub>1</sub> -Mo <sub>2</sub>	Mo <sub>1</sub> to Mo <sub>2</sub>	.6207
Mo <sub>1</sub> -SS <sub>2</sub>	Mo <sub>1</sub> to SS <sub>2</sub>	.6207

E-2187

TABLE 2. - THERMAL CONDUCTANCE DATA FOR STAINLESS STEEL 304 - STAINLESS STEEL 304 INTERFACE

[Ambient pressure,  $10^{-6}$  Torr; surface roughness,  $16 \mu$  in.]

Contact pressure, psi	Heat flow, $\dot{q}/A$ , Btu/(hr)(sq ft)	Surface temp- erature, $T_1$ , $^{\circ}\text{F}$	Surface temp- erature, $T_2$ , $^{\circ}\text{F}$	Interface temp- erature difference, $\Delta T_1$ , $^{\circ}\text{F}$	Average interface temperature, $T_i$ , $^{\circ}\text{F}$	Interface conductance, $h$ , Btu/(hr)(sq ft)( $^{\circ}\text{F}$ )
765 ↓	29,100	402	305	97	353	300
	43,450	483	347	136	415	319
	42,900	523	397	126	460	340
	60,600	695	523	172	609	352
	71,800	799	605	194	702	370
380 ↓	86,400	900	700	200	800	432
	89,100	941	726	215	834	414
	23,600	453	280	173	367	136
	27,350	518	313	205	415	133
	37,120	603	375	228	489	163
220 ↓	38,270	654	413	241	533	159
	60,400	827	512	315	670	192
	63,450	893	590	303	740	209
	75,400	1004	648	356	826	212
	85,800	1065	700	365	883	235
220 ↓	20,200	490	240	250	365	81
	32,350	659	348	311	504	104
	44,670	866	474	392	670	114
	55,100	981	544	437	763	126
	75,200	1152	601	551	876	136
220 ↓	80,400	1179	628	551	903	146
	83,700	1207	662	545	939	154

TABLE 2. - Concluded. THERMAL CONDUCTANCE DATA FOR STAINLESS STEEL 304 - STAINLESS STEEL 304 INTERFACE

[Ambient pressure,  $10^{-6}$  Torr; surface roughness, 16  $\mu$  in.]

Contact pressure, psi	Heat flow, $\dot{q}/A$ , Btu/(hr)(sq ft)	Surface temperature, $T_1$ , $^{\circ}\text{F}$	Surface temperature, $T_2$ , $^{\circ}\text{F}$	Interface temperature difference, $\Delta T_i$ , $^{\circ}\text{F}$	Average interface temperature, $T_{i, \text{OF}}$	Interface conductance, $h$ , Btu/(hr)(sq ft)( $^{\circ}\text{F}$ )
80 ↓	9,220	582	154	428	368	21.5
	14,340	598	190	408	394	35.1
	19,390	777	247	530	512	36.5
	25,200	904	302	602	603	41.9
	29,220	1021	344	677	683	43.2
	40,480	1061	455	606	758	66.8
	45,850	1326	491	835	908	55.0
No contact, surfaces separated by 1/16 in.	2,308	671	90	581	381	3.97
	2,820	770	96	673	483	4.19
	6,505	1004	138	866	571	7.51
	6,880	1195	146	1049	670	6.56
	9,660	1302	170	1132	736	8.54



TABLE 3. - THERMAL CONDUCTANCE DATA FOR MOLYBDENUM - STAINLESS STEEL 304 INTERFACE

[Heat flow from Mo to SS 304; ambient pressure  $10^{-6}$  Torr;  
surface roughness,  $16 \mu$  in.]

Contact pressure, psi	Heat flow, $q/A$ , Btu/(hr)(sq ft)	Surface temperature, $T_1$ , $^{\circ}F$	Surface temperature, $T_2$ , $^{\circ}F$	Interface temperature difference, $\Delta T_i$ , $^{\circ}F$	Average interface temperature, $T_i$ , $^{\circ}F$	Interface conductance, $h$ , Btu/(hr)(sq ft)( $^{\circ}F$ )
765 ↓	16,900	330	162	168	246	100.5
	23,950	450	200	250	325	95.6
	35,400	692	251	441	472	80.3
	40,700	822	302	520	562	78.3
	49,200	880	320	560	600	87.0
	62,000	1051	400	651	725	95.2
	75,200	1176	495	681	835	110.5
380 ↓	15,600	372	157	214	263	72.6
	21,050	488	187	301	338	69.8
	27,660	747	233	514	490	53.8
	32,750	870	269	601	569	54.5
	39,100	930	289	641	609	60.9
	46,800	1100	355	745	727	62.9
	58,400	1212	406	806	809	72.4
220 ↓	13,000	413	148	265	281	49.1
	16,900	535	177	358	356	47.3
	23,850	777	222	555	500	42.9
	26,900	900	250	650	575	41.5
	31,800	989	290	699	640	45.6
	38,000	1135	324	811	730	46.8
	47,000	1265	400	865	832	54.4
80 ↓	8,440	481	145	336	313	25.1
	16,450	821	208	613	515	26.8
	21,900	932	245	687	588	31.8
	25,720	1040	285	755	662	30.2
	23,000	1132	310	822	721	27.9
	34,100	1330	375	955	802	35.6

TABLE 4. - THERMAL CONDUCTANCE DATA FOR MOLYBDENUM - MOLYBDENUM INTERFACE

[Ambient pressure,  $10^{-6}$  Torr; surface roughness,  $16 \mu$  in.]

Contact pressure, psi	Heat flow, $\dot{q}/A$ , Btu/(hr)(sq ft)	Surface temperature, $T_1$ , $^{\circ}\text{F}$	Surface temperature, $T_2$ , $^{\circ}\text{F}$	Interface temperature difference, $\Delta T_i$ , $^{\circ}\text{F}$	Average interface temperature, $T_i$ , $^{\circ}\text{F}$	Interface conductance, $h$ , Btu/(hr)(sq ft)( $^{\circ}\text{F}$ )
765 ↓	50,400	325	292	33	309	1,527
	75,000	444	394	50	419	1,500
	148,000	573	484	89	528	1,663
	105,400	573	517	56	545	1,882
	181,500	693	589	104	641	1,745
	219,700	792	690	102	741	2,152
	236,800	841	743	98	792	2,416
	256,520	916	800	116	858	2,211
	295,300	978	865	113	922	2,612
	338,000	1100	984	116	1042	2,915
	28,780	247	212	35	230	822
	48,680	362	306	56	329	869
	71,800	484	402	82	443	875
	142,100	599	482	117	540	1,214
380 ↓	100,400	606	510	96	560	1,045
	170,000	731	595	136	663	1,250
	205,100	854	690	164	772	1,252
	223,000	897	743	154	820	1,446
	245,300	955	781	174	868	1,411
	276,000	1024	850	174	947	1,585
	327,800	1135	965	170	1050	1,929

TABLE 4. - Concluded. THERMAL CONDUCTANCE DATA FOR MOLYBDENUM - MOLYBDENUM INTERFACE  
E-2187

[Ambient pressure,  $10^{-6}$  Torr; surface roughness,  $16 \mu$  in.]

Contact pressure, psi	Heat flow, $\frac{q}{A}$ Btu/(hr)(sq ft)	Surface temperature, $T_1$ , $^{\circ}\text{F}$	Surface temperature, $T_2$ , $^{\circ}\text{F}$	Interface temperature difference, $\Delta T_1$ , $^{\circ}\text{F}$	Average interface temperature, $T_1$ , $^{\circ}\text{F}$	Interface conductance, $h$ , Btu/(hr)(sq ft)( $^{\circ}\text{F}$ )
220 ↓	46,000	394	308	86	351	535
	69,800	524	408	116	466	601
	134,600	658	475	183	567	735
	95,400	654	510	144	582	662
	159,500	799	581	218	690	727
	191,400	891	667	224	779	854
	209,000	959	709	250	834	836
	227,200	1012	760	252	886	902
	256,200	1092	819	273	956	939
	299,600	1202	926	276	1064	1,095
80 ↓	22,300	317	160	157	238	142
	50,300	659	313	346	486	145
	96,100	900	344	556	622	168
	122,700	1149	457	692	803	177
	148,500	1396	566	830	981	179
	181,500	1542	656	886	1099	205

TABLE 5. - THERMAL CONDUCTANCE DATA FOR STAINLESS STEEL 304 - MOLYBDENUM INTERFACE

[Heat flow from SS 304 to Mo; ambient pressure,  $10^{-6}$  Torr;  
surface roughness,  $16 \mu$  in.]

Contact pressure psi	Heat flow, $\dot{q}/A$ Btu/(hr)(sq ft)	Surface temp- erature, $T_1$ , $^{\circ}F$	Surface temp- erature, $T_2$ , $^{\circ}F$	Interface temp- erature difference, $\Delta T_i$ , $^{\circ}F$	Average interface temperature, $T_i$ , $^{\circ}F$	Interface conductance, $h$ , Btu/(hr)(sq ft)( $^{\circ}F$ )
765 ↓	40,240	301	244	57	273	706.0
	40,970	318	261	56	289	731.0
	52,990	385	304	80	345	658.0
	57,200	402	317	84	359	680.0
	74,740	524	400	124	462	602.0
	93,380	694	496	198	595	472.0
	105,691	770	540	230	655	460.0
	121,820	1014	650	364	832	335.0
	122,140	1113	675	438	894	279.0
380 ↓	33,450	364	274	90	319	371.0
	49,250	461	335	126	398	391.0
	66,790	591	411	180	503	370.0
	84,990	769	505	264	637	321.0
	97,840	840	560	280	700	350.0
	114,410	1056	633	423	847	270.0
	103,560	1201	687	514	944	201.0
220 ↓	28,730	396	280	116	343	247.0
	44,950	517	354	163	435	275.0
	59,600	670	447	223	559	267.0
	77,580	835	530	305	682	254.0
	90,000	922	594	328	758	276.0
	105,140	1100	630	470	865	223.0
	97,950	1223	698	525	960	186.0
80 ↓	50,450	854	488	366	671	137.0
	56,000	1105	620	485	862	115.0
	63,410	1253	735	518	994	122.0